5-2015

# CAPILLARY CHANNEL POLYMER FIBER-BASED SCAFFOLDS FOR NEURAL REGENERATION

Atanu Sen
*Clemson University*, atanu@g.clemson.edu

# CAPILLARY CHANNEL POLYMER FIBER-BASED SCAFFOLDS FOR NEURAL REGENERATION

---

A Dissertation
Presented to
the Graduate School of
Clemson University

---

In Partial Fulfillment
of the Requirements for the Degree
Doctor of Philosophy
Bioengineering

---

by
Atanu Sen
May 2015

---

Accepted by:
Dr. Ken Webb, Committee Chair
Dr. Frank Alexis
Dr. Alexey Vertegel
Dr. Bruce Gao

# ABSTRACT

Over 50 million Americans are affected by ailments to the central nervous system (CNS) and it impacts the American economy over $400 billion a year. The number of people in the United States who have spinal cord injury (SCI) has been estimated to be approximately 276,000 persons as of 2014 with a range from 240,000 to 337,000 persons. The annual incidence of SCI, not including those who die at the scene of the accident is approximately 12,500 new cases each year. Due to the limited regenerative capacity of the adult CNS and lack of clinically effective therapies, these conditions commonly result in permanent functional deficits. SCI damages both ascending sensory and descending motor axonal pathways interrupting the transmission of synaptic signals between the brain and peripheral tissues. Although damaged axons attempt an initial regenerative response, this is rapidly aborted due to the presence of growth inhibitory molecules in CNS myelin and the glial scar and intrinsic limitations of adult CNS neuronal biochemistry such as the ability to maintain cAMP levels and upregulate the expression of 'regeneration-associated genes'. On the other hand, TBI, stroke, and Parkinson's disease result in neuronal cell death. The CNS has limited capacity to replace lost neurons because the neurons themselves are terminally differentiated and post-mitotic. Although neural stem cells (NSCs) have been identified in specialized regions of the adult brain such as the sub-ventricular zone (SVZ) and the sub-granular zones (SGZ), their number is insufficient and the pathological environment inadequate to support an effective regenerative response.

The end goal of this project is to develop a biomimetic scaffold using grooved fibers for neural regeneration. This goal was met with a two-pronged approach. In the first approach, grooved fibers immobilized with bioactive adhesive molecule were developed to topographically guide regenerating axons. In the second approach, grooved fiber

staples were used as cell-laden microcarriers and integrated into a composite hydrogel which demonstrated its ability to serve as a platform for cell proliferation. This latter approach can be translated into an injectable *in situ* crosslinkable scaffold that can be used for neural stem cell (NSC) delivery with the prospect of stem cell differentiation into neurons to replenish cell loss.

The first part of this research focused on immobilizing a bioactive 140 kDa fragment of L1 neural cell adhesion molecule on uniquely designed groovy capillary channel polymer (CCP) fibers. L1-CAM is an attractive candidate for growth of spared axonal growth cones upon injury. It mediates CNS maturation, by means of neurite outgrowth, adhesion, fasciculation, migration, survival, myelination, axon guidance, synaptic plasticity and regeneration after trauma. High levels of L1 are expressed by growing axons during development and after SCI and there is a positive correlation between their expression and axonal growth. CCP fibers with surface immobilized L1-CAM were demonstrated to guide growth of primary neurons *in vitro.* In the latter part of this research, a methodology to fabricate CCP fiber staples was developed and these were employed as cell-laden microcarriers. These microcarriers were then integrated into a composite hydrogel blend and demonstrated high cell proliferation *in vitro* compared to control gels. This composite system can be a promising platform for NSC delivery and differentiation into neurons.

## ACKNOWLEDGMENTS

The Department of Bioengineering has been my safe haven for my stay here at Clemson University. Ever thankful for this opportunity to serve as research and teaching assistant at this wonderful institution. I would like to thank Prof. Martine LaBerge – Chair of Department of Bioengineering, for her belief in me and to provide me an opportunity to pursue my PhD. No words to describe the support given to me by our department's graduate student coordinator – Ms. Maria Martin. Maria, all your support during tough times have been invaluable and helped me enormously for all these years, can never forget and cannot be thankful enough. I would like to thank my committee members – Prof. Frank Alexis, Prof Alexey Vertegel and Prof. Bruce Gao for their guidance and support.

***"A teacher Takes a hand Opens a mind Touches a heart Shapes the future"***

***"A disciple is not a vessel to be filled, but a lamp to be lit."***

These words are for my mentor Prof. Ken Webb. Working with Prof. Webb over the years, I realized things more than just science, probably I realized 'life'. I remember once in my early stages, he had mentioned in a one on one meeting: 'Your success is very important to me'. And with time I realized how he meant every word of it. I learned the virtues of 'patience' and 'perseverance' from numerous failed experiments in the laboratory, which in course of time became the mantra for life in general. His utmost respectful, humble and kind attitude towards other fellow human beings is a trait that I always appreciate and try to emulate,

and probably it rubbed into me overtime. I appreciate the considerable time and effort invested by him in correcting abstracts and manuscripts on innumerable occasions. **'*Thank you*'** Prof. Webb for the opportunity and for shaping my character and my life.

I was fortunate to have labmates – Jeremy Zhang, Ho-Joon Lee and Sooneon Bae with whom I had a smooth sail and never had any issues. I acknowledge Dr. Jeoung Soo Lee for scientific discussions and guidance to my project at times. Two colleagues deserve special mention – Srikanth Sivaraman and Saketh Ram Karamched, thankful for your much needed support towards the finish.

I would like to extend my gratitude to my Maa, Baba and my sister. I know I did you proud with my achievement, eternally grateful for your unconditional love and support. Special thanks to my maternal aunt Leena Barua in Canada, your support through all these years and especially in the finishing stages have been of enormous help. Shout out to my buddies across the globe – Bishal Nath (India), Vikas Kohli (Canada) and Srikant Chandrashekaran (Australia); you have been awesome, thanks for the happy times you have time and again given to me, and look forward to more and more such times ahead.

## TABLE OF CONTENTS

**TABLE OF CONTENTS (contd.)** Page

**TABLE OF CONTENTS (contd.)**

Chapter Page

**TABLE OF CONTENTS (contd.)**

Chapter Page

## LIST OF FIGURES

Figure Page

## LIST OF FIGURES (contd.)

Figure Page

## LIST OF FIGURES (contd.)

Figure Page

## LIST OF TABLES

Table Page

## CHAPTER ONE

# INTRODUCTION

### 1. **CNS injuries and diseases** (TBI, SCI, Neurodegenerative diseases)

Over 50 million Americans are affected by ailments to the central nervous system (CNS) and it impacts the American economy over $400 billion a year. Traumatic insults to the central nervous system (CNS) such as in spinal cord injury (SCI) and traumatic brain injury (TBI), result in impaired motor and sensory functions; cystic cavity and glial scar formation thereby causing disruption of signaling pathways. Apart from spinal cord injury (SCI) and traumatic brain injury (TBI), neurological diseases such as Alzheimer's disease, Parkinson's disease, and Huntington's disease result in neuronal loss. Furthermore, if blood supply is impaired by hemorrhage or ischemia, the functional consequences worsen, as the CNS has limited capability to replace or regenerate lost neurons. In the adult CNS, the damaged axons do not regenerate spontaneously because of the extrinsic inhibitory environment and their intrinsic limited regenerative ability as well. In addition, replacement of lost neurons in debilitating cases of neurodegeneration by neural stem cells is also limited in the adult CNS. However, it is now known that various neural engineering and neuroprotective strategies can enable regeneration and replacement of surviving and lost neurons respectively. One approach to engineering the SCI pathology, is to transplant physical support that provides topographic cues for directional guidance. Such topographic support should be able to mimic the native ECM (extracellular matrix) environment of the neuronal niche. Other approaches include cellular therapy wherein

transplanted cells provide trophic biochemical support and can also replenish lost neurons by differentiating in response to the environmental niche at the defect site.

### 1.1.1 Spinal Cord Injury (SCI)

The number of people in the United States who have spinal cord injury (SCI) has been estimated to be approximately 276,000 persons as of 2014 with a range from 240,000 to 337,000 persons [1]. The annual incidence of SCI, not including those who die at the scene of the accident is approximately 12,500 new cases each year. This greatly compromises the quality of life of affected individuals and has a significant socioeconomic impact. The average individual cost borne with just SCI cases is $250,000 and amounts to a sum of about $10,000,000,000 in medical expenses every year. The pathophysiology of SCI involves two stages [2]. The primary injury involves initial mechanical infliction which results in direct compression of the spinal cord by bone fragments and spinal cord disc material that causes damage to axons and neuron membrane. The spinal cord can swell in this situation resulting in secondary ischemia. The secondary injury cascade involves cell apoptosis in response to toxic chemicals released from damaged cells, axons and blood vessels in addition to glutamate excitotoxicity. The neural engineering challenge comes in to reinnervate surviving axons by guidance from the rostral to the caudal end across the gap to restore the neuronal circuit.

### 1.1.2 Traumatic Brain Injury (TBI)

Traumatic brain injury (TBI) is one of the major causes of morbidity in the United States, impacting the lives of 1.5 million new patiently annually. The annual mortality due to TBI amounts to approximately 50,000 contributing to about 30% of all injury deaths [3] with an additional 230,000 patients requiring hospitalization. As of 2010, about 2.5 million

patients exist overall in US itself while approximately 6.5 million exist worldwide [4]. The repurcussions can last from anywhere between few days to lifetime disabilities. The severity of a TBI may range from mild to severe. A mild injury would result in a brief change in mental status or consciousness while severe case would involve in an extended period of unconsciousness or amnesia after the injury. The effects involved with TBI can include impaired thinking or memory, movement, sensation (e.g., vision or hearing), or emotional functioning (e.g., personality changes, depression). TBI is often referred to as a 'silent epidemic' because of these complications may not be obvious. These issues not only affect the patients but can have lasting socioeconomic effects on families and communities. Neurons show limited ability for repair and no therapy exists currently to reverse the neuronal injury complications. Unlike SCI, TBI involves neuronal cell death and requires cell replacement strategies.

### 1.1.3. Stroke

Brain stroke is the second leading cause of death worldwide. It can be classified into hemorrhagic, ischemic or embolic in origin. 500,000 new cases of brain strokes are reported each year in the US itself, which causes a great socioeconomic burden of approximately $54 billion/year absorbing 6% of the health care budgets. Ischemic stroke accounts for the majority of the stroke types, amounting to 80% of all brain strokes. Although no effective treatment is available for cerebral ischemic stroke till date, current treatments focus on thrombolysis and neuroprotection, which have demonstrated limited benefits in few patients. Most neuroprotective drugs investigated for stroke have failed in clinical trials during the last two decades [5].

### 1.1.4 Parkinson's disease (PD)

PD is a neurodegenerative disorder that affects movement and balance in addition to impairing cognitive abilities. It is found in 2% of the adult population over 65. These symptoms are triggered by the loss of dopaminergic (DA) neurons in the substantia nigra as well as a decrease in the levels of dopamine in the caudate and putamen. The current treatment method is administration of oral L-3, 4-dihydroxyphenylalanine (L-DOPA), which can be converted to dopamine in the body. However, this treatment is less effective with progression of degeneration with adverse effects as dyskinesias (movement disorders that are characterized by involuntary muscle movements) [6, 7].

## 1.2. **Structure/Function of PNS and CNS**:

The nervous system consists of the central nervous system (CNS) and the peripheral nervous system (PNS). The CNS includes the brain, spinal cord, optic, olfactory and auditory systems. It conducts and interprets signals conducted to it by the sensory neurons and also provides excitatory stimuli to the PNS. The PNS includes the cranial nerves from the brain, the spinal nerves from the spinal cord, sensory nerve cell bodies (dorsal root ganglia) and their processes. Peripheral nerves innervate muscle tissue, transmitting sensory and excitatory input to and from the spinal column [8, 9].

The spinal cord can be anatomically divided into the cervical, thoracic, lumbar, sacral, and coccygeal regions. The center of the spinal cord is a butterfly-shaped region referred to as gray matter which contains the somata, neuroglia and blood vessels. The gray matter is ensconced within the white matter which consists of axons and neuroglia. The nerves on each side of the cord are subdivided into roots. The dorsal root carries sensory/afferent neurons which conduct sensory information to the CNS while ventral root carries motor/efferent neurons which convey the response from the CNS to the

end/effector organs such as muscles and glands. The cell bodies of the sensory neurons are located in the dorsal root ganglia just next to the spinal cord while the cell bodies of the motor neurons are located in the ventral horns of the spinal cord or brainstem (Fig.1.1).

In the PNS, nerve fibers are enveloped in a protective sheath called endoneurium composed predominantly of oriented collagen fibers. Several axons are bundled together into fascicles, each surrounded by a protective sheath known as the perineurium formed from many layers of fibroblasts and collagen. Several fascicles are bundled together by the outermost connective tissue layer called epineurium composed of loose fibrocollagenous tissue forming the anatomically defined nerve cable/trunk. Peripheral nerves are well vascularized by capillaries within the support tissue of the nerve trunk or by vessels that penetrate the nerve from surrounding arteries and veins.

The cellular components of the nervous system are neurons and glial cells. Neurons are the basic structural and functional elements of the nervous system consisting of a cell body (soma or perikaryon) from which axons and dendrites emanate. Dendrites transmit electrical signals to the soma from preceeding neurons and the axon conducts impulses away to the next neuron. Sensory nerve soma cluster into ganglia. Glial cells also referred to as neuroglia include Schwann cells which ensheath axons in the PNS and astrocytes and oligodendrocytes in the CNS. These are support cells that aid the functioning of neurons. A basement membrane called neurilemma envelopes the outer surface of this Schwann cell layer. CNS axons lack the neurilemma but have insulating myelin sheath formed by oligodendrocytes. Similarly, in PNS, the Schwann cells produce myelin which serves to increase the propagation velocity of the nerve impulse. Astrocytes create the blood-brain barrier that barricades the CNS from blood proteins and cells.

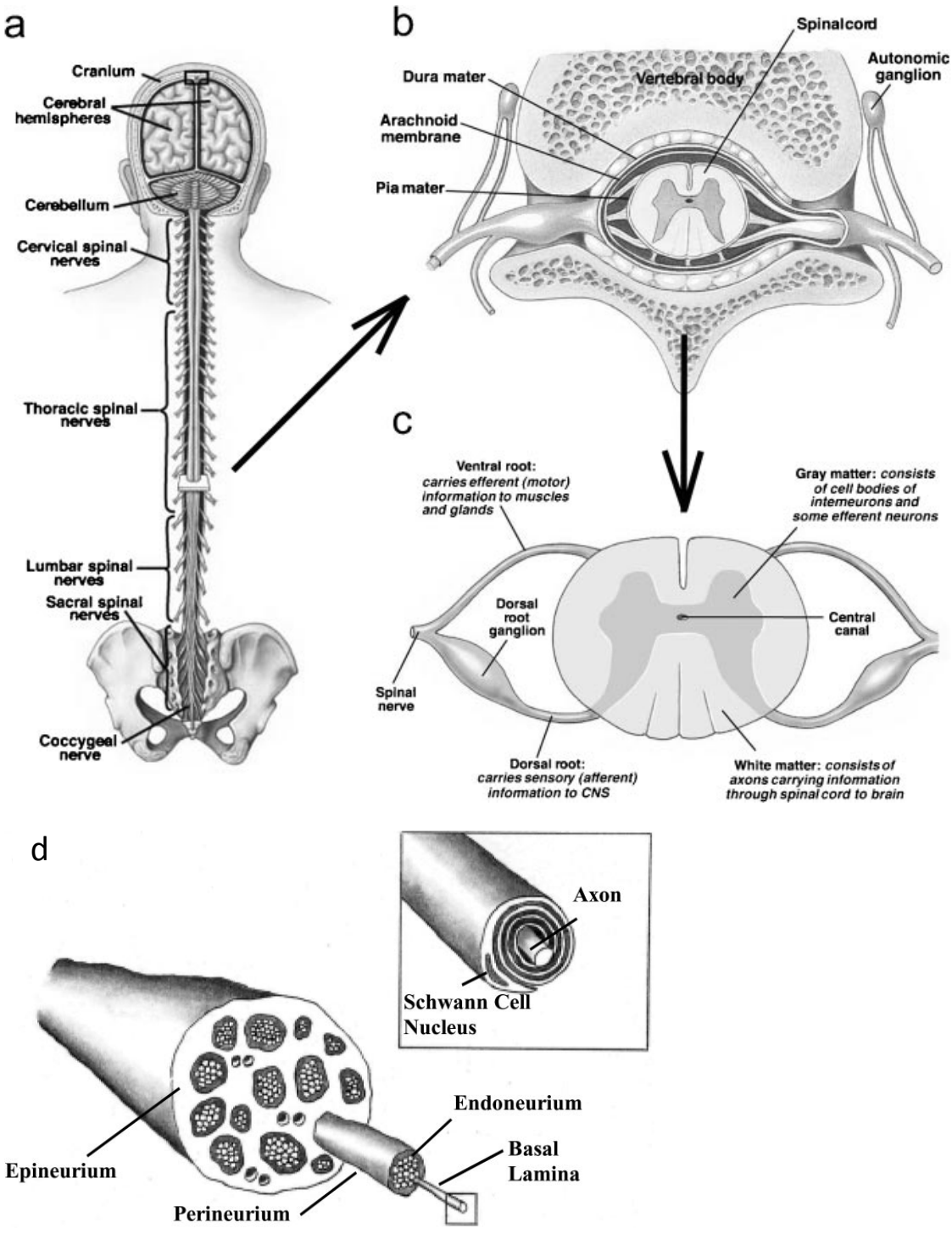


**Fig.1.1** Anatomy overview of the spinal cord (a) The spinal cord anatomy (b,c) Cross-section of the spinal cord showing gray,white matter and neighboring ganglia (d) Connective tissue arrangement of the nerve bundle [8]

## 1.3. **Pathology of nerve injury**:

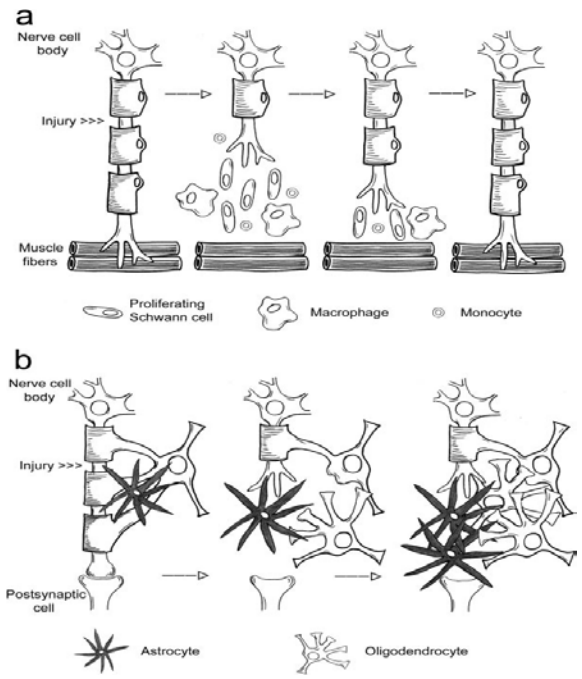


**Fig.1.2.** Responses to axotomy in the (a) PNS and (b) CNS [8, 10].

### 1.3.1. PNS injury:

The most severe PNS injury results in complete nerve transection. Such trauma results in axons being torn away from their cell bodies and eventually degrade; the distal stump of the transected nerve undergoes anterograde degeneration accompanied by disintegration of the cytoskeleton and cell membranes into their molecular constituents and shedding of myelin by the endogenous Schwann cells and PNS glial cells. This degeneration phenomena is referred to as Wallerian degeneration (WD) - a process that occurs before nerve regeneration and can be described as a myelin and neuronal debris cleaning/clearing process that essentially prepares the distal stump for reinnervation [11]. WD commences with axoplasm and axolemma degradation induced by activation of

axonal proteases and calcium influx. The success of regenerative response depends on the sparing of connections between the proximal fiber fascicles and the endoneurium of the severed distal segments. In case of a crush lesion, the continuous endoneurial basal lamina provides guidance for regenerating axons from the proximal nerve stump to the distal end. However in case of axotomy, complete separation of the proximal and distal stumps impedes reinnervation and often leads to the formation of neuroma [12]. At the transection site, Schwann cells (SCs) infiltrate to clear the myelin and neuronal debris by phagocytosis. Hematogenous macrophages are recruited by SC induced chemoattraction [12]. Both macrophages and SCs also produce neurotrophin cytokines to enhance axon growth. Schwann cells are involved in ECM production and are a versatile source of trophic factors [13]. After the initial extrusion of myelin sheaths, the Schwann cells having lost contact with the viable axons dedifferentiate and proliferate by mitosis to align within the remnant basal lamina endoneurial tubes to form bands of Büngner, which provides a growth substrate for the growth cone formed at the tip of the severed axon in the proximal nerve stump. This growth cone transduces guidance cues into intracellular signals for neurite extension and orientation extending into the ECM, retracting upon encountering inhibitory molecules or in absence of positive cues [14].

### 1.3.2. CNS injury:

In case of SCI, the spinal cord generally experiences 4 types of forces namely – flexion, extension, rotation and compression. A combination of two of more of these forces may lead to injury that can result in dislocated vertebrae and fractured vertebral bodies. Such injuries lead to concussion, contusion or laceration of the spinal cord. In case of concussion, no transient loss of function resulting in anatomical damage is involved.

However, contusion and laceration injuries involve anatomical damage that lead to permanent deficits [15].

SCI response can be listed into 3 phases upon injury – acute phase, subacute phase and late chronic phase. The acute phase occurs immediately upon injury and is characterized by mechanical damage to neural and other soft tissues, including endothelial cells of the vasculature resulting in hemorrhage, localized edema, and loss of microcirculation by thrombosis and vasospasm. Hemorrhage begins in the highly vascularized gray matter near the central canal and spreads radially to the posterior horns and into the white matter [16]. Over a time course of minutes to weeks the debilitating effects of ischemic cellular death, ionic shifts (formation of free radicals), release of nitric oxide and proteases, and edema continue from the acute phase [17]. The spinal cord parenchyma is invaded by the inflammatory cells. Apoptosis i.e. cell death occurs and involves reactive gliosis that includes the increased expression of glial fibrillary acidic protein (GFAP) and astrocytic proliferation. The subacute phase follows necrosis and is accompanied with inflammatory response due to microglia and astrocyte mediate reactive gliosis along with disruption of the blood-brain barrier which allows blood-borne immune cells from the periphery to infiltrate the spinal cord. Upregulation of cell surface proteins such as major histocompatibility complex (MHC II) on the microglia results in their transformation into macrophages. Reactive astrocytes begin to proliferate within 2 days of injury and accumulate at the lesion site within a week. However, myelin debris cannot be cleared by astrocytes and inflammatory microglia, which is another impediment to regeneration scope in the CNS. Finally, in the late chronic phase, which occurs over a time course of days to years, apoptosis continues, together with scarring, demyelination and cyst formation. The phenomenon of post traumatic cystic cavitation makes the CNS injury more complex and expands the lesion size leading to a scar encapsulated cavity many times the size of the initial wound [18]. A glial scar develops in days to weeks after

the injury, and glial hypertrophy peaks at 2-3 weeks after the injury [19]. Axons in the CNS do not tend to regenerate in their native environment because several glycoproteins as myelin in the native extracellular environment and glial scar are weaved by astrocytes, oligodendrocytes, and microglia which are inhibitory for regeneration and impenetrable. Fibroblasts, monocytes, and macrophages may also be present in the glial scar. Macrophages infiltrate the CNS lesion to remove myelin but this occurs slower than PNS because of the blood-spine barrier restricting macrophage entry into the nerve tissue to just the site of compromised barrier integrity. Absence of SCs in the CNS also results in low cell adhesion molecule (CAMs) expression in the distal end of the injured spinal cord limiting macrophage recruitment. Astrocytes in the CNS proliferate and become “reactive astrocytes,” producing glial scars that inhibit regeneration (Fig.1.2). A phenomenon that can further impede regeneration is progressive cavitation in which after days to weeks, the CNS injury can expand in size leading to a scar encapsulated cavity many times the size of the initial wound. The underlying mechanism is mediated by activated macrophages inducing astrocyte abandonment and migration away from the neuronal processes [18].

### 1.4. Topographic guidance approaches: How to bridge the gap?

In order to bridge the transection gap and bring about functional axon regeneration, the graft should contain growth supporting cues and function as a guiding substrate. Cues appropriate to the axon must be built into scaffolds if they are to provide positive enhancement of neural regeneration. Guidance cues may be diffusible chemicals or surface contact chemicals inherent in the physical structure of the surface. Conventional hydrogel scaffolds are isotropic, providing no directional cues and thus

depend entirely on exogenously delivered neurotrophic factors for directional axon growth. Biomaterials that enhance proliferation of supporting cells should support more satisfactory reinnervation than those that target just the neuron.

Most work done towards nerve regeneration have been towards the PNS, but the concepts can well be translated to the CNS as well. Scaffolds have been designed to reinnervate PNS neurons across nerve gaps which is not the barrier for the CNS injury model. A detailed understanding of the biological/biochemical microenvironment of the bands of Büngner in the PNS injury site needs to be understood and all its properties incorporated into a biointeractive 'intelligent' nerve graft. For instance, one of the properties of the bands of Büngner is the alignment of Schwann cells in the endoneurial tubes; such a cellular alignment can be brought about by controlled topography of the graft. These smart nerve guides should be readily formed into a conduit with desired dimensions, be sterilizable and tear resistant; withstand handling and suturing, withstand patient movements throughout tissue regeneration period, be biodegradable, pliable, semipermeable and porous; have ability to deliver bioactive factors and incorporate support cells, lend protection from inhibitory molecules, stimulate remyelination, be internally oriented to support cell migration and resist collapse during implantation (Fig.1.3). Biodegradable scaffold obviates the need for a second surgery to remove the implant. A polymer foam with high porosity allows higher cell attachment due to higher surface area and also determines the diffusion of different biomolecules as growth promoters or inhibitors.

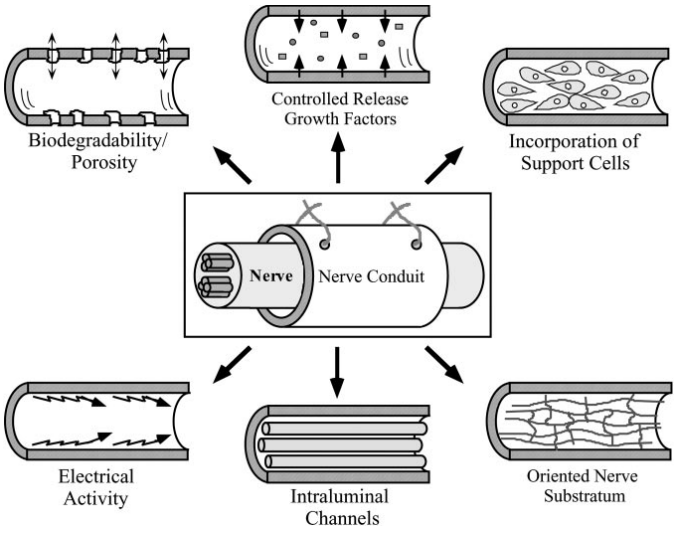


**Fig.1.3.** Properties of the ideal nerve guidance channel [20]

In the case of PNS, the degree of reinnervation with such external support is also dependent upon the length of the gap, shorter gaps as 1-4 mm being relatively easier to repair than larger gaps (>10mm) which may require extensive exogenous support for the regenerating fibers to cross and reconnect. An ideal growth substrate should have all such guidance cues as ECM protein, growth factors and support cells distributed preferably anisotropically in 3D to maximize availability to the growing fibers [21]. For short nerve gaps (< 5 mm), the severed ends can be sutured by coaptation as long as no tension is created at the injury site. For larger gaps, autologous grafts (typically the sural nerve at the back of the leg) have been termed as the ‘gold standard’ for nerve grafts because of their superior nerve regeneration potential as compared to any other alternative. However, limitations include morbidity at the donor site, constraints on the amount of donor nerve at site of harvest, requirement of dual surgeries, size and fasciculation mismatch between the two sites, limited functional recovery, and possible formation of painful neuromas [22]. The rate of success needs to be improved by tissue engineering intervention to increase the intrinsic regenerative capability while also suppressing the effect of extrinsic barriers to regeneration.

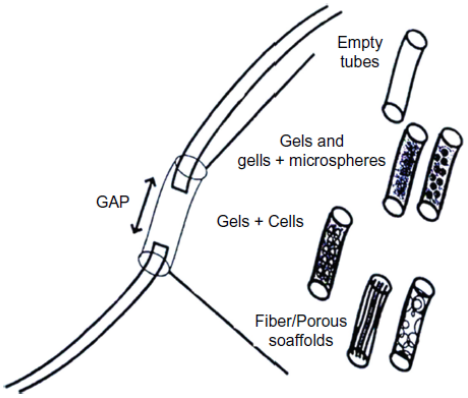


**Fig.1.4.** Tubes or guide types for peripheral nerve repair [23]

Nerve guidance conduits (NGCs) is the clinically approved alternative for autograft repair in PNS injury model. These conduits have the advantages of limited myofibroblast infiltration, reduced neuroma and scar formation, reduced collateral sprouting and no donor site morbidity; ultimately being able to guide regenerating neurons from the proximal to the distal target [24]. However, the use of these hollow NGCs is currently limited to a nerve gap of 4 cm [25]. Inadequate regeneration in the hollow NGC is attributed to the impeded formation of ECM components during the initial stages of regeneration which involves the formation of the fibrin cable through the lumens of the NGCs [26]. Without the formation of the ECM bridge, the formation of glial bands of Bungner is limited. The approach to guide the nerves through the NGCs is to pack microfilament fibers through the lumens, however, this approach requires advanced processing techniques. The use of aligned polymeric nanofibers by itself is a feasible alternative to the use intraluminal fibers/filaments. A critical nerve gap of 17 mm was successfully bridged by aligned electrospun thin films made of poly (acrylonitrile-co-methylacrylate; PAN-MA) [27]. These aligned fibers with diameter 400-600 nm, showed significantly higher nerve regeneration compared to unaligned films.

### 1.4.1. Autologous non-nerve grafts-

Tissues harvested from the patient are immunologically compatible and composed of natural, non-toxic materials with optimal donor-host integration characteristics and oriented micro-structure. Blood vessels [28], skeletal muscle [29], epineurial sheaths [30], tendons [31] have been used as autologous nerve grafts. Combination of vein-skeletal muscle graft was also tried [32]. Autologous venous nerve conduit (AVNC) in combination with autologous SCs and Matrigel showed good axonal growth over a transection of 6 cm [33]. The limitations of such biological tissues include need of dual surgeries, tissue reactions, early fibrosis, scar infiltration and lack of precise control of the conduit's mechanical properties.

### 1.4.2. Non-autologous non-nerve grafts-

Allogenic and xenogeneic sources of nerve grafts are widely available. The limitations include requirement of pre-treatment of such grafts to prevent any immune response, inflammation or disease transmission to the patient. Various decellularization techniques as freeze thawing, detergent treatment and irradiation are used to render the graft sterile and non-immunogenic.

### 1.4.3. Biologically derived polymers-

Naturally occurring polymers as collagen, fibrin, Matrigel, fibronectin, alginate, silk have been explored. Polysialic acid (PSA) is a relatively new biocompatible and bioresorbable material for artificial nerve conduits which is involved in steering processes like neuritogenesis, axonal path finding, and neuroblast migration [34]. Natural polymers are an obvious choice as nerve scaffolds due to their inherent cell binding sites and biocompatibility but design considerations such as poor mechanical properties, batch to

batch variability and their propensity to swell is problematic in the widespread use of such materials.

### 1.4.4. Synthetic polymers-

Synthetic polymers are widely researched for nerve implants owing to their ability to be tailored in terms of mechanical properties such as strength and degradability. They do not possess any biological recognition sites and serve as a blank slate, therefore require the integration/conjugation of biomolecules. Various such polymers include silicone, polyesters (such as PLA, PLGA, PGA, PHB, PCL), polyphosphoesters [as Poly (bis (hydrozyethyl) terephthalate-ethyl phosphoester/terephthaloyl chloride)), Poly (caprolactone-co-ethyl ethylene phosphate)], PNiPAAm, PAN-MA, polyurethane, polyorganophosphazene and methacrylate based hydrogels (PHEMA). Polymers with electrical activity as polypyrroles (Ppy) have also been explored to induce nerve repair by electrical stimulation, one such instance being immobilizing NGF to Ppy to bring about additive effect of electrical and chemical stimuli for nerve repair [35]. Nonbiodegradable synthetic polymers as silicone, pHEMA are less preferred because of their need to be removed or their inability to be removed after regeneration has taken place.

**Contact Guidance:**

Neurons are highly responsive to natural cues in the surrounding microenvironment. This behavior is very prominent during growth and development and during regeneration as well. A regenerating axon is dependent on guidance provided by physical topography and the chemistry of the scaffold surface in addition to biochemical signaling molecules in the microenvironment. Since regeneration is a response to physical, chemical and biochemical support in the axon's milieu, the tissue engineering

strategy for CNS injury repair is to recreate the environmental cues in a way induce neural growth [36-38]. The ability of cells to respond to topographical features have been shown widely [39-42]. “Contact guidance” refers to the phenomenon where a cell is polarized along the length axis of a topographical feature [43].

The appropriate geometry and size that can influence cellular behavior is being considered in the purview of topographic guidance. The nature and distribution of topographic cues provided by the bioscaffold will determine the cellular attachment, alignment, migration and proliferation of the cells. During neural tissue development, aligned extracellular matrix (ECM) or glial tracts, guide neural migration and differentiation [44-46]. Inspite of the limited capability of surviving neurons to grow, engineering substrates with specific topographies can guide cell behavior. The mechanisms involved in cellular interaction with the surface of the biomaterial substrate are complex but involve cell membrane receptors sensing the topographical details of dimensions, texture and stiffness and in the case of neurons that results in neuronal extension. The filopodial extensions which are actually a result of organization of the neuronal cytoskeleton, emanating from the growth cone continuously feel the surface and advance or retract depending upon the physical and chemical cues in their microenvironment. The dimensions of the scaffold can determine the constraints on the growth cone cytoskeletal organization. This behavior has been studied widely by many groups wherein neurons have been seeded on photolithographically patterned surface of grooves and ridges of various dimensions. A different body of topography related work has been done with electrospun fibers. Both these bodies of work will be elucidated further in the next two sections.

### 1.4.4.1. Topographic guidance using photolithographic anisotropic grooved features

Topographic structures such as grooves and ridges were found to influence the direction of axonal growth when these structures were of size in the order of microns. Various groups have worked on creating structures of grooves and ridges by photolithography or reactive ion etching on silicon or PDMS and studied the effect of dimensional features on guidance of neurites (Fig.1.5).

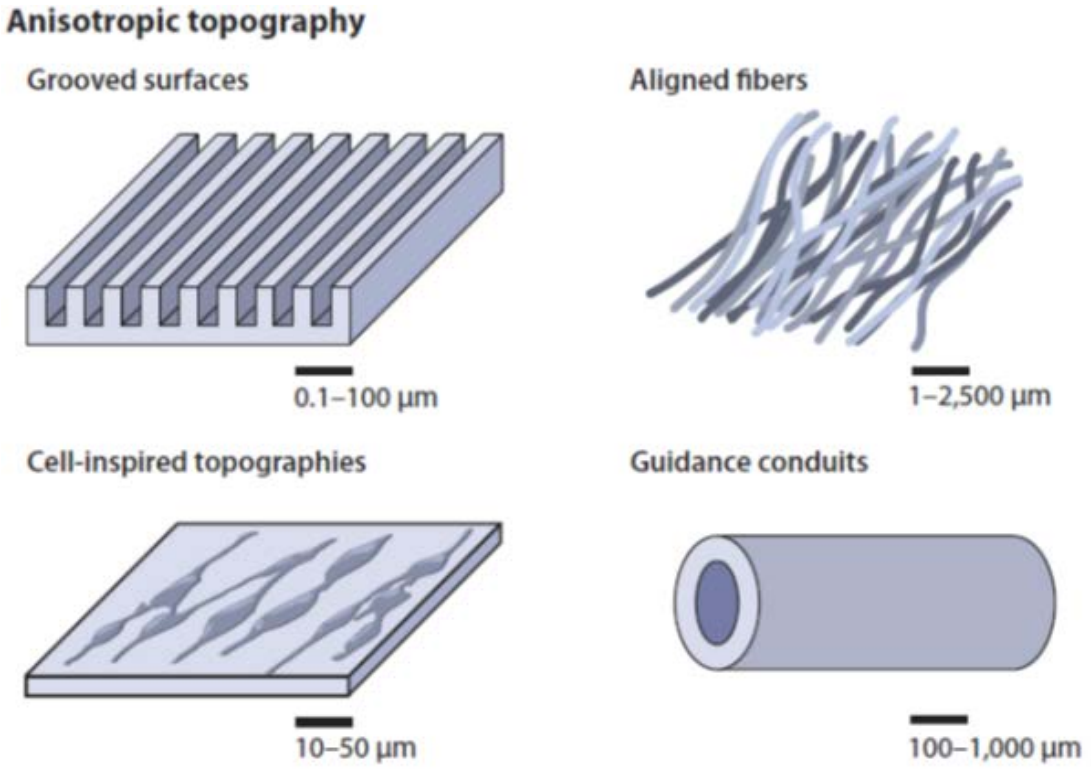


**Fig.1.5.** Topographies presented to neurons in vitro [47].

Axons can be guided by nanosized patterns (grooves and ridges) down to 100nm on a polymer material; their growth is observed on ridges in the pattern rather than in grooves, although groove width affected guidance [48]. Hippocampal neurites were shown

to grow perpendicular to narrow and shallow grooves (130 nm deep and 1µm wide) but parallel to wider and deeper grooves (1100 nm deep and 4 µm wide) [49]. The effect of microchannel width and depth was also studied with PC-12 cells wherein it was found that width of 20-30 um was most effective in maintaining neurite direction [50]. In narrow channels, neurites would extend more along the long axis with lower angular orientations i.e. more parallel to the channel. Neurites tend to grow parallel to the channel wall in narrow microchannels, but perpendicular to the channel wall in wider microchannels (40–60 µm), where neurites grow until they reach the channel wall.

An interesting piece of work has shown how neurites from DRGs possess the unusual capability to pull themselves out of grooves (depth 50 um, width 30-200 um) by climbing up the walls and suspending themselves without any underlying solid support, this phenomenon being referred to as 'neurite bridging' (Fig.1.6) [43].

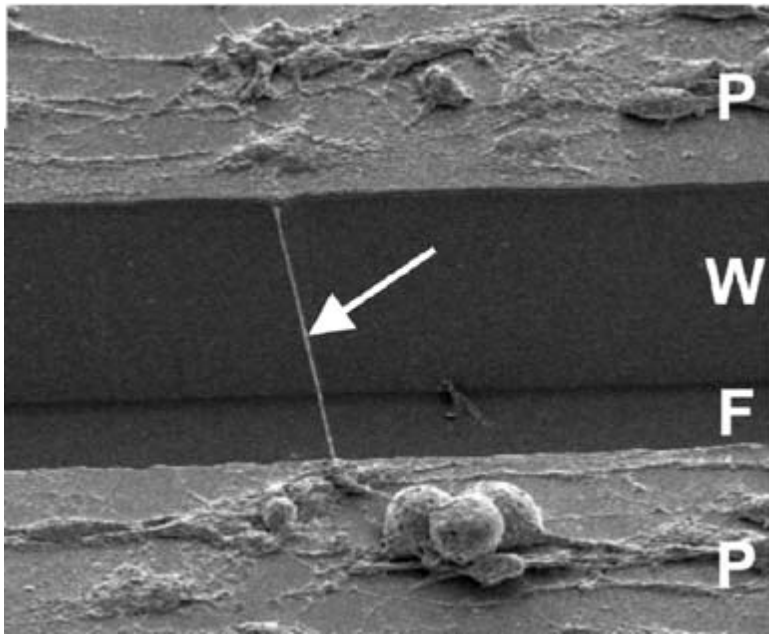


***Fig.1.6.*** Scanning electron micrograph of DRG after 24 h culture on laminin-coated, micropatterned PDMS substrate. A neurite (arrow) bridges between two adjacent plateaus without interacting with the groove wall or groove floor. P, plateau; G, groove; W, groove wall; F, groove floor [43].

In 1987, Clarke et al also showed that topography can indeed influence the mannerism of cell locomotion. Using a groove-ridge system, they showed that at steps, be it grooves or ridge edges, the chick embryonic neural cells would try to make the most cytoskeletally conservative decision [41]. The lamellipodia formed protrusions/filopodia at the edge. This is different for different cells and also depends upon the angle of approach to such an edge. Cells do not extend around external angles at 17 degree greater than horizontal plane due to cytoskeletal inflexibility i.e if the angle to be changed is higher than 17 degree their locomotion in that direction is inhibited. At 10 um steps, almost all cells are stranded or trapped on ridge or grooves. For neurons this limit is 4 um which means that at 4 um steps, they do not step down or up. Even neurons confined in 7 um wide and 2 um deep grooves, failed to cross-over and double back and forth the edges. Frequency of ascent was lower than descent. Thus for neurons 2 um deep grooves is enough to contain them without any crossover. Clark et al followed up this work with some more findings in 1990 [42]. They found that alignment was inversely proportional to spacing and that groove depth proved to be much more important in determining cell alignment, which increased with depth. The outgrowth of neurites appeared unaffected on the 1um patterns, the growth cones having crossed many grooves and ridges. On 2 um deep patterns neurite outgrowth was markedly aligned to groove direction, though crossing over edges did occur. The finding that deeper grooves promoted higher orientation of neurons was corroborated in other works as well [51].

Baranes et al observed that ridges as low in height as 10 nm influenced the manner neurons in which interacted with them. Two main factors in this interaction was the height of the ridge and the angle of approach of the neuron to the ridge [52]. The higher the height and the more the angle of approach of the neuron, the more neuronal processes were affected. From 10-100 nm, the number of such affected processes increased. Neurons

oriented themselves on the ridges and aligned along the axis of the ridge; when encountering edge of the ridge they would send off a bifurcated process.

It has also been shown that an aligned monolayer of astrocytes resulted in aligned growth of DRG neurites atop them [53]. This is because of organized cue (laminin, fibronectin, NCAM, CSPG) production by the astrocytes onto which the neurites grow. DRG neurites were shown to grow on underlying SC layer and follow the SC patterns on PDMS conduits and films in parallel or perpendicular orientations. Neurites were found to extend maximum length on parallel SC tracks and found to turn on perpendicular oriented SC tracks [54]. Britland et al have shown that neurites did not align to 12-100 μm pitch grooves which were less than 1 μm deep [55]. The proportion of aligned neurites increased with groove depth. Cells growing in 12 um wide grooves were more aligned than in wider grooves. Maximum neurite alignment was seen when 6 μm deep, 25 μm wide grooves contained superimposed parallel adhesive tracks. For groove depths less than 1 um, neurites could cross across orthogonally patterned adhesive strips. In similar work by Clarke et al, spiral ganglion neurons (SGNs) were shown to align parallelly along microchannels with ridge periodicity of 50 um and channel depths of 0.6-1um [56]. It was also shown that fibroblasts were unable to align to these microchannels which suggests cell specific responses to topographic cues.

Sorribas et al immobilized cysteine terminated RGDC peptide to patterned chips with grooves and ridges and found that outgrowth along narrow lines of 5 to 15 um RGDC patterns was more frequent than along 25 um lines [57]. Johansson et al nano-imprinted patterns on PMMA consisting of parallel grooves with depths of 300nm and varying widths of 100–400 nm [48]. The distance between two adjacent grooves was 100–1600 nm. They found that nano-imprinted patterns with groove sizes higher than 100nm could be conducive to neurite growth with preference to grow on the ridge edges. No protein was coated on these surfaces but NGF was used in media.

Growth cones were shown to have decision making capability which is a summation of growth permissiveness preference and straightness preference [58]. Neurons prefer to travel straight because it is cytoskeletally most favorable; if needed to change directions, they bend to the least possible angular orientation. In this work, micropatterned substrate was photolithographically fabricated; PDL was coated on the plateaus and the substrate dipped in Matrigel solution (1:10), thus Matrigel would be in the grooves. In case of shallow grooves with 2.5-4.6 microns depth, neurons disregarded such topography and could cross-over with neglect of any topographical variation. For intermediate depth grooves 11-15 micron depth, the percentage of neurons which could disregard topography decreased. With increase in depth of the grooves, the neurons extended on the plateaus and at the ridge could either go left/right/down the ridge or go straight into the matrigel; they preferred going straight into the matrigel than turning 90 deg.

Topography dimensions in the range of 300 nm to 2 um in the form of lines of holes, did not affect neuron adhesion to quartz substrate [59]. % polarization was higher on the line topographies compared to holes and smooth surface. Axon elongation data indicated that both the 300 nm and 2 $\mu$m grooves appeared to catalyze axon growth relative to the smooth surface and the 300 nm holes.

The question that arises at this point is, what goes on at the biochemical level inside the neurites in response to topographical substrates? Using nanoimprint lithography technique, Ferrari et al demonstrated that neurons form focal adhesion contact with the substratum followed by intracellular ROCK1/2-myosin II activity to induce the polarity in the neurite by inducing focal adhesion (FA) maturation [60]. On the substrate, the neurite seeks to form stable FAs, following which cytoskeletal machinery triggers association of actin, vinculin, FAK, paxilin and talin in response to the tension of FA formation with the

substrate. Inhibition of ROCK1/2-Myosin II was found to impair the cell polarity thus proving the hypothesis correct.

#### 1.4.4.2. Topographic guidance using electrospun fibers

Electrospinning is a straightforward, cost-effective and versatile technique earlier used in the textile industry and has recently been used in the medical field for fabricating sheets of fibers at the nanoscale [61]. This technique spins continuous nano-featured scaffolds with large surface area–volume ratio and interconnected porous geometry with spatial orientation. Also, it does not involve heating or chemical reactions during nerve guidance conduit (NGC) synthesis. Thus, a material not stable to heat or chemical reactions can be processed by electrospinning into microfibrous or nanofibrous form. Nanofibrous scaffolds can dimensionally mimic the fibrillar structure of the ECM matrix intricately and their interaction with the growth cone can provide contact guidance cues thereby directing neurite outgrowth. Electrospun scaffolds provide superior cues for the differentiation of neurons and neurite outgrowth owing to their high porosity and large surface area which in turn leads to higher concentrations of adsorbed serum proteins. The porosity influences the diffusion and adhesion of serum proteins and growth factors [14]. Unidirectional aligned scaffolds are more useful in replicating the ECM environment and promote directional contact guidance to a much greater extent than random counterparts. Polymerization of cytoskeletal microtubules causes the traction force to be generated in the direction of protrusion by filopodia and lamellipodia formation. Probably along the direction of alignment, the rate of cytoskeletal polymerization is highest, requires expenditure of least metabolic energy and the signaling between axons is also enhanced [62, 63]. Fiber diameters of electrospun nanofibrous mats approach that of collagen fiber bundles, between 50 and 500 nm. Various factors as inter-fiber distance, fiber diameter, size of cells and the chemical and interfacial properties of the fibers influence the migration

of the cells in the 3D scaffold. The flexibility in controlling fiber size and fiber orientation makes this technique superior to other methods of scaffold formation such as self-assembly, phase separation and solvent casting.

The basic electrospinning setup consists of a spinneret, fiber collector and a high voltage power supply (Fig.1.7). The spinneret is connected to a syringe reservoir containing the working polymer solution to be electrospun. A syringe pump is used to control the feed rate of the solution into the spinneret. Upon application of a high voltage to the spinneret, a pendent droplet of the polymer solution at the tip of the spinneret becomes highly electrified which induces charge accumulation on the surface of the droplet subsequently allowing the droplet to elongate into a conical shape, better known as the Taylor cone. This deformation is caused by two electrostatic forces–electrostatic repulsion between the surface charges of the droplet and Columbic force exerted by the strong external electric field applied. When the applied electric field crosses a threshold value, the electrostatic force overcomes the viscoelastic force and surface tension of the polymer droplet resulting in a finely charged jet forced from the tip of the Taylor cone. This jet then undergoes an unstable stretching and whipping process accompanied by rapid evaporation of the solvent, followed by the formation of a series of ultra-fine dry fibers. These fibers can be collected in the form of an interconnected, nonwoven mat on a grounded metallic target due to the potential difference between the tip and the target. Different types of fiber collectors are available as plate, cylinder, and disc. The alignment of the fiber is rather complicated due to the bending instability of the polymer jet, but it can be attained by tuning the rotational speed of the collector. The fibers are on the order of several nanometers (5 nm to 1 $\mu$m). Varying the applied electric field, polymer molecular weight, polymer concentration, solution flow rate, needle/needle tip size, mandrel speed and spinneret size can manipulate the fiber diameter.

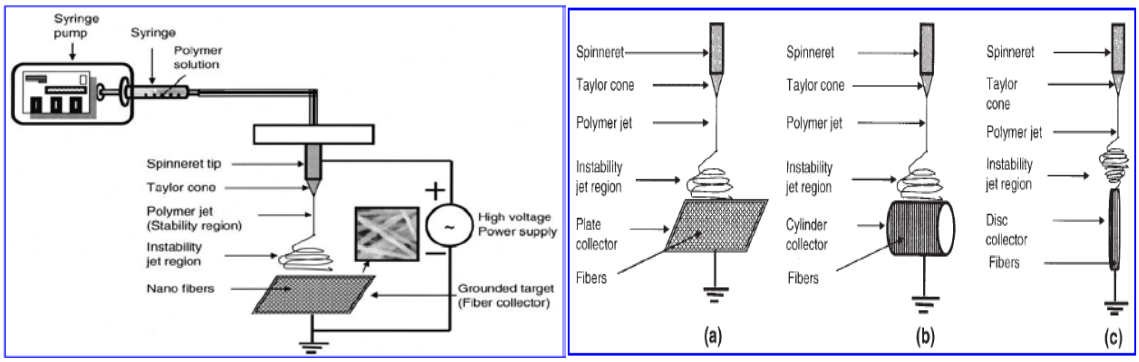


***Fig.1.7.*** *(Left)* Schematic representation of electrospinning apparatus *(Right)* Different types of fiber collectors. **(a)** Plate type; **(b)** cylinder type; **(c)** disc type [61].

Polyesters such as PLLA, PGA and PCL are the most commonly used synthetic, biodegradable, and biocompatible polymers for neural repair. PLGA nanofibrous conduit was successfully able to regenerate nerves across a 10 mm sciatic gap in rats without any exogenous therapeutic agent [64]. Various studies have evaluated these materials as electrospun mats having aligned and/or random fiber orientations. PLLA aligned nanofibers (ANF) having an average diameter of 300 nm were spun at higher mandrel speed while the random counterpart (RNF) having average diameter of 700 nm was formed at lower speed. The average pore size was in the range of 100 nm in width. Neural stem cells (NSCs) were found to align themselves in case of ANFs while no topographical guidance was observed in case of RNFs (Fig.1.8) [65]. The relation of axon diameter appeared to be crucial for axonal guidance. Although alignment is a requirement for the success of such nanofibrous scaffolds, the caveat in the degree of alignment lies in the fact that high and precise alignment can lead to lower inter-fiber distance which may in turn limit the penetration of cells into the scaffold and detrimentally cause the implant to be perceived as a 2D surface with grooves instead of a porous 3D scaffold [14]. The type of neurons also defines the success of such research. For instance, neurites from dorsal root ganglia (DRG) explants growing radially, sharply turned to align themselves when in

contact with fibers aligned at a different angle [63, 66], while cortical neurons cultured on random, nonwoven electrospun PLGA and PLLA scaffolds demonstrated little evidence of contact guidance. Also cortical neurons are more influenced by the fiber density than contact guidance [67]. PCL/PLGA electrospun fibers made into a porous, flexible tube elicited sciatic nerve regeneration across a 10 mm gap without significant inflammation [68]. Collagen IV deposition was found in the lumens along with myelinated axons.

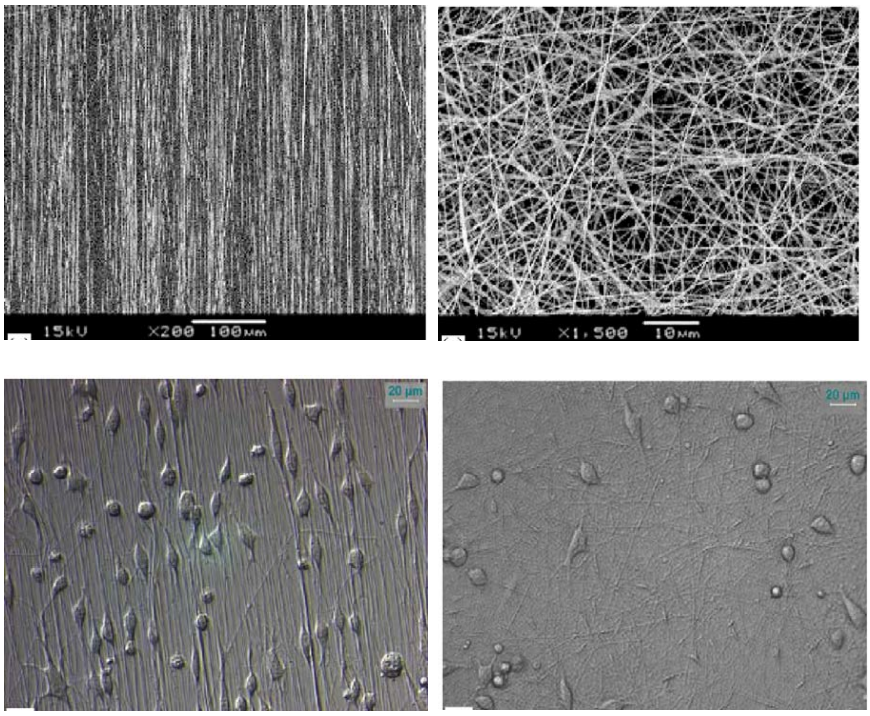


**Fig.1.8.** (Top) SEM micrographs of PLLA (left) ANF (right) RNF; (Bottom) Phase contrast micrographs of NSC growth on (left) ANF (right) RNF [65]

Microfibers of PHBV-PLGA copolymer were electrospun into an aligned mat to serve as an inner core component ensheathed by an outer porous micropatterned PHBV-P(LD)LA-PLGA film [69]. The films were made macroporous by using PEG as a porogen which was leached in water after solvent casting on a PDMS mold (Fig.1.9). Fig.1.9 shows the maximum pore size observed on the patterned film is around 4–5 µm which is smaller

than the size of most neural cells. This pore size of the micropatterned film would allow the nutrients to permeate whilst not allowing the permeation of inflammatory scar tissue cells forcing them to remain outside the tube, while allowing the axons to align and migrate along the axis of the micropatterns on the inner lumen. This work integrated two oriented components – an aligned electrospun fibrous mat (inner core) and a porous micropatterned film (outer enveloping tube) in the same structure to maximize topographic guidance cues for directing growth of axons along the axis of the fibers and grooves of the films emphasizing that the importance of alignment of the cells in regeneration. Apart from the engineered two in one design, a large surface area to volume ratio was being made available to the axonal growth. The outer film rolled around the fibrous core and was formed into a tube by using acrylate based adhesive; a limitation of this approach is the formation of a seam which may break in vivo by stress propagation or can also elicit inflammation response as fibrous capsule.

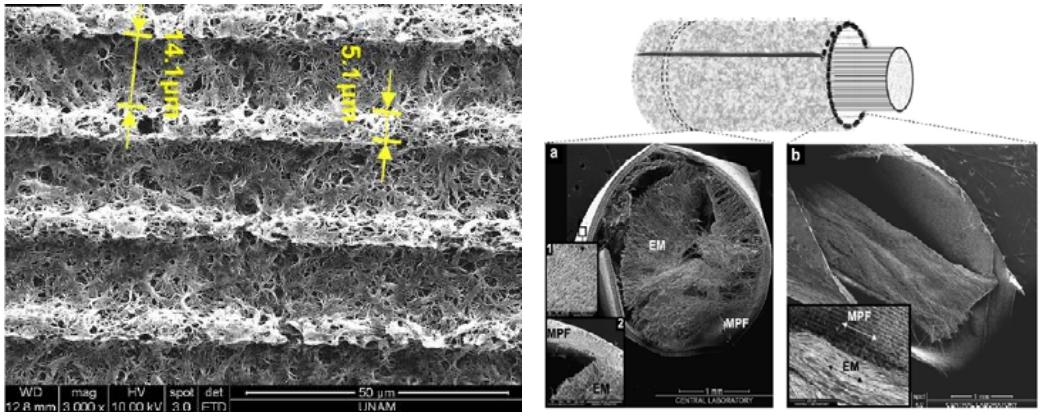


**Fig.1.9.** *(Left)*-Scanning electron micrographs of micropatterned polymeric films obtained from the PDMS replica of the Si template porous micropatterned PHBV–P(L-D,L)LA–PLGA (2:2:1, w/w) film.*(Right)*- Formation of 3D construct and (a–b) various cross sectional views of the construct by SEM (EM: electrospun mat, MPF: porous micropatterned film). Inset 1 of a: SEM image of the exterior surface of the tubular construct. Inset 2 of a & an inset of b: SEM images of certain parts of the constructs at higher magnifications [69].

Synthetic basal lamina fibers made from trichloroacetic acid (TCA) precipitated BD Matrigel™ was electrospun to deposit nonwoven nanofiber mats. The nanorough

topography (average surface roughness of 23 nm) was found to contribute to DRG neurite process growth and allowed Schwann cell movement and clustering [70]. The neurite extension on such electrospun fibers was higher than just coating the Matrigel on coverslip. Although the authors confirmed by SDS-PAGE that the proteins did not degrade upon processing, it may seem that there could be possible denaturation of integrin-recognition motifs when exposed to electric fields and splaying. This technology has been shown to not be detrimental to cell membrane integrity when cellular suspensions in PDMS were electrosprayed and high cell viability recorded thereupon [71] which lays to rest any doubts of denaturation and loss of bioactivity in using electrospinning. More so, blending with synthetic polymers helps maintain the integrity of such chemotactic motifs in biomolecules/biopolymers.

To that end, blended electrospinning can be an efficient technique to introduce a biochemical guidance cue into the nanofibrous scaffold. Laminin was blended in PLLA fibers and found to promote higher PC-12 outgrowth than covalently conjugated and adsorbed groups [72]. Blended electrospinning is a rapid and simple modification technique compared to covalent immobilization and physical adsorption which involve several steps to achieve protein conjugation to the nanofibrous scaffold. In addition, the presence of laminin molecules on the surface and in the interior of the blended nanofibers can provide the necessary signals for cell interaction as the synthetic polymer degrades.

PCL/gelatin (70:30) blend fibers were fabricated wherein incorporation of gelatin enhances the hydrophilicity of PCL scaffold due to amine and carboxyl groups [73]. Higher gelatin content in the blend (50:50) resulted in poor mechanical properties, lower fiber diameter, lower % elongation and pore size since more fibers could overlap with each other. In a separate study by the same group, PCL/collagen electrospun fibers were found to be less effective in SC adhesion and proliferation than plasma treated PCL films [74] although Schnell et al have shown that PCL/collagen electrospun blend fibers are the most

optimum material for nerve regeneration [75]. Surface collagen conjugated electrospun fibers of copolymer of methyl methacrylate (MMA) and acrylic acid (AA) (PMMAAA) promoted neural stem cell viability and neurite length with increasing collagen content [76].

Gupta et al fabricated PCL/gelatin blend nanofibrous scaffold in aligned and random orientations to study the effect on Schwann cell growth, proliferation and alignment [77]. The random scaffold showed higher cell proliferation than the aligned scaffold because of higher porosity, more interconnected pores, and higher roughness in the form of grooves and ridges in the former. However, this result is in stark contrast to other similar research where it is mostly established that aligned fibers demonstrate higher proliferation because of the affinity of the neural cells to arrange themselves in a pattern [66, 78]. This anomaly could probably have been due to low pore size of 1-2 μm or high compactness of the aligned fiber scaffold that impeded Schwann cell migration and proliferation. The hydrophobicity of PCL was decreased upon blending with gelatin and was still able to retain similar tensile strength. The elastic modulus of PCL/gelatin was enhanced compared to PCL which shows better resistance to deformation. Blending of gelatin resulted in integration of amine, hydroxyl and carboxyl peaks into the polymer and made the material hydrophilic. Similar work was also done with PLCL/gelatin blend [PLCL=Poly-l-lactide co ε-Caprolactone] which characterized the mechanical strength of gelatin composite electrospun scaffolds wherein the Young's modulus increased and porosity decreased because of lower fiber diameter [79].

Aligned electrospun PLLA fibers immobilized with Laminin and bFGF via di-Amino-PEG and heparin as linkers showed neurite extension parallel to the fiber alignment compared to random fiber scaffold [62]. The heparin in this case helps protect the bioactivity of the biomolecules. More branching of neurites was observed in the random scaffolds while more axonal directionality was achieved in the aligned form.

Uniaxially aligned poly (acrylonitrile-co-methylacrylate) (PANMA) electrospun fibers stacked in 3D facilitated Schwann cell migration and DRG axonal elongation across a 17 mm nerve gap, similar to Bands of Büngner [80]. The endogenous deposition of ECM protein laminin by the Schwann cells along the direction of alignment was confirmed to support the guidance of the neurite fronts without any exogenous delivery of regenerative agents such as NGF, laminin or cellular implants. In another study on PANMA, aligned nanofiber films were compared with thin solvent casted smooth films to investigate the potential role of differential fibronectin protein adsorption on topography-dependent neural cell responses [81]. Aligned nanofiber films promoted enhanced adsorption of fibronectin compared to smooth films. Fibronectin adsorption mediated the ability of the aligned fiber topographical cue to influence Schwann cell migration and neurite outgrowth such that the cells could align themselves, proliferate and produce their own ECM matrix. However, PAN-MA is non-degradable may cause nerve compression in the long run. A degradable polymer in this regard with rate of degradation and byproducts that do not interfere with the regeneration process and Bands of Bungner formation would be ideal.

It has been demonstrated that it is the increased surface area of aligned fibrous scaffold that results in successful nerve regeneration than contact guidance [82]. PCLEEP fibers were electrospun directly onto PCLEEP film so as to form a tube with fibers at the center in two different orientations- longitudinal and circumferential; both were found to bridge 15 mm sciatic gap with higher numbers of myelinated axons and larger cross-sectional areas as compared with hollow PCLEEP tubes. The fibers when electrospun as PCLEEP/GDNF blends facilitated a more significant recovery as a synergistic effect with high surface area. The introduction of phosphate group to the PCL polymer in this case helped increase the flexibility and degradation rate.

PLCL [copolymer of poly (L-lactide-co-caprolactone)] was electrospun into the luminal region as aligned and onto an outer region as randomly oriented nanofibers into a

one-step nerve conduit synthesis to form a bilayer seamless conduit [83]. This direct electrospinning of bi-layer nanofibrous conduits is a fast process that obviates the otherwise tedious and unreliable option of rolling and sealing sheet [69]. The seamless construction of the bi-layer nanofibrous conduit also presents a smooth and even luminal surface for nerve growth and poses no risk of mechanical failure by stress propagation.

Neurites were shown to extend radially from DRG explants and change direction to align along direction of PLLA fibers [66]. Neurites on highly aligned substrates were longer than neurites on random and intermediate fibers. However, there is a limit to how closely neurites can follow fibers even when the fibers are well aligned because of less space between them. It was also observed that the neurites grew fastest on aligned fibers. Neurite growth slows in cases of random fibers wherein growth cones need to make choices between two paths or materials.

The specificity and accuracy of fiber alignment was enhanced by insulating the area of the needle around the tip to dampen the electrical field around the needle resulting in more fibers being deposited onto the collection disk [84]. PLLA fiber density was enhanced by using this technique and resulted in reduced chances for fiber crossing which can otherwise impede functional recovery by delaying the growth cone in making a directional orientation decision.

Double layers in 3D of varying degrees of PLLA fiber alignment influenced DRG neurite extension where neurites were able to penetrate from the top to the underlying layer and make sharp turns to follow the long-axis of fibers in the underlying layer [63].

Polyamide electrospun nanofibers covalently conjugated with D5 peptide (specific to the alternatively spliced fibronectin type III region of human Tenascin C) were found to elicit neurite outgrowth in vitro and in vivo [85, 86]. The limitation of this scaffold was its random folding during implantation because of which regenerating axons could be impeded and can result in nerve compression. In another study, NGF was covalently

conjugated onto electrospun PCL/PCL-PEG-diamine nanofibrous meshes using ethylenediamine carbodiimide-Hydroxybenzotriazole (EDC/HOBt) chemistry [87].

**1.5. Stem cell differentiation in response to topography**:

Multipotent stem cells can differentiate into the three cell lineages of the CNS-neurons, astrocytes and oligodendrocytes depending upon the environment [88, 89]. In recent years, neurons and glia have been generated successfully from stem cells in culture, fuelling efforts to develop stem-cell-based transplantation therapies for human patients [90]. NSCs are multipotent and self-renewing stem cell populations that are present in both the developing and adult mammalian CNS. NSCs are responsible for generating the neurons and glial cells of the developing brain and for the ability of the adult brain to regenerate after injury/disease [91]. During the early embryonic stages, they exist as neuroepithelial stem cells in the embryonic neural tube. Upon progression of symmetric division, NSCs exist as radial glia cells and begin to generate neuronal lineages by asymmetrically dividing within the germinal ventricular zone (GVZ). NSCs then acquire gliogenic competency and produce glial progenitor cells, which proliferate mostly in a second germinal or subventricular zone (SVZ) as well as the subgranular zone (SGZ), which is positioned between the dentate gyrus and the hilus of the hippocampus. By the postnatal stage, most of the radial glia transforms into astrocytes and the ventricular zone disappears. Some portions of the SVZ remain in adulthood and become host sites for adult neurogenesis [92]. These specific sites are highly significant for CNS tissue engineering. For this approach, there are two methods in which neural stem cells can be used to promote this regeneration. One option could be by activation of the endogenous stem cells or otherwise, by transplantation of neural stem cells [93, 94].

Stem cells can be isolated and transplanted to the diseased brain and spinal cord, either directly or after predifferentiation/genetic modification in culture to form specific types of neuron and glia. Stem cells could provide clinical benefits by neuronal replacement, remyelination and neuroprotection. The possibility of stable expansion and differentiation into neurons make human NSCs an attractive cell source for reconstructive transplantation strategies in CNS trauma and neurodegenerative diseases. NSCs are undifferentiated stem cell populations that are present in both the developing and adult mammalian CNS which can both self-renew and generate the three major cell types that constitute the CNS, i.e. neurons, astrocytes, and oligodendrocytes, a characteristic known as multipotency [91, 94]. NSCs display sensitivity to substrate presentation of topographical cues via changes in cell morphology which transmits biomechanical responses to the nucleus through cytoskeletal linked signaling pathways as Wnt and Shh [95].

ANSCs that were cultured on aligned fibers elongated along the major fiber axis and significantly more number of cells differentiated into the neuronal phenotype as compared to random non-aligned fibers [96]. The aligned fiber substrates promoted neuronal lineage specification of NSCs with an efficiency of 82% within days of seeding on laminin coated nanofibers [97]. With rat hippocampus adult NSCs (rNSCs) an increase of 20% neuronal differentiation was observed on nanofibers compared to tissue culture plastic [98]. With increase in fiber diameter, rat Neural Stem Cells (rNSCs) showed reduced migration, spreading and proliferation in the presence of FGF-2 and serum free medium. Under the differentiation condition (in retinoic acid and FBS), rNSCs spread and assume glial cell shape and preferentially differentiate into oligodendrocytes, whereas they elongate on 749-nm and 1452-nm fibers and preferentially differentiate into neuronal lineage.

Hippocampal progenitor cells differentiated into neurons on Polystyrene-Laminin micropatterned substrates [16x13x4 micron (groove width x groove spacing x groove depth] in individual culture or astrocyte co-culture [99]. On planar non patterned substrates, differentiation into neurites was not observed.

A multi-architectural chip (MARC) containing topographies varying in geometry and dimension was developed to facilitate topography-induced neural differentiation *in vitro* from human embryonic stem cells (hESCs) [100]. The differentiation period was shortened to 7 days as compared to longer time periods required in conventional differentiation methods, to derive a population of 20–25% Tuj1-positive neurons, 10% MAP2-positive oligodendrocytes from hESCs growing on anisotropic gratings (250x250x250 nm grating dimensions) and a population of 25–40% GFAP-positive astrocytes from hESCs growing on the isotropic pillars.

NSCs seeded on laminin-coated aligned polystyrene fibers were shown to induce differentiation into 82% neuronal lineage for cells seeded on the fibers [101]. It was also interestingly observed that neighboring cells in close proximity of few millimeters to the cells differentiated into neurons on fibers also differentiated into 72% neurons, anticipated mostly due to paracrine signaling. As opposed to this phenomenon, the NSCs farther away from the fibers mostly yielded glia (Fig.1.10).

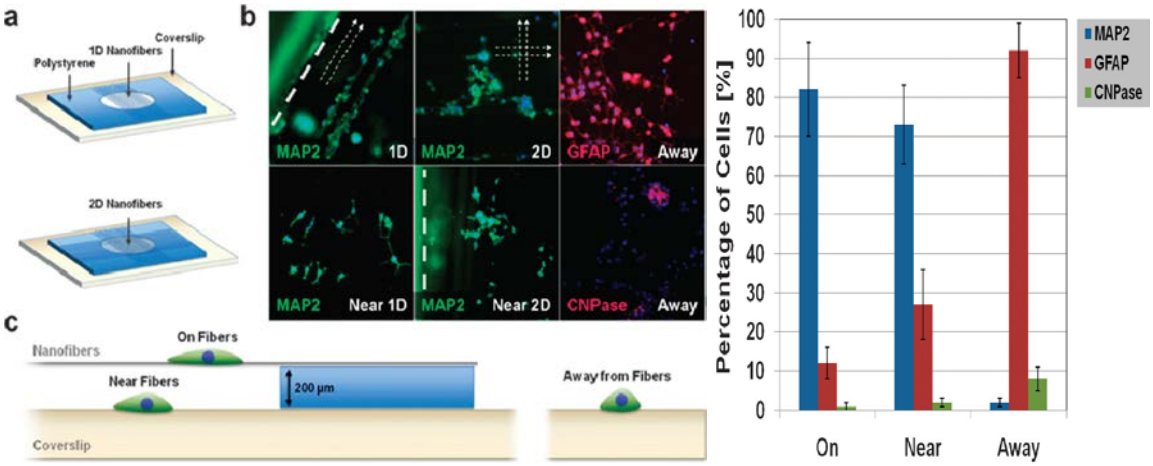


**Fig. 1.10.** *(Left)* Immunofluorescence staining of NSCs seeded on aligned 2D and 1D STEP-aligned, polystyrene fiber meshes. (a) Schematic of used 1D and 2D substrates. (b) Significantly enhanced neuronal differentiation (>80%) by MAP2 staining (green) is seen on both 2D and 1D STEP fiber meshes versus a planar control, on which glial differentiation dominates (red); bold dotted lines indicate substrate edges; arrows indicate directions of fiber alignment (blue: nuclear DAPI stain). (c) Cross-section of the fiber substrate. Not only NSCs seeded on fibers undergo preferred neuronal differentiation but also NSCs directly underneath the fiber mesh, most likely due to paracrine signals from NSCs on fibers, while NSCs on a planar surface far away from fibers undergo mostly glial differentiation [101].
*(Right)* Quantification of immunofluorescence staining (MAP2 for neurons, GFAP for astrocytes, and CNPase for oligodendrocytes) of NSCs on 2D and 1D STEP-aligned polystyrene fiber meshes, and on planar substrates ‘‘near’’ and ‘‘away’’ from cells on fibers.

Adult rat NSCs were found to differentiate into neurons on 749 nm electrospun polyethersulfone fibers; the number of cells differentiated being 20% higher than on polystyrene culture plate control [102]. PLLA electrospun fibers both in micro and nano scales were equally capable of orienting NSCs, although the nanoscale fibers increased neuronal differentiation over the microscale fibers (average diameters 250 nm and 1.25 µm) [65].

Embryonic stem (ES) cells are known to differentiate into neuronal lineage upon formation of embryoid bodies and retinoic acid (RA) induction. However, Xie et al were able to induce neuronal differentiation in ES cells using electrospun aligned fibers without the need for formation of embryoid bodies [103]. Human embryonic stem cells seeded onto the 350-nm ridge/groove pattern arrays differentiated into neuronal lineage after five days, in the absence differentiation-inducing agents [104]. This work is highly encouraging

since it shows that topography alone can induce differentiation of ESCs without the need for embryoid body formation or biochemicals such as RA.

### 1.6. CCP fiber scaffolds for tissue regeneration:

The regeneration of certain tissues as tendons, ligaments, nerves and muscles, require cell alignment along one or more axes for optimum functioning. For myocardial tissue to function effectively by contraction signal transmission over long distances, cardiomyocytes are organized into parallel cardiac muscle fibers with intracellular contractile myofibrils oriented parallel to the long axis of each cell [105]. For load bearing tissues as tendons and ligaments, axial alignment of cells and fibers is important. Nerve tissue engineering focuses on alignment of neurons in a direction from proximal to distal end across the injury gap for nerve regeneration processes [106, 107]. The alignment and topographically controlled orientation of neurons on anisotropic groove and ridge features has been widely explored. However, these anisotropic structures are not translatable to clinical applications wherein 3-dimensional arrangement of cells in an implantable scaffold is required.

A unique design of polymer fibers called capillary-channeled polymer (CCP) fibers has been fabricated for aligned tissue engineering applications in 3D. These fibers have eight deep grooves (or channels) running continuously along their longitudinal axis in its cross-section- 2 major and 6 minor (Fig.12). This unique geometry enhances the surface area for ligand presentation and cell adhesion by more than two-fold when compared to round fibers of comparable dpf (denier per filament) [108, 109]. Lu et al prepared CCP fibers from two polymers, poly(L-lactic acid) (PLA) and poly(ethylene terephthalate) (PET) and seeded them with two cell types- rat skin fibroblasts (RSFs) and rat aortic smooth

muscle cells (RASMCs) to assess the cell alignment capability [110]. Both cell types were found to attach and extend their cytoplasmic lamellipodia in addition to proliferating and depositing ECM proteins as laminin and collagen within the grooves. RASMCs and RSFs showed highly aligned actin and vimentin cytoskeleton, respectively.

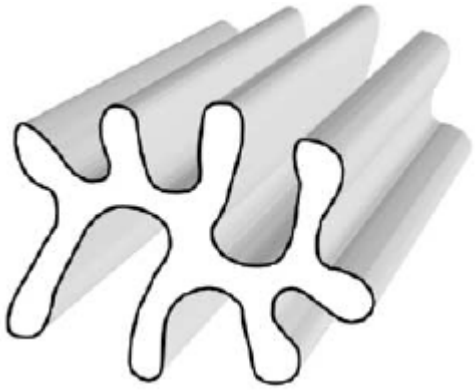

**Fig.1.11.** Cross-sectional view of CCP fibers [110]

In another study, CCP fibers prepared by melt extrusion were cultured with normal human dermal fibroblasts (NHDF) and compared versus round fiber controls [108, 109]. They demonstrated that the cells aligned better along the grooves of the CCP fiber than the round cross-section counterpart in addition to aligned collagen deposition along the grooves. The authors found this work promising towards regeneration of highly-organized cellular structures such as the anterior cruciate ligament (ACL) of the knee.

**2. Role of Cell adhesion molecules (CAMs) in nervous system:**

The nervous system is a highly organized orchestra of cell migration, differentiation, survival and connection between neurons and their postsynaptic targets [111]. During early development of the nervous system, neurons seek synapse formation

by axon elongation and cell-cell adhesion. A crucial step during tissue morphogenesis is the ability of cells to contact tightly and interact specifically with other cells. The architecture of tissues is determined mainly by various cell adhesion mechanisms that bind cells together along with their connections to the internal cytoskeleton. The neurons polarize and formation of synaptic connections results in formation of an ordered nervous tissue. After the developmental processes stop, synaptic contacts still remain viable. In adults, the various stages of evolving plasticity include learning, memory consolidation, and neuronal regeneration. This requires that the nervous system have structural flexibility to enable contact-mediated attraction or repulsion of neuron-neuron or neuron-glia contacts.

Such processes are mediated by membrane proteins called cell adhesion molecules (CAMs). Some of the key processes involving CAMs include formation of neural tube and neural crest, neuron and glia migration, axonal outgrowth and guidance, stabilization of synapses and plasticity, selection of targets, myelination and nerve regeneration post-injury [112].

Cell adhesion molecules (CAMs) play a critical role in cell-cell adhesion and cell-ECM interaction in both developing and maturing nervous system. SCI perturbs the stable state of the tissue environment and requires the interplay of CAMs and neurotrophins both inhibitory and growth promoting to bring about the neuronal outgrowth across the lesion. CAMs should act not only as adhesion molecules at the extracellular level but also as signal transduction molecules at the intracellular level. Most CAMs identified belong to either of 3 different families- Immunoglobulin superfamily (Ig), integrins, and cadherins [113]. Integrins are heterodimeric cell-surface receptors that induce axonal elongation in neurons by binding to ECM molecules such as laminin, fibronectin and tenascin and also to Ig superfamily molecules to promote cell-cell adhesion. Cadherins are Ca2+ dependent

homophilic CAMs that bring about morphogenesis in both neuronal and non-neuronal systems. Ig superfamily is the largest family of proteins, as NCAM, L1CAM, TAG-1, Myelin associated glycoprotein (MAG) and P0. We will focus on L1CAM and its role in neuronal outgrowth, growth cone motility and signal transduction in order to consider its integration in a neural engineered scaffold.

### 2.1. Role of L1-CAM in axonal growth:

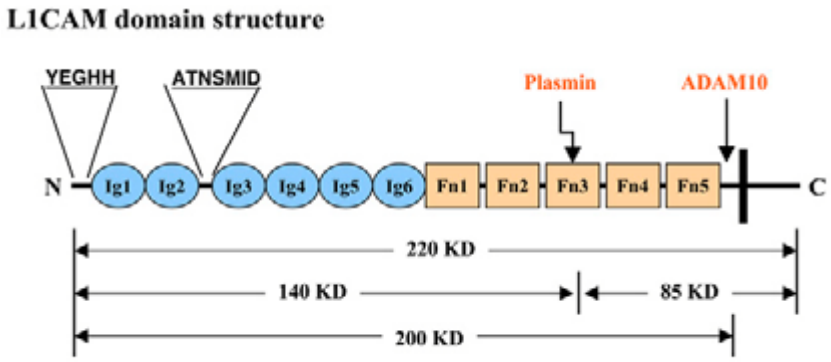


**Fig.1.12.** Schematic of L1-CAM [114]

L1CAM is a neuronal cell adhesion molecule (CAM) that belongs to the immunoglobulin (Ig) superfamily that is conducive to CNS development in humans. It mediates CNS maturation, by means of neurite outgrowth, adhesion, fasciculation, migration, survival, myelination, axon guidance, synaptic plasticity and regeneration after trauma [114, 115]. It is mainly expressed on neurons possessing strong regenerative capability such as retinal ganglional cells (RGCs), dorsal root ganglion (DRGs) and neurons in the thalamic reticular nucleus [116]. L1 exhibits homophilic interactions i.e. can functionally interact with one another and heterophilic binding with other CAMs, signaling

receptors, and extracellular matrix proteins. High levels of L1 are expressed by regenerating neurons during development and after SCI and there is a positive correlation between their expression and axonal growth, the expression levels being low during maturation. Recently, Schwann cells have been engineered to express L1 to promote myelination and motor recovery after SCI. Herein we discuss the L1 mechanism in growth cones- highly specialized membranous extension at the distal tip of growing axons which act as sensory structures that interact with localized cues in the environment to produce the directed growth of axons toward their appropriate targets [117].

L1CAM molecule is made up of 6 Ig domains and 5 fibronectin domains (Fig.1.12). The extracellular domain binds to at least 8 distinct molecules. Interaction with these molecules could either be cis or trans depending on whether the interaction is on the same cell membrane or on different cell membranes respectively.

Depending upon the extracellular conformation of L1CAM, binding could be modular or cooperative. The extracellular chain could either be horseshoe shaped or extended linear as shown in Fig.1.13. Modular binding takes place in the extended linear form of L1 where single domain of L1 binds to specific molecule. For instance, Ig6 domain binds to integrins and Ig1 binds to neurocan/NP-1.

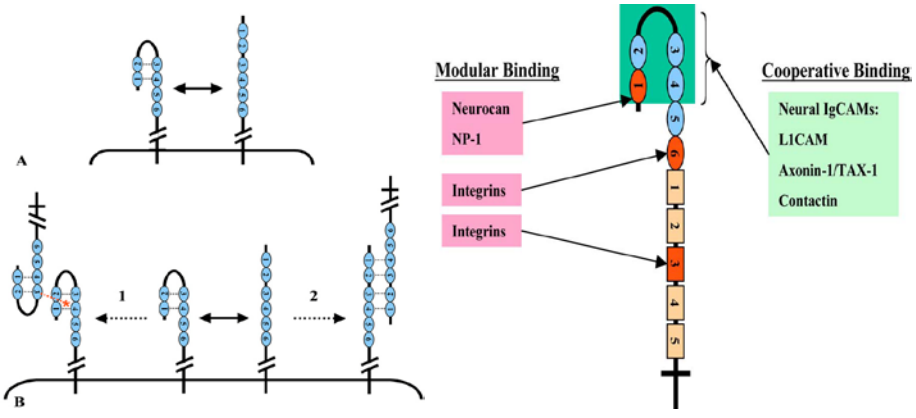


**Fig.1.13.** *Left*- Homophilic binding of L1 in horseshoe or extended forms; *Right*- Modular and cooperative binding of L1 with different molecules [114]

**Inside-out regulation of L1CAM-mediated adhesion:**

The ability of L1 to stimulate neurite growth implies that it can activate second-messenger systems which in turn lead to neuron growth. When cells in suspension medium are dropped over a substrate, the membrane receptors bind non-covalently to the protein ligands adhered to the material surface. When neurons attach, the ligands and receptors diffuse in the plasma membrane and react in the small region of contact. The sequence of events taking place at such region of contact is depicted in Fig.1.14.

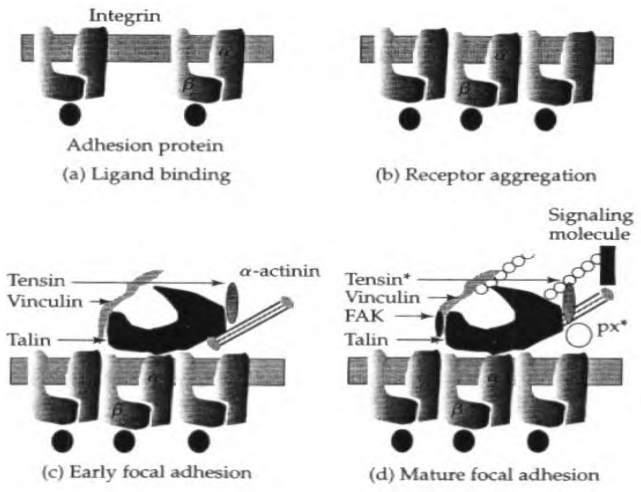


**Fig.1.14.** Sequence of events at region of neuron attachment [118]

Following ligand binding, the receptors aggregate by decrease of inter-receptor distance. The clustered receptors then bind cytoskeletal molecules to their cytoplasmic portions. Subsequently, signal transduction mechanisms as focal adhesion kinase (FAK) binding and tyrosine phosphorylation stimulate the interaction of cytoskeleton and signaling molecules with focal contact proteins. The actin polymerization brings about changes in shape of the cell becoming more oblong and spread out with lamellipodia/filopodia formation.

L1CAM-mediated adhesion can be controlled by at least 4 mechanisms in an outside manner (Fig.1.15) [119]:

1. Lateral oligomerization of L1CAM

2. Internalization and recycling of L1CAM

3. Proteolytic cleavage of L1CAM ectodomain

4. Transcriptional regulation of L1CAM expression

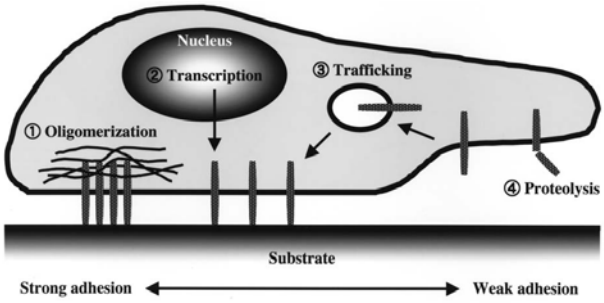


**Fig.1.15.** Four distinct mechanisms involved in the inside-out regulation of IgCAM-mediated adhesion. These four pathways cooperatively regulate cell adhesion both spatially and temporally [119].

Amongst these oligomerization and internalization/recycling are the major mechanisms of the inside-out regulation. Oligomerization of the L1 is mediated by both its cytoplasmic and extracellular domains. The cytoplasmic domain interacts with ankyrin partially mediated by phosphorylation/dephosphorylation of tyrosine kinase and phosphatase (Fig.1.16c). Ankyrin is referred to as a ‘clutch’ molecule which regulates the slippage and restraining forces for neuronal migration/growth. Ankyrin in turn binds to spectrin (Fig. 1.16d). Spectrin in turn binds to actin and initiates actin polymerization to form F-actin. Retrograde flow of F-actin leads to formation of filopodia from the lamellipodia which leads to neuronal migration- desired after SCI.

**Endocytotic L1 trafficking in neuronal growth cones**

The motility of the growth cone depends on cytoskeletal dynamics of F-actin and microtubules located in the peripheral (P) and central (C) domains respectively. Spatially localized actin polymerization/depolymerization and actin-myosin interactions generate a retrograde movement of F-actin, which is a traction force-generating system to move the growth cone in the forward direction. L1 is internalized at the C-domain and centrifugally transported to the P-domain and reinserted into the plasma membrane at the leading edge. Forward translocation of growth cone requires strong adhesion at the leading edge and weak adhesion at the rear (Fig.1.16a).

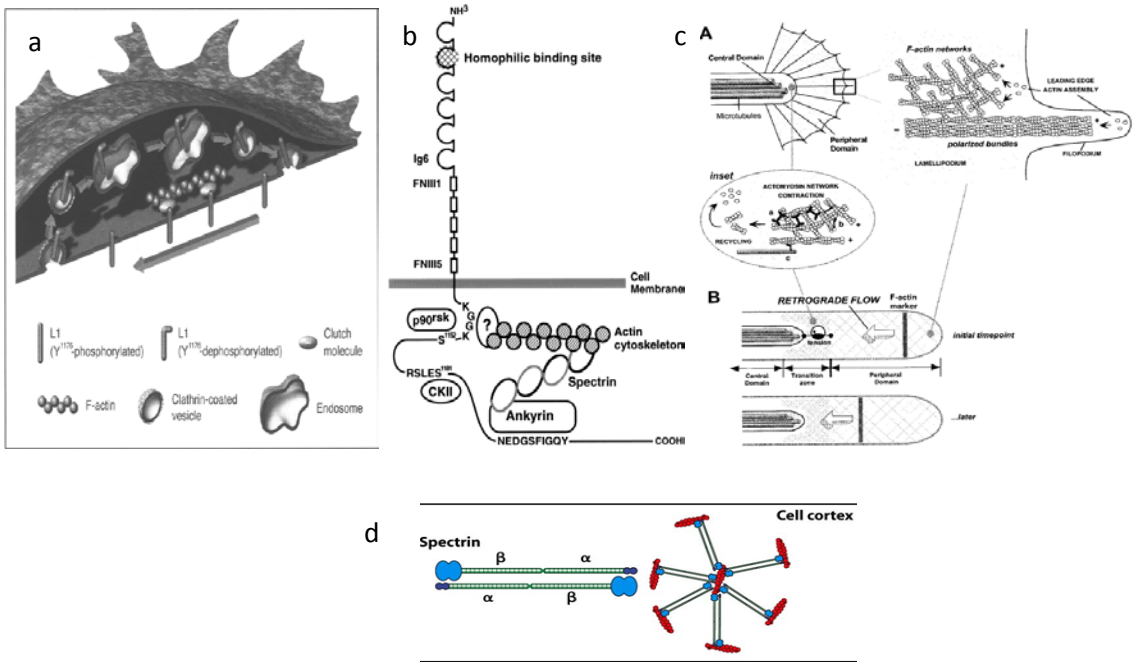


**Fig.1.16.** (a). *Left*- Molecular mechanism of L1-mediated growth cone migration (b). *Middle*- L1 interaction at its cytoplasmic domain with other cytoplasmic proteins (c). *Right*- Cytoskeletal organization and actin dynamics in growth cones. (d). *Bottom*- Schematic of Spectrin which plays a role in actin polymerization by binding to ankyrin [113, 118, 120]

The cytoplasmic domain of L1 has an alternatively spliced RSLE (Arg-Ser-Leu-Glu) sequence expressed only in neurons but not in Schwann cells. This results in a YRSL sequence which matches the tyrosine-based sorting motif Yxxφ where x is any amino acid

and φ is one with a bulky hydrophobic side group. Tyrosine based signals interact with clathrin-associated adaptor AP-2 composed of 4 subunits (α,β1/β2,μ2,σ2), resulting in endocytosis of signal bearing molecules by clathrin coated vesicles. Clathrin is triskelion in shape which coats outside of the protein, forms hexagonal shape on the network. AP-2 complex is a protein that interacts with both clathrin, as well as sorting signals in the cargo proteins.

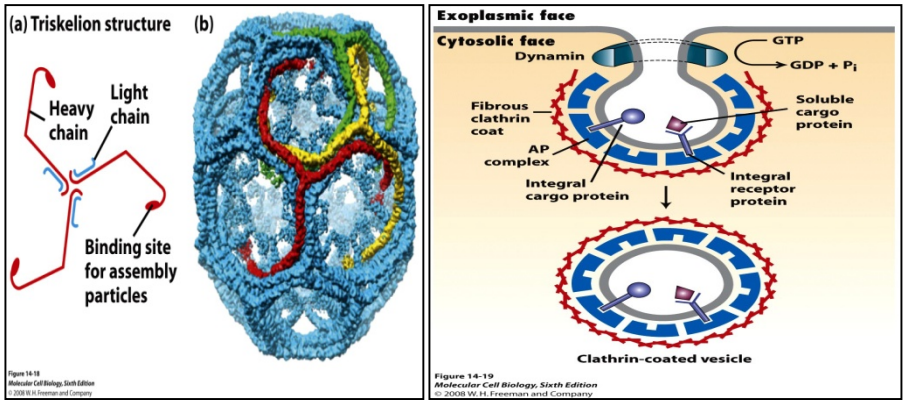


**Fig.1.17.** *Left*- Clathrin triskelion structure; *Right*- Model of dynamin-mediated pinching off clathrin/AP-coated vesicles [119]

A cytosolic protein dynamin is essential for the membrane fission event which results in formation of clathrin coated vesicles. After a vesicle bud forms, dynamin polymerizes over the neck (Fig.1.17). Dynamin-catalyzed hydrolysis of GTP provides energy for release of the vesicle from the donor membrane. The membrane proteins in the donor membrane are incorporated into vesicles by interacting with AP complexes in the coat. Src is implicated in the clathrin-mediated endocytosis via the phosphorylation of clathrin and dynamin. L1 endocytosis is triggered by $Y^{1176}$ dephosphorylation. Src on the one hand induces L1 endocytosis by phosphorylating clathrin at C-domain by dephosphorylating $Y^{1176}$ and also prevents L1 endocytosis at the P-domain by phosphorylating $Y^{1176}$, this role leads to the creation of weaker and stronger adhesion respectively.

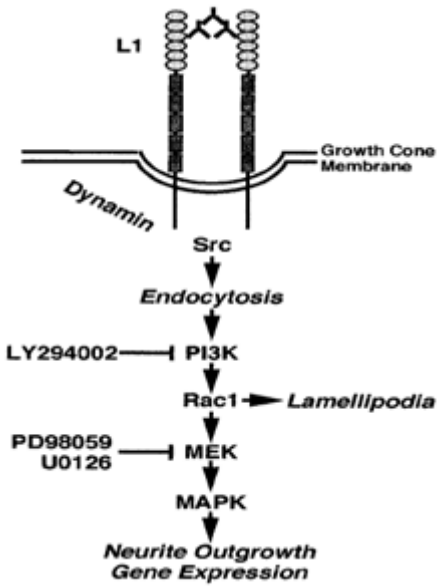


**Fig. 1.18.** Proposed L1-signaling pathway [121]

Cross-linking of L1 molecules on the growth cone membrane is proposed to induce dynamin-mediated endocytosis of L1 via the Src tyrosine kinase, leading to initiation of an intracellular signal transduction cascade involving the sequential activation of PI3-kinase, Rac, MEK, and mitogen-activated protein kinase (MAPK). It is suggested that Rac activation in the growth cone causes cytoskeletal changes resulting in lamellipodia and that MAPK may have nuclear effects on gene expression, both of which may be needed for neurite outgrowth (Fig.1.18).

**Conclusion:**

Topographic cues influence various cell types such as neurons and glia. But such cues work in conjunction with biochemical cues by providing desired directional and biological response as well. A synergism of physical and trophic support is required to design a biomaterial scaffold to achieve functional regeneration in CNS related pathologies. A vast

plethora of therapeutic modules can be integrated with biomaterials to devise the ‘silver magic’ bullet that can heal injuries to the CNS. While entubulation and intraluminal strategies have failed because of issues of collapse, fabrication difficulty respectively, the approach of fiber-based scaffolds has gained more recognition and promise because of higher stability, higher surface area and higher match to the natural environmental ECM niche. This dissertation work in the initial stages focused on development of acellular synthetic biomaterial-based bridges for directional guidance growth of primary neurons. This acellular scaffold was developed by integration of a novel biochemical cue L1-CAM with the unique groovy topography of CCP fibers for neurite guidance. In later stages, an injectable defect conforming cell laden microcarrier biomaterial was developed. The microcarrier approach is aimed towards a stem cell based scaffold which can act as a cell proliferation platform and also as a differentiation inducing platform to replenish cell loss in CNS related injuries and diseases.

**Dissertation arrangement**

The following manuscript is arranged in chapters that highlight individual studies that relate to the overall aims of the project. Chapter 2 enlists the aims, rationale and novelty of this dissertation work. Chapter 3 focuses on highlighting CCP fibers as probable scaffold for guided CNS tissue regeneration. In Chapter 4, a model niche has been developed with fibroblasts in a composite hydrogel based on polyethelene glycol (PEG), Hyaluronic acid, peptide GRGDS and CCP staples. In Chapter 5, we are using NSCs within the optimized hydrogels described in Chapter 4 for brain regeneration after traumatic injury or neurodegenerative disease models.

## References:


[1] University of Alabama BNSCISCN. Spinal Cord Injury (SCI) Facts and Figures at a Glance. 2014.
[2] McDonald JW, Sadowsky C. Spinal-cord injury. The Lancet 2002;359:417-25.
[3] Faul M, Xu L, Wald MM, Coronado VG. Traumatic brain injury in the United States: emergency department visits, hospitalizations, and deaths. Atlanta (GA): Centers for Disease Control and Prevention. National Center for Injury Prevention and Control 2010;2:1-9.
[4] Walker PA, Aroom KR, Jimenez F, Shah SK, Harting MT, Gill BS, et al. Advances in progenitor cell therapy using scaffolding constructs for central nervous system injury. Stem Cell Reviews and Reports 2009;5:283-300.
[5] Lapchak PA. A critical assessment of edaravone acute ischemic stroke efficacy trials: is edaravone an effective neuroprotective therapy? Expert opinion on pharmacotherapy 2010;11:1753-63.
[6] Di Stefano A, Sozio P, Iannitelli A, Cerasa LS. New drug delivery strategies for improved Parkinson's disease therapy. 2009.
[7] Olanow CW, Kieburtz K, Schapira AH. Why have we failed to achieve neuroprotection in Parkinson's disease? Annals of neurology 2008;64:S101-S10.
[8] Schmidt C, Leach J. N EURAL T ISSUE E NGINEERING: Strategies for Repair and Regeneration. Annual review of biomedical engineering 2003;5:293-347.
[9] C.Guyton A. Textbook of Medical Physiology,11th Edition.
[10] Brück W. The role of macrophages in Wallerian degeneration. Brain pathology 1997;7:741-52.
[11] Mey J, Brook G, Hodde D, Kriebel A. Electrospun Fibers as Substrates for Peripheral Nerve Regeneration. [Without Title] 2011:1-40.
[12] Stoll G, Müller HW. Nerve injury, axonal degeneration and neural regeneration: basic insights. Brain pathology 1999;9:313-25.
[13] Bunge RP. The role of the Schwann cell in trophic support and regeneration. Journal of neurology 1994;242:S19-S21.
[14] Nisbet DR, Forsythe JS, Shen W, Finkelstein DI, Horne MK. Review paper: a review of the cellular response on electrospun nanofibers for tissue engineering. Journal of Biomaterials Applications 2009;24:7.
[15] Schwab ME, Bartholdi D. Degeneration and regeneration of axons in the lesioned spinal cord. Physiological reviews 1996;76:319-70.
[16] Hagg T, Oudega M. Degenerative and spontaneous regenerative processes after spinal cord injury. Journal of neurotrauma 2006;23:263-80.
[17] Ramer LM, Ramer MS, Steeves JD. Setting the stage for functional repair of spinal cord injuries: a cast of thousands. Spinal Cord 2005;43:134-61.
[18] Fitch MT, Doller C, Combs CK, Landreth GE, Silver J. Cellular and Molecular Mechanisms of Glial Scarring and Progressive Cavitation: In Vivo and In VitroAnalysis of Inflammation-Induced Secondary Injury after CNS Trauma. The Journal of neuroscience 1999;19:8182.
[19] Hulsebosch CE. Recent advances in pathophysiology and treatment of spinal cord injury. Advances in physiology education 2002;26:238.
[20] Hudson TW, Evans GRD, Schmidt CE. Engineering strategies for peripheral nerve repair. The Orthopedic clinics of North America 2000;31.
[21] Bellamkonda RV. Peripheral nerve regeneration: an opinion on channels, scaffolds and anisotropy. Biomaterials 2006;27:3515-8.

[22] Lee SK, Wolfe SW. Peripheral nerve injury and repair. Journal of the American Academy of Orthopaedic Surgeons 2000;8:243.
[23] Biazar E, Khorasani MT, Montazeri N. Types of neural guides and using nanotechnology for peripheral nerve reconstruction. International Journal of Nanomedicine;2010.
[24] Lundborg G. A 25-year perspective of peripheral nerve surgery: evolving neuroscientific concepts and clinical significance. The Journal of hand surgery 2000;25:391-414.
[25] de Ruiter GC, Malessy MJ, Yaszemski MJ, Windebank AJ, Spinner RJ. Designing ideal conduits for peripheral nerve repair. Neurosurgical focus 2009;26:E5.
[26] Koh H, Yong T, Teo W, Chan C, Puhaindran M, Tan T, et al. In vivo study of novel nanofibrous intra-luminal guidance channels to promote nerve regeneration. Journal of neural engineering 2010;7:046003.
[27] Kim H, Tator CH, Shoichet MS. Design of Protein-Releasing Chitosan Channels. Biotechnology progress 2008;24:932-7.
[28] Risitano G, Cavallaro G, Merrino T, Coppolino S, Ruggeri F. Clinical results and thoughts on sensory nerve repair by autologous vein graft in emergency hand reconstruction* 1. Chirurgie de la main 2002;21:194-7.
[29] Meek MF, Varejao ASP, Geuna S. Use of skeletal muscle tissue in peripheral nerve repair: Review of the literature. Tissue engineering 2004;10:1027-36.
[30] Karacao lu E, Yüksel F, Peker F, Güler MM. Nerve regeneration through an epineurial sheath: its functional aspect compared with nerve and vein grafts. Microsurgery 2001;21:196-201.
[31] Brandt J, Dahlin LB, Lundborg G. Autologous tendons used as grafts for bridging peripheral nerve defects. Journal of Hand Surgery (British and European Volume) 1999;24:284.
[32] Benedetto GD, Zura G, Mazzucchelli R, Santinelli A, Scarpelli M, Bertani A. Nerve regeneration through a combined autologous conduit (vein plus acellular muscle grafts). Biomaterials 1998;19:173-81.
[33] Strauch B, Rodriguez DM, Diaz J, Yu HL, Kaplan G, Weinstein DE. Autologous Schwann cells drive regeneration through a 6-cm autogenous venous nerve conduit. Journal of reconstructive microsurgery 2001;17:589-95.
[34] Haile Y, Haastert K, Cesnulevicius K, Stummeyer K, Timmer M, Berski S, et al. Culturing of glial and neuronal cells on polysialic acid. Biomaterials 2007;28:1163-73.
[35] Gomez N, Schmidt CE. Nerve growth factor immobilized polypyrrole: Bioactive electrically conducting polymer for enhanced neurite extension. Journal of Biomedical Materials Research Part A 2007;81:135-49.
[36] Newgreen D. Physical influences on neural crest cell migration in avian embryos: contact guidance and spatial restriction. Developmental biology 1989;131:136-48.
[37] Nagata I, Nakatsuji N. Rodent CNS neuroblasts exhibit both perpendicular and parallel contact guidance on the aligned parallel neurite bundle. Development 1991;112:581-90.
[38] Ebendal T, Jacobson C-O. Tissue explants affecting extension and orientation of axons in cultured chick embryo ganglia. Experimental cell research 1977;105:379-87.
[39] Ito Y. Surface micropatterning to regulate cell functions. Biomaterials 1999;20:2333-42.
[40] Curtis A, Wilkinson C. Topographical control of cells. Biomaterials 1997;18:1573-83.
[41] Clark P, Connolly P, Curtis AS, Dow JA, Wilkinson CD. Topographical control of cell behaviour. I. Simple step cues. Development 1987;99:439-48.
[42] Clark P, Connolly P, Curtis AS, Dow JA, Wilkinson CD. Topographical control of cell behaviour: II. Multiple grooved substrata. Development 1990;108:635-44.
[43] Goldner JS, Bruder JM, Li G, Gazzola D, Hoffman-Kim D. Neurite bridging across micropatterned grooves. Biomaterials 2006;27:460-72.

[44] Rakic P. Mode of cell migration to the superficial layers of fetal monkey neocortex. Journal of Comparative Neurology 1972;145:61-83.
[45] O'Rourke NA, Sullivan DP, Kaznowski CE, Jacobs AA, McConnell SK. Tangential migration of neurons in the developing cerebral cortex. Development 1995;121:2165-76.
[46] Nadarajah B, Alifragis P, Wong RO, Parnavelas JG. Ventricle-directed migration in the developing cerebral cortex. Nature neuroscience 2002;5:218-24.
[47] Hoffman-Kim D, Mitchel JA, Bellamkonda RV. Topography, cell response, and nerve regeneration. Annual review of biomedical engineering 2010;12:203.
[48] Johansson F, Carlberg P, Danielsen N, Montelius L, Kanje M. Axonal outgrowth on nano-imprinted patterns. Biomaterials 2006;27:1251-8.
[49] Rajnicek A, Britland S, McCaig C. Contact guidance of CNS neurites on grooved quartz: influence of groove dimensions, neuronal age and cell type. Journal of cell science 1997;110:2905.
[50] Mahoney MJ, Chen RR, Tan J, Mark Saltzman W. The influence of microchannels on neurite growth and architecture. Biomaterials 2005;26:771-8.
[51] Davidson P, Bigerelle M, Bounichane B, Giazzon M, Anselme K. Definition of a simple statistical parameter for the quantification of orientation in two dimensions: Application to cells on grooves of nanometric depths. Acta Biomaterialia 2010;6:2590-8.
[52] Baranes K, Chejanovsky N, Geva N, Sharoni A, Shefi O. Topographic cues of nanoscale height direct neuronal growth pattern. Biotechnology and Bioengineering 2012.
[53] Biran R, Noble MD, Tresco PA. Directed nerve outgrowth is enhanced by engineered glial substrates. Experimental Neurology 2003;184:141-52.
[54] Richardson JA, Rementer CW, Bruder JM, Hoffman-Kim D. Guidance of dorsal root ganglion neurites and Schwann cells by isolated Schwann cell topography on poly (dimethyl siloxane) conduits and films. Journal of neural engineering 2011;8:046015.
[55] Britland S, Perridge C, Denyer M, Morgan H, Curtis A, Wilkinson C. Morphogenetic guidance cues can interact synergistically and hierarchically in steering nerve cell growth. Experimental Biology Online 1997;1:1-15.
[56] Clarke JC, Tuft BW, Clinger JD, Levine R, Figueroa LS, Guymon CA, et al. Micropatterned methacrylate polymers direct spiral ganglion neurite and Schwann cell growth. Hearing research 2011.
[57] Sorribas H, Padeste C, Mezzacasa T, Tiefenauer L, Leder L, Fitzli D, et al. Neurite outgrowth on microstructured surfaces functionalized by a neural adhesion protein. Journal of Materials Science: Materials in Medicine 1999;10:787-91.
[58] Li N, Folch A. Integration of topographical and biochemical cues by axons during growth on microfabricated 3-D substrates. Experimental cell research 2005;311:307-16.
[59] Fozdar DY, Lee JY, Schmidt CE, Chen S. Hippocampal neurons respond uniquely to topographies of various sizes and shapes. Biofabrication 2010;2:035005.
[60] Ferrari A, Cecchini M, Serresi M, Faraci P, Pisignano D, Beltram F. Neuronal polarity selection by topography-induced focal adhesion control. Biomaterials 2010;31:4682-94.
[61] Murugan R, Ramakrishna S. Nano-featured scaffolds for tissue engineering: a review of spinning methodologies. Tissue engineering 2006;12:435-47.
[62] Patel S, Kurpinski K, Quigley R, Gao H, Hsiao BS, Poo MM, et al. Bioactive nanofibers: synergistic effects of nanotopography and chemical signaling on cell guidance. Nano letters 2007;7:2122-8.
[63] Xie J, MacEwan MR, Li X, Sakiyama-Elbert SE, Xia Y. Neurite outgrowth on nanofiber scaffolds with different orders, structures, and surface properties. ACS nano 2009;3:1151-9.

[64] Bini TB, Gao S, Tan TC, Wang S, Lim A, Hai LB, et al. Electrospun poly (L-lactide-co-glycolide) biodegradable polymer nanofibre tubes for peripheral nerve regeneration. Nanotechnology 2004;15:1459.
[65] Yang F, Murugan R, Wang S, Ramakrishna S. Electrospinning of nano/micro scale poly (L-lactic acid) aligned fibers and their potential in neural tissue engineering. Biomaterials 2005;26:2603-10.
[66] Corey JM, Lin DY, Mycek KB, Chen Q, Samuel S, Feldman EL, et al. Aligned electrospun nanofibers specify the direction of dorsal root ganglia neurite growth. 2007.
[67] Nisbet DR, Pattanawong S, Ritchie NE, Shen W, Finkelstein DI, Horne MK, et al. Interaction of embryonic cortical neurons on nanofibrous scaffolds for neural tissue engineering. Journal of neural engineering 2007;4:35.
[68] Panseri S, Cunha C, Lowery J, Del Carro U, Taraballi F, Amadio S, et al. Electrospun micro- and nanofiber tubes for functional nervous regeneration in sciatic nerve transections. BMC biotechnology 2008;8:39.
[69] Yucel D, Kose GT, Hasirci V. Polyester based nerve guidance conduit design. Biomaterials 2010;31:1596-603.
[70] de Guzman RC, Loeb JA, VandeVord PJ. Electrospinning of matrigel to deposit a basal lamina-like nanofiber surface. Journal of Biomaterials Science, Polymer Edition, 21 2010;8:1081-101.
[71] Jayasinghe SN, Townsend-Nicholson A. Stable electric-field driven cone-jetting of concentrated biosuspensions. Lab Chip 2006;6:1086-90.
[72] Koh HS, Yong T, Chan CK, Ramakrishna S. Enhancement of neurite outgrowth using nano-structured scaffolds coupled with laminin. Biomaterials 2008;29:3574-82.
[73] Ghasemi-Mobarakeh L, Prabhakaran MP, Morshed M, Nasr-Esfahani MH, Ramakrishna S. Electrospun poly (-caprolactone)/gelatin nanofibrous scaffolds for nerve tissue engineering. Biomaterials 2008;29:4532-9.
[74] Prabhakaran MP, Venugopal J, Chan CK, Ramakrishna S. Surface modified electrospun nanofibrous scaffolds for nerve tissue engineering. Nanotechnology 2008;19:455102.
[75] Schnell E, Klinkhammer K, Balzer S, Brook G, Klee D, Dalton P, et al. Guidance of glial cell migration and axonal growth on electrospun nanofibers of poly-[epsilon]-caprolactone and a collagen/poly-[epsilon]-caprolactone blend. Biomaterials 2007;28:3012-25.
[76] Li W, Guo Y, Wang H, Shi D, Liang C, Ye Z, et al. Electrospun nanofibers immobilized with collagen for neural stem cells culture. Journal of Materials Science: Materials in Medicine 2008;19:847-54.
[77] Gupta D, Venugopal J, Prabhakaran MP, Dev VR, Low S, Choon AT, et al. Aligned and random nanofibrous substrate for the in vitro culture of Schwann cells for neural tissue engineering. Acta Biomaterialia 2009;5:2560-9.
[78] Subramanian A, Krishnan UM, Sethuraman S. Fabrication of uniaxially aligned 3D electrospun scaffolds for neural regeneration. Biomedical Materials 2011;6:025004.
[79] Lee J, Tae G, Kim YH, Park IS, Kim SH. The effect of gelatin incorporation into electrospun poly (l-lactide-co--caprolactone) fibers on mechanical properties and cytocompatibility. Biomaterials 2008;29:1872-9.
[80] Kim Y, Haftel VK, Kumar S, Bellamkonda RV. The role of aligned polymer fiber-based constructs in the bridging of long peripheral nerve gaps. Biomaterials 2008;29:3117-27.
[81] Mukhatyar VJ, SalmerÃ³n-SÃ¡nchez M, Rudra S, Mukhopadaya S, Barker TH, GarcÃa AJ, et al. Role of fibronectin in topographical guidance of neurite extension on electrospun fibers. Biomaterials 2011.

[82] Chew SY, Mi R, Hoke A, Leong KW. Aligned Protein-Polymer Composite Fibers Enhance Nerve Regeneration: A Potential Tissue Engineering Platform. Advanced functional materials 2007;17:1288-96.
[83] Zhu Y, Wang A, Patel S, Kurpinski K, Diao E, Bao X, et al. Engineering bi-layer nanofibrous conduits for peripheral nerve regeneration. Tissue Engineering Part C: Methods 2011;17:705-15.
[84] Wang HB, Mullins ME, Cregg JM, Hurtado A, Oudega M, Trombley MT, et al. Creation of highly aligned electrospun poly-L-lactic acid fibers for nerve regeneration applications. Journal of neural engineering 2009;6:016001.
[85] Meiners S, Ahmed I, Ponery AS, Amor N, Harris SL, Ayres V, et al. Engineering electrospun nanofibrillar surfaces for spinal cord repair: a discussion. Polymer International 2007;56:1340-8.
[86] Ahmed I, Liu HY, Mamiya PC, Ponery AS, Babu AN, Weik T, et al. Three dimensional nanofibrillar surfaces covalently modified with tenascin-C□derived peptides enhance neuronal growth in vitro. Journal of Biomedical Materials Research Part A 2006;76:851-60.
[87] Cho YI, Choi JS, Jeong SY, Yoo HS. Nerve growth factor (NGF)-conjugated electrospun nanostructures with topographical cues for neuronal differentiation of mesenchymal stem cells. Acta Biomaterialia 2010;6:4725-33.
[88] Chow SY, Moul J, Tobias CA, Himes BT, Liu Y, Obrocka M, et al. Characterization and intraspinal grafting of EGF/bFGF-dependent neurospheres derived from embryonic rat spinal cord. Brain research 2000;874:87-106.
[89] Cao Q, Zhang YP, Howard RM, Walters WM, Tsoulfas P, Whittemore SR. Pluripotent stem cells engrafted into the normal or lesioned adult rat spinal cord are restricted to a glial lineage. Experimental Neurology 2001;167:48-58.
[90] Lindvall O, Kokaia Z. Stem cells for the treatment of neurological disorders. Nature 2006;441:1094-6.
[91] Temple S. The development of neural stem cells. Nature 2001;414:112-7.
[92] Conti L, Cattaneo E. Neural stem cell systems: physiological players or in vitro entities? Nature Reviews Neuroscience 2010;11:176-87.
[93] Okano H, Sawamoto K. Neural stem cells: involvement in adult neurogenesis and CNS repair. Philosophical Transactions of the Royal Society B: Biological Sciences 2008;363:2111-22.
[94] Okano H. Neural stem cells and strategies for the regeneration of the central nervous system. Proceedings of the Japan Academy Series B, Physical and biological sciences 2010;86:438.
[95] Mathai KI, Sudumbraker S, Sahoo P. Stem cell therapy for spinal cord injury: A plea for rationality. The Indian Journal of Neurotrauma 2008;5:7-10.
[96] Lim SH, Liu XY, Song H, Yarema KJ, Mao H-Q. The effect of nanofiber-guided cell alignment on the preferential differentiation of neural stem cells. Biomaterials 2010;31:9031-9.
[97] Bakhru S, Nain AS, Highley C, Wang J, Campbell P, Amon C, et al. Direct and cell signaling-based, geometry-induced neuronal differentiation of neural stem cells. Integrative Biology 2011;3:1207-14.
[98] Christopherson GT, Song H, Mao H-Q. The influence of fiber diameter of electrospun substrates on neural stem cell differentiation and proliferation. Biomaterials 2009;30:556-64.
[99] Recknor JB, Sakaguchi DS, Mallapragada SK. Directed growth and selective differentiation of neural progenitor cells on micropatterned polymer substrates. Biomaterials 2006;27:4098-108.
[100] Ankam S, Suryana M, Chan LY, Kywe Moe AA, Teo BK, Law JB, et al. Substrate topography and size determines the fate of human embryonic stem cells to neuronal or glial lineage. Acta Biomaterialia 2012.

[101] Bakhru S, Nain AS, Highley C, Wang J, Campbell P, Amon C, et al. Direct and cell signaling-based, geometry-induced neuronal differentiation of neural stem cells. Integr Biol 2011;3:1207-14.
[102] Christopherson GT, Song H, Mao HQ. The influence of fiber diameter of electrospun substrates on neural stem cell differentiation and proliferation. Biomaterials 2009;30:556-64.
[103] Xie J, Willerth SM, Li X, Macewan MR, Rader A, Sakiyama-Elbert SE, et al. The differentiation of embryonic stem cells seeded on electrospun nanofibers into neural lineages. Biomaterials 2009;30:354-62.
[104] Lee MR, Kwon KW, Jung H, Kim HN, Suh KY, Kim K, et al. Direct differentiation of human embryonic stem cells into selective neurons on nanoscale ridge/groove pattern arrays. Biomaterials 2010;31:4360-6.
[105] McDevitt TC, Angello JC, Whitney ML, Reinecke H, Hauschka SD, Murry CE, et al. In vitro generation of differentiated cardiac myofibers on micropatterned laminin surfaces. Journal of biomedical materials research 2002;60:472-9.
[106] Recknor JB, Recknor JC, Sakaguchi DS, Mallapragada SK. Oriented astroglial cell growth on micropatterned polystyrene substrates. Biomaterials 2004;25:2753-67.
[107] Miller C, Jeftinija S, Mallapragada S. Micropatterned Schwann cell-seeded biodegradable polymer substrates significantly enhance neurite alignment and outgrowth. Tissue engineering 2001;7:705-15.
[108] Sinclair KD, Webb C, Brown PJ. Capillary channel polymer fibers as structural templates for ligament regeneration. Am Assoc Text Chem Colorists 2008;8:36-40.
[109] Sinclair KD, Webb K, Brown PJ. The effect of various denier capillary channel polymer fibers on the alignment of NHDF cells and type I collagen. Journal of Biomedical Materials Research Part A 2010;95:1194-202.
[110] Lu Q, Simionescu A, Vyavahare N. Novel capillary channel fiber scaffolds for guided tissue engineering. Acta Biomaterialia 2005;1:607-14.
[111] Lee AY. The cell recognition molecule L1 and cognition. Chinese Journal of Physiology 2005;48:169.
[112] Colman D, Filbin M. Cell adhesion molecules. Basic neurochemistry 1999:139-53.
[113] Giannone, G., et al. (2009). "Multi-level molecular clutches in motile cell processes." Trends in cell biology **19**(9): 475-48
[114] Haspel J, Grumet M. The L1CAM extracellular region: a multi-domain protein with modular and cooperative binding modes. Front Biosci 2003;8:s1210-s25.
[115] Maness PF, Schachner M. Neural recognition molecules of the immunoglobulin superfamily: signaling transducers of axon guidance and neuronal migration. Nat Neurosci 2007;10:19-26.
[116] Zhang Y, Yeh J, Richardson P, Bo X. Cell adhesion molecules of the immunoglobulin superfamily in axonal regeneration and neural repair. Restorative Neurology and Neuroscience 2008;26:81-96.
[117] Golas PL, Matyjaszewski K. Click chemistry and ATRP: a beneficial union for the preparation of functional materials. QSAR & Combinatorial Science 2007;26:1116-34.
[118] Truskey, G. A., et al. (2004). Transport phenomena in biological systems, Pearson/Prentice Hall Upper Saddle River NJ
[119] Kamiguchi H. The mechanism of axon growth. Molecular Neurobiology 2003;28:219-27.
[120] Lodish, Molecular Cell Biology, Sixth Edition, W.H.Freeman & Company
[121] Schmid R-S, Pruitt WM, Maness PF. A MAP Kinase-Signaling Pathway Mediates Neurite Outgrowth on L1 and Requires Src-Dependent Endocytosis. J Neurosci 2000;20:4177-88.

# CHAPTER 2

# AIMS AND RATIONALE

The central nervous system (CNS) is vulnerable to a variety of traumatic injuries including spinal cord injury (SCI), traumatic brain injury (TBI), and ischemic stroke; as well as various neurodegenerative diseases such as Parkinson's, Alzheimer's and Huntington's diseases. Due to the limited regenerative capacity of the adult CNS and lack of clinically effective therapies, these conditions commonly result in permanent functional deficits. SCI damages both ascending sensory and descending motor axonal pathways interrupting the transmission of synaptic signals between the brain and peripheral tissues. Although damaged axons attempt an initial regenerative response, this is rapidly aborted due to the presence of growth inhibitory molecules in CNS myelin and the glial scar and intrinsic limitations of adult CNS neuronal biochemistry such as the ability to maintain cAMP levels and upregulate the expression of 'regeneration-associated genes'. On the other hand, TBI, stroke, and Parkinson's disease result in neuronal cell death. The CNS has limited capacity to replace lost neurons because the neurons themselves are terminally differentiated and post-mitotic. Although neural stem cells (NSCs) have been identified in specialized regions of the adult brain such as the sub-ventricular zone (SVZ) and the sub-granular zones (SGZ), their number is insufficient and the pathological environment inadequate to support an effective regenerative response.

The goal of neural tissue engineering is to use combinations of biomaterial scaffolds; adhesive and trophic biomolecules; and in some cases therapeutic cell transplantation to overcome injury- and pathology-induced barriers and deficiencies and promote regeneration and functional recovery. In general, the guiding principle for all approaches has been to attempt to recapitulate a microenvironment more closely

resembling that of the growth-supportive embryonic CNS or adult peripheral nervous system (PNS). Tissue engineering for SCI has focused on delivery of bioactive signals that can both stimulate and direct axonal regeneration. Examples include fabrication of tubular or multi-lumen scaffolds and the provision of bioactivity either through recombinant proteins/genes or transplantation of various stem and glial cell populations. Tissue engineering strategies for large-scale TBI, stroke, and Parkinson's disease have emphasized neuronal cell replacement through stem cell transplantation. One aspect of the developing CNS / adult PNS that has only recent begun to gain widespread attention is the presence and bioactivity of topographic structural microarchitecture. In the developing CNS, primitive radial glia form highly aligned structures that guide pioneering axons, which subsequently provide a pathway for later arriving axonal projections. In addition, recent studies have shown that substrate topography can play an important role in NSC differentiation, most importantly, in terms of increasing differentiation into neurons as opposed to various glial cell types. Thus, topography can offer an important contribution towards strategies for CNS repair aimed towards both axonal regeneration and cell replacement through transplantation and differentiation of NSCs.

Previously, capillary channel polymer (CCP) fibers have been reported that possess micrometer-scale, aligned surface grooves. These fibers have been shown to provide increased surface area and support increased fibroblast alignment relative to traditional fibers with a round cross-section. The overall objective of this dissertation was to investigate the application of CCP fibers to the development of scaffolds for CNS regeneration. In the first study, CCP fibers in combination with the L1 neural cell adhesion molecule were evaluated as a potential scaffold design for long-distance axonal regeneration following SCI. Next, CCP fibers were fabricated into 'staples' 100-200 micrometers in length and investigated as injectable microcarriers using NIH 3T3

fibroblasts as a model cell line. In the final study, the ability of CCP staples to increase neuronal differentiation of NSCs was examined.

The specific aims were as follows:

***Specific Aim 1. To develop acellular fibrous scaffolds for axonal regeneration integrating topographic guidance and trophic bioactivity.***

**Approach**

Specific studies were conducted to evaluate the bioactivity of a cell adhesion molecule L1-CAM and protein laminin for neurite outgrowth on 2D polylactide films and investigate the effect of fiber channel dimensions on neurite orientation and extension.

**Novelty & Innovation**

A novel acellular scaffold was devised by integration of cell adhesion molecule L1-CAM and CCP fibers into a biomaterial for neural engineering scaffold.

***Specific Aim 2. To fabricate fiber 'staples' and test their utility as microcarriers within hybrid hydrogels***

**Approach**

CCP fibers were used to make short staples. The viability of these staples for cell adhesion and purported use as injectable microcarriers was validated. These cell laden staples were encapsulated into hydrogels and cell proliferation was quantified.

**Novelty & Innovation**

A strategy for fabrication of CCP fiber staples amenable to cell adhesion was developed. A novel hydrogel/staple composite injectable scaffold was designed which served as a cell proliferation platform.

***Specific Aim 3. To evaluate effect of hydrogel/staple composite on neural stem cell (NSC) differentiation***

**Approach**

The composite scaffold developed in Aim 2 was used to investigate NSC differentiation in response to staple topography and chemical inducer Retinoic acid.

**Novelty & Innovation**

For the first time, CCP fiber staples are being considered for NSC differentiation in response to the unique grooved topography.

# CHAPTER 3

# ENGINEERING GUIDED NEURON GROWTH USING CCP FIBERS

## INTRODUCTION

SCI inflicts functional deficits that are mostly severe with no effective treatment. At the basic research level, the strategies being investigated include (a) trophic support-encouraging the survival and growth of damaged axons using neurotrophins [1], (b) targeting the downstream signaling molecules such as cAMP to induce axonal outgrowth [2], (c) neutralizing inhibitory molecules such as chondroitin sulphate proteoglycans (CSPGs) by using enzymatic treatment with chondroitinase [3] or Nogo with blocking antibodies to the Nogo receptor [4], and (d) providing a permissive growth environment by biomaterial implantation and/or cell transplantation [5]. The various cells explored include neural stem cells, subventricular zone astrocytes [6], and glial cells such as olfactory ensheathing cells [7], Schwann cells [8] and oligodendrocyte precursor cells [9]. However, the delivery mechanism of cell transplants with optimum survival and integration in addition to patient safety has been an enormous challenge because of the hostile environment at the lesion site. The major hindrances with direct cell transplantation include (a). cell isolation, propagation and stabilization for storage, (b). in vitro testing for biological activity and potency and stemness for stem cells, (c). viability and functional integration of cells into target tissue, (d). ectopic differentiation including chances of tumorigenicity [10]. These difficulties with cell transplants call for surgically implanting acellular scaffolds at the site of injury which would anchor the transplanted cells, provide adhesive/topographic activity and topographic guidance. These scaffolds can be loaded with proteins or ECM to

control the attachment, growth and differentiation of cells. Apart from trophic support, these scaffolds should be able to provide physical and structural topographic guidance to surviving neurons from adjacent tissue by infiltrating the scaffold.

The vast majority of studies examining cell alignment, survival, and differentiation have used two dimensional (2-D) cultures. Neuron growth behavior in response to groove width and depth has been studied by photolithographically fabricated models. Neurons can be directionally guided by topographic manipulations of patterns such as grooves and ridges [11-17]. These groups were able to show that neurons would follow directed guidance in 4-10μm deep and 10μm wide grooves. Although such studies have been able to demonstrate neuron growth behavior with respect to dimensionality, these models have seldom been translatable to 3D scaffolds for tissue engineering. The aim of the work presented here was to develop a novel scaffold which potentially provides guidance to axons in the injured spinal cord and facilitating signal transduction as well with a view towards clinical application. We demonstrate the use of uniquely designed Capillary Channel Polymer (CCP) fibers for guided growth of neurons. A unique design of polymer fibers called capillary-channeled polymer (CCP) fibers has been fabricated for aligned tissue engineering applications in 3D. These fibers have eight deep grooves (or channels) running continuously along their longitudinal axis in its cross-section- 2 major and 6 minor. This unique geometry enhances the surface area for ligand presentation and cell adhesion by more than two-fold when compared to round fibers of comparable dpf (denier per filament) [18].

Apart from topographic guidance, biochemical cues are required to induce signaling within the axon or the growth cone. Most researchers have used laminin-coated scaffolds for promoting neuronal adhesion and axon elongation. Laminin is a heterotrimeric glycoprotein consisting of α, β, and γ subunits that signals though a variety

of integrins and constitutes a major component of basement membrane ECM. When integrin receptors activate, they in turn activate a focal adhesion complex and the mitogen-activated protein kinase which causes neurites to grow. For tissue engineering scaffolds, laminin is not coated directly to the substrate, but onto polylysine or polyornithine coated surfaces [19, 20]. In some cases, laminin has also been integrated in the bulk of the polymer [21]. Presenting the laminin-derived IKVAV or RGDS peptide epitopes has shown to enhance the growth of neurites from DRG neurons along direction of nanofibers [22].

In this work, we consider the use of another biomolecule for making the scaffold promote neurite elongation. In order to provide trophic support and enhance adhesion of neurons, a biomolecule of interest - L1-CAM (cell adhesion molecule) has shown great promise [23]. L1 neural CAM is a member of the immunoglobulin superfamily and plays an important role in the overall development of both the central and peripheral nervous systems, making it an attractive candidate for promoting neural regeneration following injury. Although L1 used for experimental studies is primarily mammalian-derived, insect cell expression system has been used to express a 140 kDa L1 fragment described previously to provide an alternative source of recombinant L1 with equivalent bioactivity [24].

We hypothesized that the unique design of the CCP fibers can provide high directional support and guidance to neurons. In order to investigate neurite extension in response to fiber grooves of various dimensions, we have melt extruded polylactide (PLA) fibers, physisorbed L1 on them and seeded Chicken forebrain neurons (CFN) and dorsal root ganglia (DRG) neurons as well. We also compared the effect of different ligands as laminin and polylysine on neurite lengths on these fibers. This study was able to show that L1-CAM is crucial for axon elongation and is superior to the effect of laminin which has

been widely used by other researchers worldwide. Also, this study was able to demonstrate the directional growth of neurons along the grooves of the CCP fibers.

## MATERIALS AND METHODS

### Fabrication of CCP fibers

Capillary channel polymer (CCP) fibers were melt extruded from polylactide (PLA, Natureworks, Minnetonka, MN) as previously described [18]. Briefly, an extruder with a 30 hole custom spinneret was used to produce CCP fibers at an extrusion temperature of 240 °C, flow rate of 8.76 cc/min and take up speeds indicated in Table 1.

**Table 1.** CCP fibers of different dimensions made by varying extrusion conditions

| Fiber Sample | Polymer throughput rate (m/min) |
|---|---|
| A | 590 |
| B | 350 |
| C | 270 |
| D | 160 |
| E | 115 |
| F | 109 |
| G | 50 |

### Morphology and characterization of CCP fibers

The dimensions of the CCP fibers were measured from fiber samples embedded in Optimal Cutting Temperature compound (OCT, Tissue Tek, Fisher Scientific, MA) and

sectioned using cryotome (Microm, HM 505N, ThermoFisher Scientific, MA). ImagePro Plus software (ICube, Crofton, MD) was used to measure the groove dimensions. At least 10 individual fibers were measured from a representative sample for each group. The fibers were imaged by SEM using TM-3000 (Hitachi).

**Expression and purification of L1-CAM**

L1-CAM was expressed and purified as described previously [24]. Briefly, High Five™ (Life Technologies, Carlsbad, CA) cells were plated in T-175 flasks (2.5 x $10^7$ cells/flask) and infected with recombinant baculovirus. The supernatant was harvested 72 hour post-infection, dialyzed and purified by chromatography column (# 731-1550, Polyprep, Biorad, Hercules, CA). The purified protein was sterile-filtered through a 0.2 µm syringe filter (#180-1320, Nalgene, ThermoFisher Scientific) and stored at 4˚C. The concentration of L1-CAM was determined by BCA (bicinchoninic acid) assay kit (ThermoFisher Scientific).

**Preparation of 2D polystyrene samples**

96 well plate wells were coated with L1-CAM at varying concentrations of 0-50 ug/ml. PBS was used to make the dilutions. The L1-CAM was incubated at room temperature overnight for physisorption followed by washing twice with PBS. Cell culture media containing BME with 10% FCS, 20 mM KCL, 33mM glucose and 50 U/ml penicillin and streptomycin was placed into each well and incubated at 37°C for 15 minutes prior to neuron plating.

**Preparation of 2D spin cast samples**

Microscopic glass slides were cut with a diamond scribe into 2.5 cm x 1.5 cm pieces and cleaned with acetone and water and blow dried with compressed air. The slides were then treated with Piranha solution (3:1 Sulfuric acid : 30% Hydrogen peroxide) and rinsed thoroughly with distilled water. Poly-l-lactide (PLLA, Natureworks, Minnetonka, MN) was dissolved at 10% w/v in dichloromethane and spin coated on the glass slides at 2000 rpm and dried in vacuum for 48 hours to completely remove the dichloromethane. The samples were physisorbed with either 20µg/ml L1-CAM or laminin (#23017-015, Life technologies, Carlsbad, CA) overnight at room temperature followed by washing twice with sterile Phosphate Buffer Solution (PBS). For the dual coated samples, polylysine (0.01% in water) was coated on the samples for 1 hour, followed by washing twice with sterile distilled water, after which either laminin or L1-CAM was adsorbed at 20 µg/ml overnight. For controls, 0.01% polylysine (MW 150000-300000, # P1399-100MG, Sigma) was coated overnight and washed with distilled water twice. The substrates were incubated in cell culture media at 37˚C until seeding within one hour.

**Preparation of fiber samples**

Double sided tape was placed on two opposite edges of round glass cover slips (#26024, Ted Pella, Redding, CA). CCP fibers were aligned and secured between the taped portions of each coverslip. These samples were sterilized by exposure to UV for 1 hour in 24 well plate. The samples were physisorbed with either 20µg/ml L1-CAM or laminin (#23017-015, Life technologies, Carlsbad, CA) overnight at room temperature followed by washing twice with sterile Phosphate Buffer Solution (PBS). For controls,

0.01% w/v polylysine was coated overnight and washed with distilled water twice. The substrates were incubated in cell culture media at 37˚C until seeding within one hour.

**Cell preparation**

Rat cerebellar neurons were isolated from Day 3 post natal (P3) rat pups. Cerebella were stripped of meningeal tissue, minced in a small volume of L-15 medium (Gibco), transferred to a centrifuge tube and digested with 1ml 1% trypsin in HBSS for 15 min. The trypsin was then aspirated and the tissue perfused with fresh media Eagle's Basal Medium (BME) with 10% FCS. The tissue was gently triturated through fire-polished Pasteur pipettes, then incubated in 35 mm petri dishes pre-coated with polylysine (PLL, 0.5 mg/ml overnight) for 10 minutes. This 'panning' step allows astrocytes to attach leaving the neurons suspended in the media. The media was removed, centrifuged and the cells resuspended in BME with 10% FCS, 20 mM KCL, 33mM glucose and 50 U/ml penicillin and streptomycin for plating.

CFN explants (E8) were isolated from embryonic day 8 white leghorn chicken eggs according to protocol used previously [25]. Explants were minced with a small scissor and used as is or dissociated into individual neurons by triturating though fire polished Pasteur pipette and cultured on the 2D film or 3D fiber samples in Basal Medium Eagle (BME, Gibco, ThermoFisher Scientific, MA) supplemented with 6 mg/mL glucose (Sigma, MO), 1% antibiotic/antimycotic 100x stock solution (Gibco, ThermoFisher Scientific, MA), 10% fetal bovine serum (FBS, ThermoFisher Scientific, MA), and 2 mM L-glutamine (Hyclone, Logan UT) for 48 h in a humidified, 5% $CO_2$ incubator.

Dissociated dorsal root ganglion (DRG) neurons were isolated from E8 white leghorn chicken eggs as well. Dorsal ganglia were stripped of nerve roots in HBSS buffer (Gibco) with 10% glucose (Sigma, MO). The DRGs were then trypsinized for 30 minutes

followed by dissociation through fire polished Pasteur pipette. The dissociated DRGs were incubated in a petri dish to 'pan' out the Schwann cells for 4 hours at 37˚C.

**Cell adhesion and neurite outgrowth on 2D polystyrene, PLLA spin cast film and 3D fiber samples**

Rat cerebellar neurons were plated at 5000 cells/well in 96 well plates in BME with 10% FCS, 20 mM KCL, 33mM glucose and 50 U/ml penicillin and streptomycin. The neurons were allowed to attach and grow for 24 hours post-seeding at 37°C with 5% $CO_2$ in incubator after which the neurons were fixed in 4% paraformaldehyde.

Chicken forebrain neurons were plated at 150,000 cells/well in 6 well plates in BME supplemented with 6 mg/mL glucose (Sigma, MO), 1% antibiotic/antimycotic 100x stock solution (Gibco, ThermoFisher Scientific, MA), 10% FBS, and 2 mM L-glutamine (Hyclone, Logan UT) for 24 h in a humidified, 5% $CO_2$ incubator. The neurons were allowed to attach and grow for 24 hours post-seeding at 37°C with 5% $CO_2$ in a humid incubator.

Similary for the 3D fiber samples, chicken forebrain neurons were plated at 60,000 cells/well of 12 well plate.

**Immunohistochemical staining**

The CFNs were fixed 24 hrs post seeding for 1 hour in 4% paraformaldehyde (Alfa Aesar, MA) and washed three times with staining media. The CFNs were immunostained by Anti mouse β-III Tubulin produced in Rabbit (1:500, mouse IgG, Sigma, MO) to identify the neurons. As secondary antibody goat anti-rabbit IgG Alexa 488 (Life Technologies, Carlsbad, CA) was used at 1:200 dilution in staining media. The immunostained neurons were visualized with a fluorescence microscope AMG-EVOS (Fisher Scientific, MA). For the quantitative comparison of neurite outgrowth, ImagePro software was used. Only

single stand-alone neurites, not connected to other neurites were measured and quantified.

## Scanning electron microscopy (SEM)

For SEM analysis, the samples were fixed with 4% paraformaldehyde for 1 h at room temperature. The samples were washed three times with PBS (1x) and dehydrated through a graded ethanol series (50, 70, 90, 95 and 100%). HMDS (1,1,1,3,3,3-hexamethyl disilazane, United Chemical Technologies Inc., Bristol, PA) was added and left to air dry at room temperature. For SEM imaging, the samples were placed on glass cover slips mounted on stainless steel SEM stubs, coated with platinum and imaged with a Hitachi S-4800 high resolution scanning electron microscope at 10 kV image beam intensity.

## Statistical analysis

All the data presented are expressed as mean ± standard error of the mean. Single-factor analysis of variance was carried out to compare the means of different data sets, and a value of $p \leq 0.05$ was considered statistically significant.

# RESULTS AND DISCUSSION

## Effect of L1-CAM concentration on neurite length in 2D:

In order to determine the effect of L1 coating concentration on neurite length, L1-CAM was plated in 96 well plate wells overnight at concentrations ranging from 0-50 µg/ml. For the negative control, the well was submerged in PBS instead of L1-CAM. The aim of this experiment was to determine the optimum concentration of L1-CAM coating that could be most viable for neurite elongation. Rat cerebellar neurons were used for this experiment.

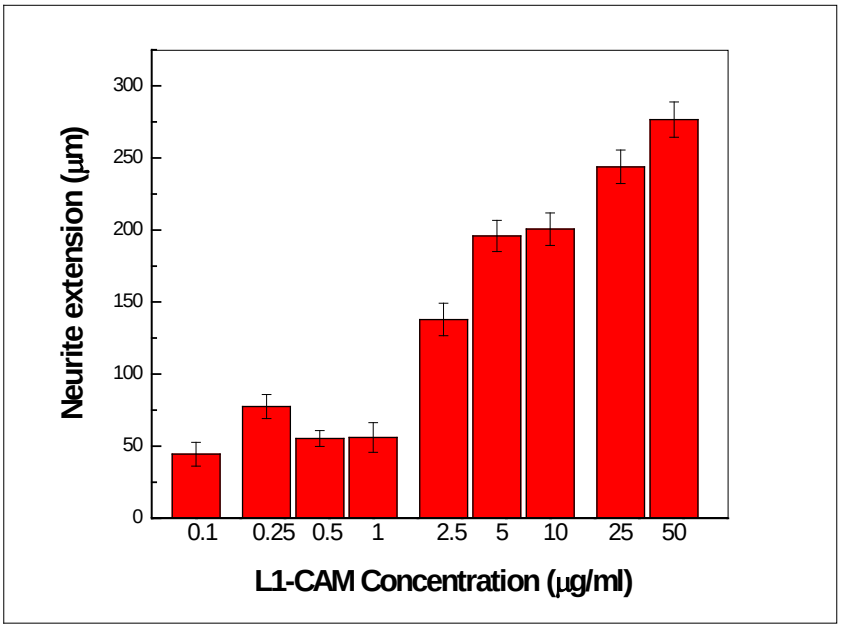


**Fig.3.1.** Dose dependent neurite extension response of L1-CAM in 2D polystyrene on rat cerebellar neurons

Neurite outgrowth increased with increasing coating concentration of L1 in a dose-dependent manner (Fig.3.1). This corroborates the fact that increased availability of the biochemical cue would trigger enhanced signaling in the axon which would in turn increase axon extension. It was observed that no neurites grew on the negative control (no L1-CAM) and highest average neurite extension (~ 276 µm) was measured at 25-50 µg/ml L1-CAM plating concentration. The neurite extension plateaued after 25 µg/ml plating concentration and therefore there was no statistically significant difference between 25 and 50 µg/ml plating concentration. For the rest of the study, we chose to use 20 µg/ml as an optimum concentration.

**Effect of ligand on neurite length in 2D:**

In order to determine the neurite elongation response of different ligands, polylactide films were coated by physisorption. It can be surmised that different ligands would elicit different responses from neurites because of different receptor ligand interactions and biochemical pathways. While laminin has been widely used as the ligand of interest in tissue engineering scaffolds, seldom has any other ligand been explored. Also, laminin is usually adsorbed on polylysine pre-coated substrates and not by itself. We compared the elongation response of chicken forebrain neurons on PLLA spin cast films coated with polylysine, laminin, polylysine/laminin, L1-CAM, and polylysine/L1-CAM. Cells are known to bind to polylysine by charge interaction, while laminin induces integrin based adhesion.

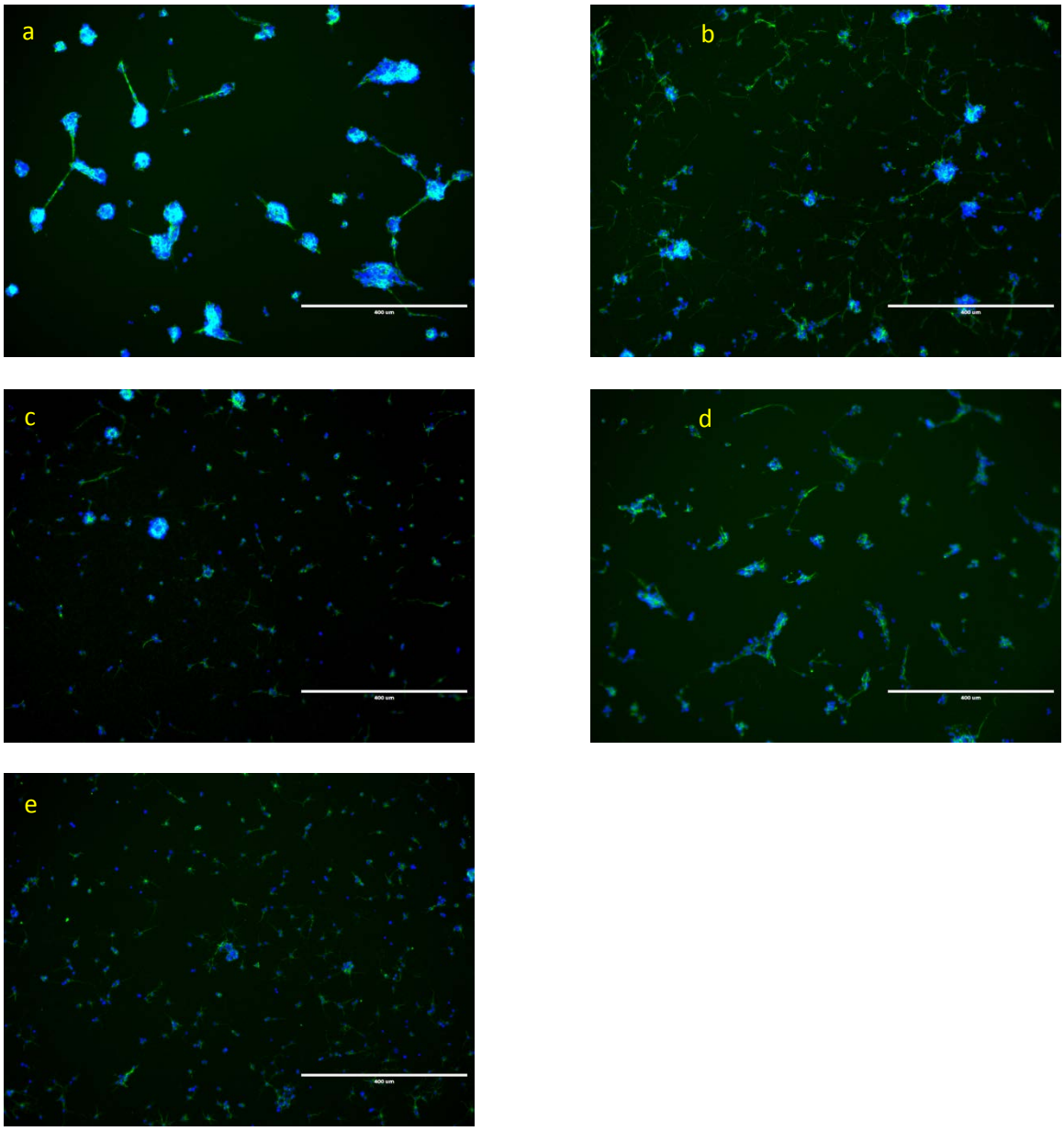


**Fig.3.2.** Dissociated Chicken forebrain neurons on different ligands (a). laminin (b). L1-CAM (c). polylysine (d). PLL/L1-CAM (e). PLL/laminin (Scale bar = 400 um)

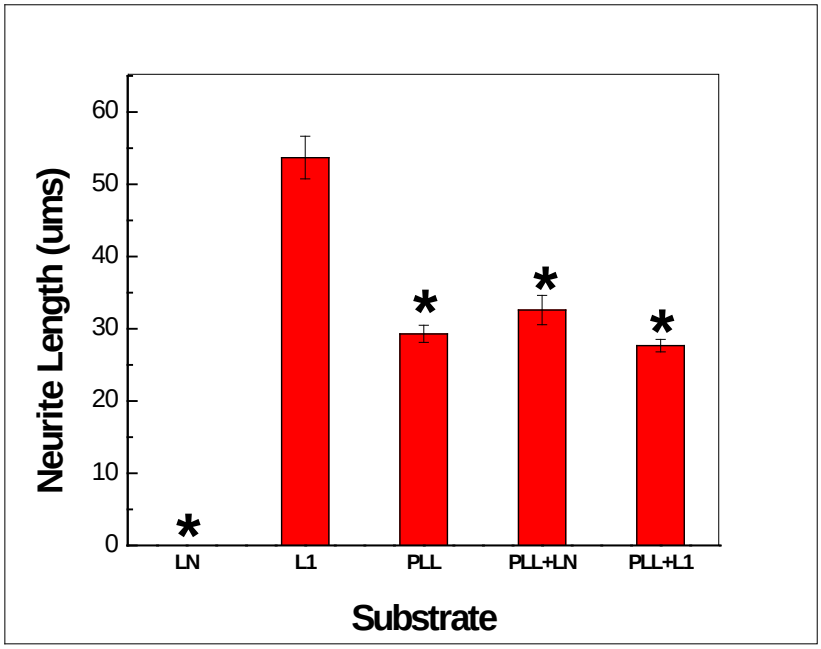


**Fig.3.3.** Comparison of neurite length extension in 2D on PLA coated with different ligands (* indicates significant different versus L1 at $p < 0.05$)

As previously described, only single stand-alone neurites, not connected to other neurites were measured and quantified (Fig.3.2). At 24 hours, it was observed that L1-CAM coated films promoted the growth of longest neurites (~54 µm), significantly higher than all other ligands. It was interesting to note that there was no significant difference in neurite extension on PLL vs PLL/LN vs PLL/L1-CAM (~30 µm) (Fig.3.3). It is interesting to note that coating L1-CAM on PLL pre-coated substrate reduces neuron growth by half, this could possibly be because of the charge interaction between positively charged PLL and negatively charged domains in L1-CAM that could cause its conformation to change to a less bioactive one than by its hydrophobic interaction on polylactide film. In addition, probably L1 adsorbs more efficiently by hydrophobic interactions with PLA than PLA/PLL. Also, it was noted that laminin when coated by itself, does not induce any single neurite extension. This means that polylysine pre-coating enables laminin to adsorb on it in a

manner that is most conformationally bioactive on the charged surface and that the bioactive sites get hidden and non-accessible to neurons when laminin interacts with a hydrophobic surface as PLA.

## Fabrication of extruded PLLA CCP fibers

Seven different CCP fibers having varying groove dimensions were fabricated by controlling the take up speed during melt extrusion. The various melt extrusion conditions are listed in Table 1.

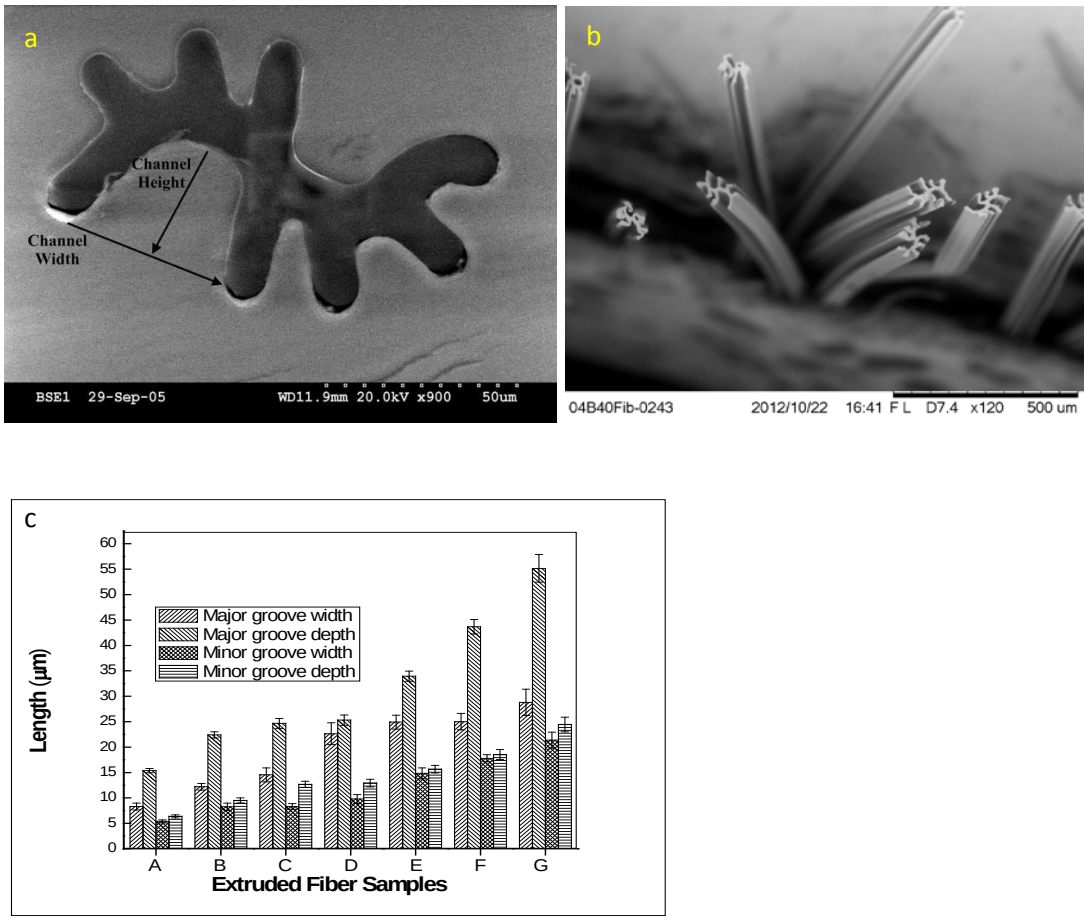


**Fig.3.4.** (a). Scanning electron microscope image of a resin embedded capillary channel polymer fiber cross-section (x900). Arrows identify how the dimensions of channel height and width were measured, within a large CC-P fiber channel [26] (b). SEM of CCP fibers (x120) (c). Fiber microtopography dimensions of 7 different dpf CCP fiber samples

It could be observed that the dimensions of major and minor groove width and depth increased with decreasing take up speed of the fibers during extrusion (Fig.3.4c).

**Effect of fiber dimensions on neurite extension:**

The next step was to check the effect of different dimension CCP fibers on neurite extension. In order to do so, chicken forebrain neurons (CFN) were seeded on L1-CAM (20 ug/ml) coated CCP fiber samples A-G.

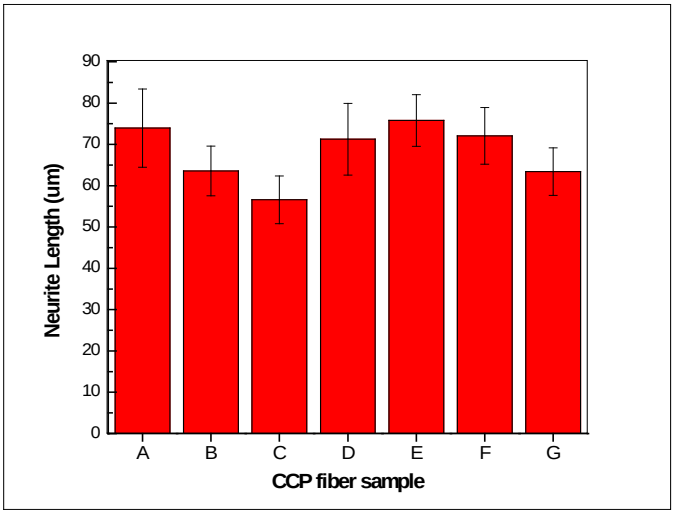


**Fig.3.5.** Effect of groove dimensions of CCP fibers on neurite extension was quantified with dissociated CFN neurons

No sigificant difference (at $p<0.05$) in neurite length was observed among the CCP fiber groups with different groove dimensions (Fig.3.5). Thus between groove width range of 5-25 µm and depth range of 5-55 µm across A-G, neurite lengths did not vary significantly. This is in agreement with widely researched effect of dimensions of anisotropic photolithographic arrangement of grooves and ridges. Neuron growth behavior in response to groove width and depths has been studied by photolithographically

fabricated 2D models [12-17]. These groups were able to show that neurons would follow directed guidance in 4-10 µm deep and 10 µm wide grooves. Thus we concluded, that all the fiber samples A-G are equally capable of directing neuron guidance. While sample A was too soft to handle and Sample B was a more handle-able sample with dimensions of groove width in the range of (7.5-12.5 µm) and groove depth in the range of (10-22.5 µm). Thus, we chose Sample B for further studies.

**Effect of CCP biofiber topography and biochemical cue L1-CAM on neurons and tissue explants:**

In order to study the effect of CCP fiber topography on neuronal guidance and extension, dissociated rat (P3) cerebellar and embryonic chicken (E8) forebrain and DRG neurons in addition to neuron tissue explants were seeded. Thus far it has been demonstrated that L1-CAM is a superior ligand for promoting neurite growth as compared to polylysine and laminin. Also, L1-CAM requires only a single physisorbed coating vs pre-coating of PLL in case of laminin. Also, sample B was chosen for studying the effect of CCP topography on neuronal guidance.

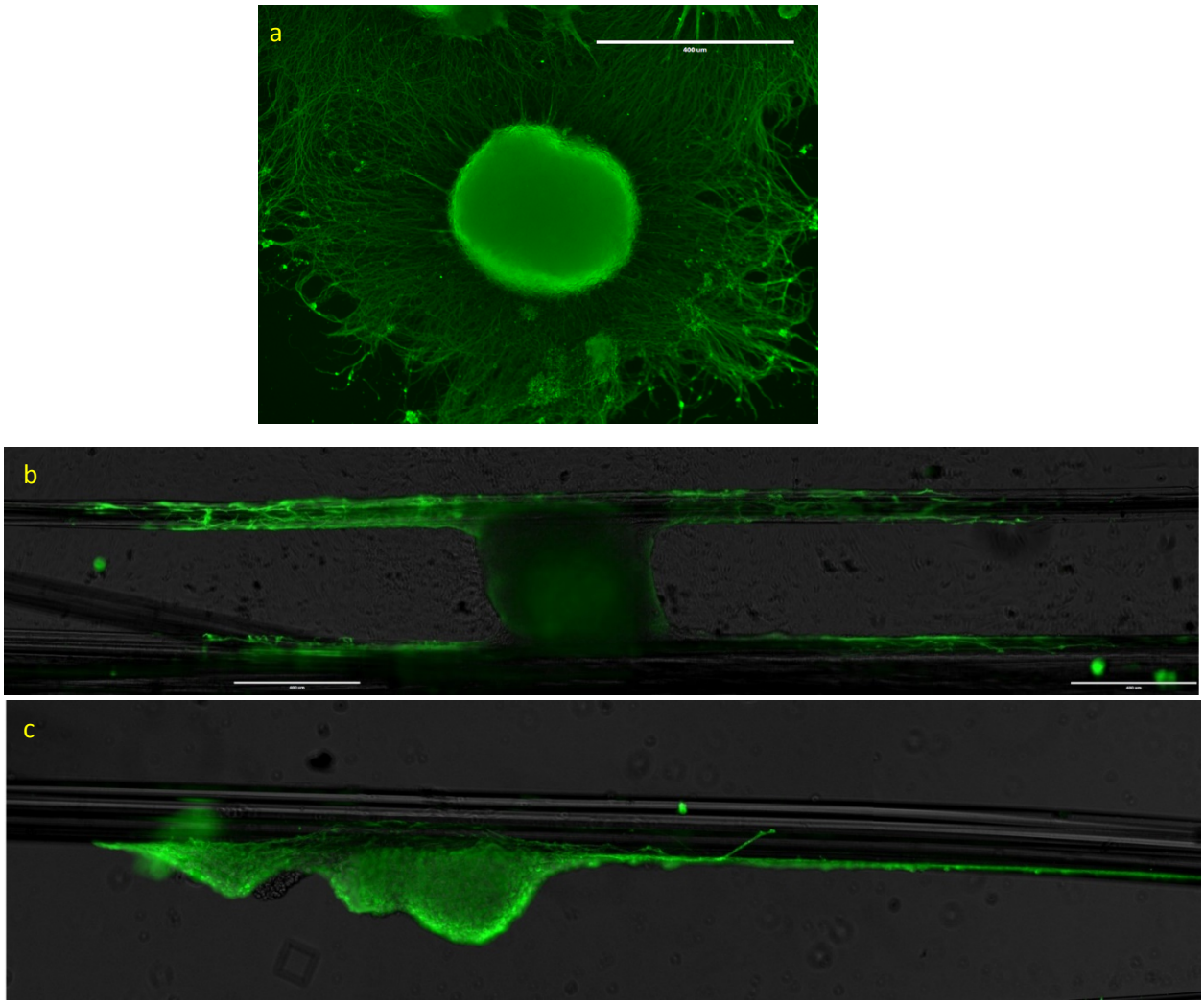


**Fig.3.6.** Effect of CCP biofiber topography on postnatal rat cerebellar neuron explants *(a)* Primary Rat cerebellar neuron explants growing randomly on L1-CAM coated PLA film in 2D (*b,c)*. Primary Rat cerebellar neuron explants directionally guided on L1-CAM coated CCP fibers in 3D (Green stain = β-III tubulin neuronal marker, Scale bar = 400 um)

It can be seen in Fig.3.6a that rat cerebellar neuron explants emanate neurons in random directions on L1 coated PLA film in 2D, while directional growth along the length of the fiber away from the explant body can be seen in 3D on L1 coated PLA fibers (Fig.3.6 b,c). We also observed similar topographic guidance response when chicken forebrain neuron explants (Fig.3.7) and cDRGs (Fig.3.8) were seeded on PLA fibers; and likewise with dissociated chicken forebrain neurons (Fig.3.9).

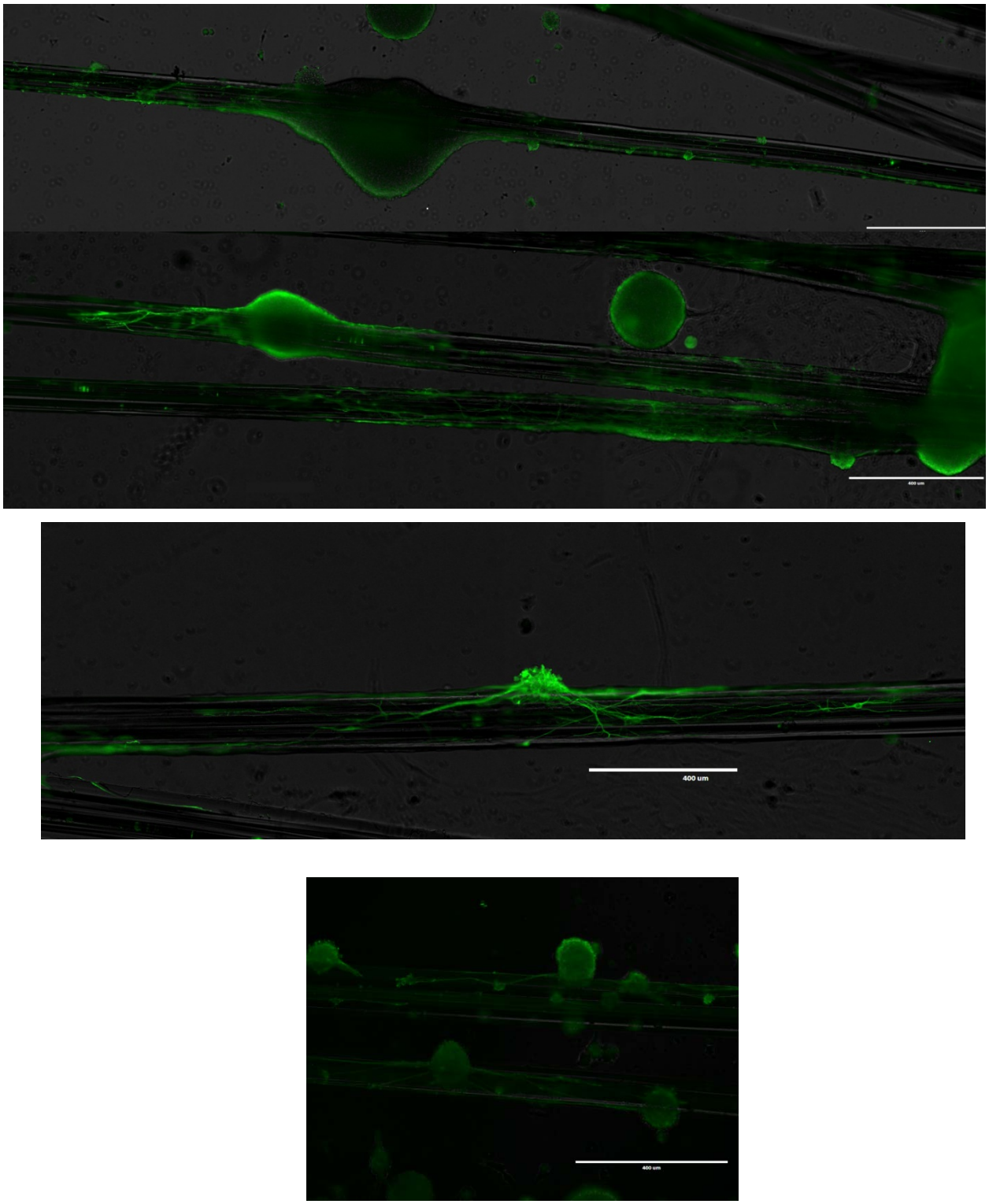


**Fig.3.7.** Effect of CCP biofiber topography on E8 chicken forebrain neuron explants (Green stain = β-III tubulin neuronal marker; Scale Bar = 400um)

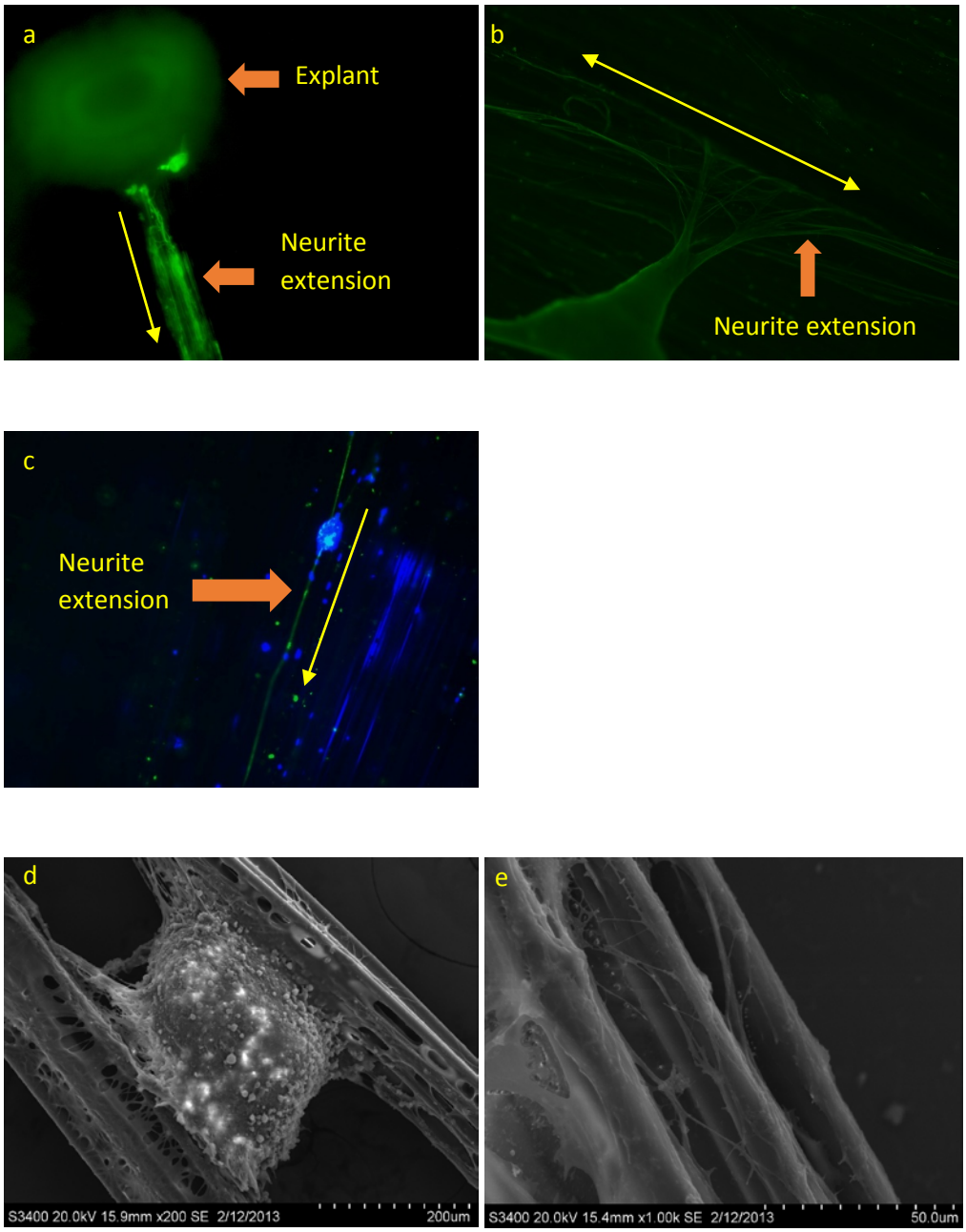


**Fig.3.8.** Topographic guidance of cDRG neurons (a,b). Neurites growing along direction of CCP fiber from cDRG explant (c). Dissociated DRG neurons growing along CCP fiber axis length (Green stain = β-III tubulin neuronal marker; Blue = DAPI; Yellow arrow shows direction of fiber axis) (d,e). SEM images showing effect of CCP biofiber topography on E8 cDRG neuron explants

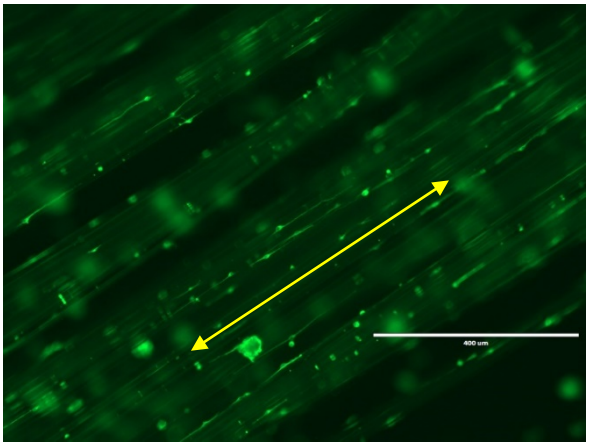

**Fig.3.9.** a). Primary chick embryonic forebrain dissociated neurons cultured on L1-CAM adsorbed CCP fibers in 3D (Green stain = β-III tubulin neuronal marker; Yellow arrow shows direction of fiber axis)

## CONCLUSION:

Micron scale topographic features can be employed *in vitro* in order to mimic the natural cellular surroundings of the ECM for nerve regeneration application. In this work, uniquely designed CCP fibers were studied for neuronal alignment and polarization response. The effect of CCP fiber dimensions on the topographic guidance of various neuronal tissue explants and dissociated cells was studied. In addition, we have studied the response of neurons on different ligands and shown that L1-CAM could possibly be used in biomaterials for triggering axon extension. L1-CAM was shown to be capable of supporting significantly greater neurite extension than the widely used ECM protein laminin. Therefore, this work will contribute towards better designing of the surface of biomaterials for neural applications, such as nerve tissue engineering scaffolds and neural prostheses.

## References:


[1] Ramer MS, Priestley JV, McMahon SB. Functional regeneration of sensory axons into the adult spinal cord. Nature 2000;403:312-6.

[2] Qiu J, Cai D, Dai H, McAtee M, Hoffman PN, Bregman BS, et al. Spinal axon regeneration induced by elevation of cyclic AMP. Neuron 2002;34:895-903.

[3] Bradbury EJ, Moon LD, Popat RJ, King VR, Bennett GS, Patel PN, et al. Chondroitinase ABC promotes functional recovery after spinal cord injury. Nature 2002;416:636-40.

[4] McKerracher L, Winton MJ. Nogo on the go. Neuron 2002;36:345-8.

[5] Jain KK. Neuroprotection in spinal cord injury. The Handbook of Neuroprotection: Springer; 2011. p. 255-80.

[6] Horner PJ, Gage FH. Regenerating the damaged central nervous system. Nature 2000;407:963-70.

[7] Franklin RJ, Barnett SC. Olfactory ensheathing cells and CNS regeneration: the sweet smell of success? Neuron 2000;28:15-8.

[8] Tuszynski MH, Weidner N, McCormack M, Miller I, Powell H, Conner J. Grafts of genetically modified Schwann cells to the spinal cord: survival, axon growth, and myelination. Cell transplantation 1998;7:187-96.

[9] Barnett SC, Thompson RJ, Lakatos A, Pitts J. Gap junctional communication and connexin expression in cultured olfactory ensheathing cells. Journal of neuroscience research 2001;65:520-8.

[10] Andressen C. Neural Stem Cells: From Neurobiology to Clinical Applications. Current pharmaceutical biotechnology 2013;14:20-8.

[11] Britland S, Perridge C, Denyer M, Morgan H, Curtis A, Wilkinson C. Morphogenetic guidance cues can interact synergistically and hierarchically in steering nerve cell growth. Experimental Biology Online 1997;1:1-15.

[12] Clark P, Connolly P, Curtis AS, Dow JA, Wilkinson CD. Topographical control of cell behaviour. I. Simple step cues. Development 1987;99:439-48.

[13] Clark P, Connolly P, Curtis AS, Dow JA, Wilkinson CD. Topographical control of cell behaviour: II. Multiple grooved substrata. Development 1990;108:635-44.

[14] Recknor JB, Sakaguchi DS, Mallapragada SK. Directed growth and selective differentiation of neural progenitor cells on micropatterned polymer substrates. Biomaterials 2006;27:4098-108.

[15] Rajnicek A, Britland S, McCaig C. Contact guidance of CNS neurites on grooved quartz: influence of groove dimensions, neuronal age and cell type. Journal of cell science 1997;110:2905.

[16] Rajnicek A, McCaig C. Guidance of CNS growth cones by substratum grooves and ridges: effects of inhibitors of the cytoskeleton, calcium channels and signal transduction pathways. Journal of cell science 1997;110:2915-24.

[17] Clark P, Britland S, Connolly P. Growth cone guidance and neuron morphology on micropatterned laminin surfaces. Journal of cell science 1993;105:203-12.

[18] Sinclair KD, Webb C, Brown PJ. Capillary channel polymer fibers as structural templates for ligament regeneration. Am Assoc Text Chem Colorists 2008;8:36-40.

[19] Bakhru S, Nain AS, Highley C, Wang J, Campbell P, Amon C, et al. Direct and cell signaling-based, geometry-induced neuronal differentiation of neural stem cells. Integr Biol 2011;3:1207-14.

[20] Bozkurt A, Deumens R, Beckmann C, Olde Damink L, SchÃ¼gner F, Heschel I, et al. In vitro cell alignment obtained with a Schwann cell enriched microstructured nerve guide with longitudinal guidance channels. Biomaterials 2009;30:169-79.

[21] Koh HS, Yong T, Chan CK, Ramakrishna S. Enhancement of neurite outgrowth using nano-structured scaffolds coupled with laminin. Biomaterials 2008;29:3574-82.

[22] Berns EJ, Sur S, Pan L, Goldberger JE, Suresh S, Zhang S, et al. Aligned neurite outgrowth and directed cell migration in self-assembled monodomain gels. Biomaterials 2014;35:185-95.

[23] Webb K, Budko E, Neuberger TJ, Chen S, Schachner M, Tresco PA. Substrate-bound human recombinant L1 selectively promotes neuronal attachment and outgrowth in the presence of astrocytes and fibroblasts. Biomaterials 2001;22:1017-28.

[24] Cribb RC, Haddadin FT, Lee JS, Webb K. Baculovirus expression and bioactivity of a soluble 140 kDa extracellular cleavage fragment of L1 neural cell adhesion molecule. Protein Expression and Purification 2008;57:172-9.

[25] Heidemann SR, Reynolds M, Ngo K, Lamoureux P. The culture of chick forebrain neurons. Methods in cell biology 2003;71:51-65.

[26] Sinclair KD, Webb K, Brown PJ. The effect of various denier capillary channel polymer fibers on the alignment of NHDF cells and type I collagen. Journal of Biomedical Materials Research Part A 2010;95:1194-202.

# CHAPTER 4

# ENGINEERING CELL PROLIFERATION USING TOPOGRAPHY AND HYDROGEL

## INTRODUCTION:

Tissue engineering and regenerative medicine encompass a broad group of strategies directed towards the structural and functional restoration of diseased or damaged tissues. Scaffolds play a central role as provisional matrices to support the adhesion, migration, proliferation, and differentiation of transplanted or endogenous cells. Early examples of scaffolds included sponges and meshes with interconnected pores and high surface area / volume ratio prepared by solvent casting / particulate leaching [1], phase separation [2], gas-foaming [3], and fiber bonding. More recent efforts in the field have focused on designing scaffolds with bioactive cues capable of directing specific cellular activities. For example, incorporation and controlled release of recombinant growth factors or gene delivery vectors has been used to enhance cell differentiation and scaffold vascularization [4-6]. In another approach, advanced fabrication techniques such as solid-free form fabrication and electrospinning have been used to prepare scaffolds with bioactive topographic / structural features [7]. Microtopographies shaped like pillars, posts and convex micro-hills have been shown to accelerate human mesenchymal stem cells (hMSC) proliferation compared to smooth controls [8, 9]. Human embryonic stem cells (hESCs) were shown to proliferate 10 times on polyurethane electrospun fibers after 18 days of seeding compared to day 5 of cell seeding [10]. These hESCs differentiated into neurons (~80% of total cell population) while very little astrocyte differentiation was observed. In comparison, about 95% of the total cell population differentiated into astrocytes on planar non fiber controls. Higher neurite length and higher neuronal differentiation was observed from ESCs seeded on aligned polycaprolactone (PCL) fibers

as compared to random counterparts [11]. Similarly, 2.5 fold higher number of adult neural stem cells (ANSCs) cells were found to differentiate into neuronal lineage on aligned PCL nanofibers compared to planar controls [12]. However, one important limitation of these types of scaffolds is that they generally must be pre-fabricated in the laboratory and therefore invasive surgery is required for their implantation.

In order to minimize surgical trauma, much attention has focused on hydrogel scaffolds that can be prepared from aqueous solutions, delivered in a minimally invasive manner by injection, and crosslinked in-situ. Hydrogels offer several additional advantages including chemical compatibility with cells and biomolecules allowing their homogenous encapsulation; shape conformation to tissue defects of irregular geometry; and structural and mechanical properties similar to the native ECM. [13]. While hydrogels prepared from natural polymers most closely resemble the ECM and possess intrinsic bioactivity, they have a limited range of mechanical properties and potential immunogenicity. On the other hand, synthetic hydrogels can be tailored to control the network physical and chemical properties, but are relatively bioinert. Hybrid hydrogels, composed of both synthetic and naturally-derived macromolecules, attempt to integrate the advantages and overcome the limitations of each material component when used alone [14-17]. For example, polyethylene glycol polymers crosslinked with protease-sensitive peptides have been shown to support cell-mediated remodeling, bone regeneration, and angiogenesis [18, 19]. In spite of these benefits, such hydrogels are predominantly amorphous in nature and cannot provide any topographic bioactivity to encapsulated cells.

Our goal was to integrate anisotropic topographic cell microcarriers providing topographic support in 3D within the bulk of hydrogel matrix while retaining compatibility with minimally invasive delivery. The concept of microcarriers was introduced by van Wezel in 1967 to produce viral vaccines and biological cell products using mammalian

cells [20]. These substrates can serve for proliferation of anchorage dependent cells at the site of defect. Another means of regeneration of various tissues is to deliver the cells as undifferentiated cells at the site and then induce to differentiate into the cell of interest at the specific location in the body. Various factors involved in designing a microcarrier include consideration of chemical composition, surface topography, porosity and charge density, all of which determine the ease of cell adhesion to the microcarrier [21]. Most primary cells and non-malignant cell lines require a substrate in order to proliferate in culture. The interaction of the cells with the substrate is thought to affect the arrangement of cellular structures involved in control of growth and other essential functions. In 1986, fibroblasts were shown to attach and proliferate on dextran microcarriers [22]. Commercially available Cytodex microcarriers were later used for expansion in 3D of a wide variety of cells as chondrocytes [23], animal derived stem cells [24-27]. This mode of expansion provides high surface area in a bioreactor and is therefore superior to expansion in regular 2D cell culture flasks. For example, 1 g of Cytodex$^{TM}$ microcarriers provides a surface area of 4400 $cm^2$, equivalent to the surface area as approximately fifty-eight 75 $cm^2$ culture flasks, which makes microcarriers for tissue culture space saving and cost effective, as well as less time and labor intensive than standard culture methods [28]. Likewise, microspheres made of PLLA have been used as microcarriers for skin epidermal and dermal cell delivery for wound healing in a porcine model [29]. More recently, keratinocyte seeded microcarriers have been used to enhance healing of full thickness wounds [30, 31]. Previous work with capillary channel polymer (CCP) fibers has shown that the surface micro-architecture of the CCP fibers, consisting of eight surface grooves parallel to the fiber axis, provided favorable geometrical constraints and promoted spreading and generation of increased cellular organization which achieved biomimetic, physical templates akin to the native ACL (anterior cruciate ligament) of the knee [32, 33]. These fibers were shown to promote significantly greater cell alignment parallel to the fiber

axis and organized ECM deposition than round fiber controls of comparable denier or perimeter. In this study, we demonstrated the development of an injectable fiber-based microcarrier for tissue regeneration. Gel-based composite systems have been shown to provide physical support for cellular focal adhesion while also facilitating cell spreading phenotype [34]. Gelatin grafted gellan (TriG) microspheres have been used as cell-laden microcarriers for hMSCs which upon encapsulation within agarose gel demonstrated two fold increase in cell proliferation compared to gel only controls [34]. The composite developed in this study is a photocrosslinked, hybrid semi-interpenetrating polymer network (semi-IPN) composed of synthetic polyethylene glycol diacrylate (PEGdA), native hyaluronic acid (HA), and the integrin binding peptide GRGDS with dispersed cell carrying CCP polylactide (PLA) staples sized approx. 180 μm. The results of these studies demonstrate that fibroblasts pre-seeded on CCP-based microcarriers exhibit significantly increased cell proliferation with PEGdA/HA semi-IPNs relative to bulk-encapsulated cells without microcarriers.

## MATERIALS AND METHODS

### Capillary channel polymer fiber staple fabrication and characterization

Capillary channel polymer (CCP) fibers were melt extruded from polylactide (PLA, Natureworks) as previously described [32]. Briefly, an extruder with a 30 hole custom spinneret was used to produce CCP fibers at an extrusion temperature of 240 °C, flow rate of 8.76 cc/min and take up speed of 270 m/min. CCP fibers were embedded in Optimal Cutting Temperature (OCT) compound and cut on a cryostat microtome (Microm HM 505 N). The OCT slices were collected in a 50 ml tube and washed three times (1

hr/wash) by sonication in distilled water (Model 75D, VWR International, West Chester, PA). After each wash, the staples were centrifuged (Accuspin 1R, Fisher Scientific) at 6000 rpm for 10 minutes and the supernatant discarded and replaced. The complete removal of OCT from the staples was verified by ATR-FTIR (Thremo-Nicolet Magna 550 FTIR spectrometer equipped with a Thermo-SpectraTech Endurance Foundation Series Diamond ATR). The staples were then recovered by lyophilization (Freezone 4.5, Labconco). For SEM imaging, the samples were placed on glass cover slips mounted on stainless steel SEM stubs, coated with platinum and imaged with a Hitachi S-4800 high resolution scanning electron microscope at 10 kV image beam intensity (Fig.3.2). The staples were also imaged by phase contrast microscopy and their size was measured using ImagePro (Media Cybernetics, Rockville, MD) software.

**Cell culture and seeding on staples**

Mouse-derived NIH3T3 fibroblasts (ATCC® CRL-1658) were cultured in 75cm$^2$ tissue culture flasks with DMEM/F-12 50:50 1X media (Mediatech, Herdon, VA) supplemented with 10% (v/v) bovine growth serum (Hyclone, Logan UT), and 50 U/mL penicillin and 50 µg/mL streptomycin (Mediatech). Medium was changed every 2 days and cells were maintained in a tissue culture incubator at 37ºC with 5% carbon dioxide ($CO_2$).

In order to improve cell adhesion, the staples were incubated with fibronectin (20µg/ml, F1141-5MG, Sigma) in a micro-centrifuge tube overnight at room temperature attached to a rotary cell culture system (Synthecon Inc., Houston, Texas) rotating at 15 rpm and then washed with 1X PBS. FN-coated staples (15mg) were seeded with 1x10$^6$ cells in 1 ml medium in a 1.5 ml micro-centrifuge tube and incubated on a rotary platform (15 rpm) housed in a cell culture incubator for 6 hr. The staples were allowed to settle and the supernatant was discarded. The cell-seeded staples were then transferred to a 24 well plate at 7.5 mg per well and incubated for 42 hours. This method allowed any remaining

non-adherent cells to be removed by attachment to the bottom of the well. The seeding efficiency on the CCP staples was assessed by viability staining at 48 hrs (Calcein AM, Life Technologies, Carlsbad, CA). To evaluate cell morphology and cytoskeletal organization, cells were fixed in 4% paraformaldehyde for 1 hour, permeabilized with 0.1% Triton X-100, and stained with Alexa 594-phalloidin and DAPI (Life Technologies). Fluorescence images were captured using an AMG EVOS microscope (Fisher Scientific, Pittsburgh, PA). For SEM imaging, cell-seeded staples were fixed in paraformaldehyde, dehydrated in a series of ethanol washes, immersed in hexamethyldisilazane (United Chemical Technologies, Bristol, PA) and air dried on glass cover slips at room temperature overnight in fume hood. The samples were then mounted on stainless steel SEM stubs, coated with platinum, and imaged at 10 kV image beam intensity (Hitachi S-4800).

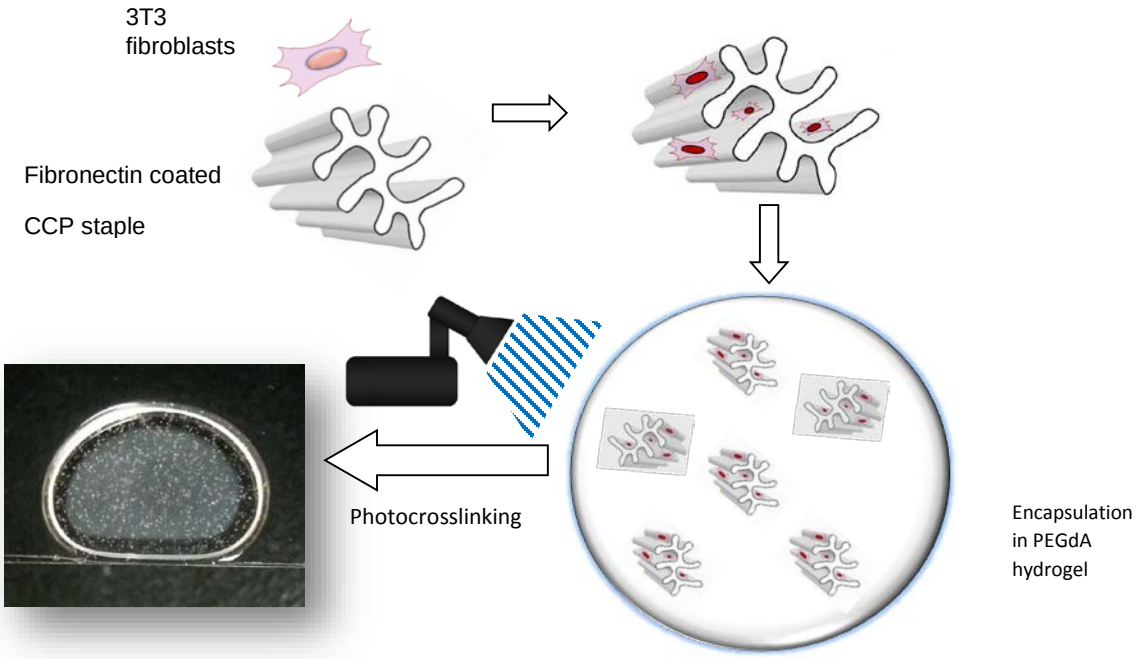


**Fig.4.1.** Schematic of 3T3 fibroblast cell seeding and culture in 3D hydrogel composites.

**Validation of injectability**

CCP staples were seeded with NIH 3T3 fibroblasts as described above. At 48 hours post-seeding, staples were suspended in medium (10 mg/ml) and passed through a 21G syringe needle (Becton Dickinson, Franklin Lakes, NJ) to validate their injectability and investigate the effect of injection on cell viability. Cells were stained with Calcein AM and compared to non-injected controls.

**Synthesis of PEG-DA macromers with ester linkages containing variable alkyl spacers**

Three different types of PEG-DA macromers with varying susceptibility to hydrolytic degradation were synthesized by a two-step process as previously reported [32]. Briefly, PEG (4000 MW, Fluka, Buchs, Switzerland) was reacted with either choroacetyl chloride, 2-chloropropionyl chloride, or 4-chlorobutuyrl chloride (Sigma-Aldrich, St. Louis, MO) in the presence of triethylamine (TEA, Sigma-Aldrich) at a 1:4:1.8 molar ratio in dry dichloromethane (Sigma-Aldrich). After 24 hrs reaction at room temperature, the reactants were filtered, washed with sodium bicarbonate and water, dried with anhydrous sodium sulfate, and then precipitated in ethyl ether. After recovery, each resulting intermediate product was reacted with sodium acrylate (5X molar ratio) in dry dimethylformamide (Acros, Morris Plains, NJ) for 30 hours at 50, 85, and 100 ºC to yield PEG-bis (acryloyloxy acetate) [PEG-bis-AA], PEG-bis-(acryloyloxy propanoate) [PEG-bis-AP] and PEG-bis-(acryloyloxy butyrate) [PEG-bis-AB], respectively. The products were purified by filtration, rotary evaporation, and precipitation in ethyl ether and dried under vacuum. The structures of each PEGdA and the degree of acrylation were determined

from the $^{1}$H-NMR (Brucker 300MHz, $CDCl_3$) spectra. All samples achieved acrylation efficiencies greater than 90%.

**Preparation of staple-hydrogel composites**

HA (2% w/v, 1.5 MDa, LifeCore Biomedical, Chaska, MN) and PEG-DA (30% w/v) stock solutions were prepared in 1X-PBS (0.1M, pH 7.4). Acryl-PEG-GRGDS was synthesized by conjugating GRGDS peptide (Bachem, Torrance, CA) to acryl-PEG-NHS (Jenkem, Beijing, China) as previously described [35]. Gel precursor solutions were prepared containing PEG-DA (6% w/v), HA (0.36% w/v 1.5 MDa), acryl-PEG-GRGDS (1 mM), 1-[4-(2-hydroxyethoxy) phenyl]-2-hydroxy-2-methyl-1-propanone (I-2959, BASF, Florham Park, NJ, 0.1% w/v), and cell seeded staples (5 mg/ml). Sample volumes (45 µl) were pipetted in between glass coverslips separated by 1 mm Teflon spacers and exposed to low intensity UV light (365nm, 10mW/cm$^2$, Black-Ray B100-AO, Upland, CA) for 5 minutes on each side of the disc. Hydrogels with encapsulated staples were cultured in Petri dishes (Becton Dickinson, San Jose, CA) with 2mL culture medium. As a control, hydrogels with the same composition were prepared with cells only and no staples. Gels (n=7 samples / group) were cultured for 21 days.

**Confocal imaging**

The viability of encapsulated cells was determined by vital staining using Calcein AM/ethidium bromide at 1, 7, 14, and 21 days post-encapsulation. Gel samples were placed in glass-bottom well chambers (Lab-Tek, Hatfield, PA) for imaging. Images of stained cells were captured via confocal laser scanning microscopy (Ti-Eclipse, Nikon, Tokyo, Japan). Cell morphology inside hydrogel was visualized and compared to assess

cell spreading and proliferation. The region of interest in the gel sample was identified and the system software was programmed to collect images at 20 µm intervals through the thickness of the gel (*z*-dimension). Macroscopic images of sample hydrogels were also captured alongside with an iphone 5 (Apple).

## Cell proliferation

At 1, 7, 14, and 21 days post encapsulation, gel samples (n=5 gels/group) were homogenized in 0.1% Triton-x and stored at -80 ºC until ready for assay. The samples were thawed and homogenized using probe sonication (10W for 1 minute, Omni-Raptor 4000, OMNI International Inc.) on ice followed by centrifugation and collection of the supernatant. The DNA content in each gel sample was then determined by PicoGreen double stranded assay (Life Technologies, Carlsbad, CA). Gels containing cells without staple microcarriers were used as control and gels without any cells were used as blanks. Serial dilution of 3T3 fibroblasts at known concentration was used to generate a standard curve. Samples were analyzed according to the manufacturer's instructions, using a Synergy H1 hybrid fluorometer (Bio-Tek, Winooski, VT) at 480 nm excitation and 520 nm emission wavelengths.

## Statistical analysis

Quantitative data for cell proliferation were compared by ANOVA using Tukey's method for post-hoc comparisons (one-way ANOVA). p values $< 0.05$ were considered to be statistically significant. All quantitative data are presented as mean ± standard error of the mean.

## RESULTS:

### Preparation of CCP staples

CCP fibers were melt extruded using a customized spinneret as previously described in Chapter 3. We used group B of the various CCP fiber samples described in the Table 1 in Chapter 3. The fibers were imaged by a microscope and found to have the following groove dimensions- major groove width (25±1.37) µm, major groove depth (34±1) µm, minor groove width (14.8±1.08) µm, minor groove depth (15.67±.75) µm. The average length of staples made from these fibers was found to be 184.8±11µm. The staples were imaged by SEM (Fig.4.2).

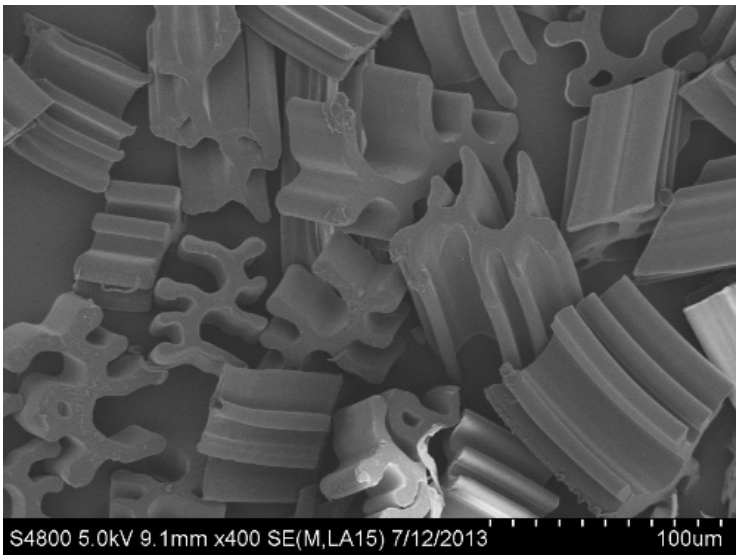


**Fig.4.2.** SEM image of CCP staples (x400)

## Cell culture and seeding on staples

Cells were found to be efficiently seeded in the grooves of the CCP staples after 6 hour rotary followed by 42 hour static seeding. The adhered cells were seen to spread in the grooves by actin/DAPI staining which clearly illustrates the polarization of the cell nuclei and cytoskeleton (Fig.4.3a). Also the filopodial projections could be observed by SEM imaging (Fig.4.3b). This combined method of rotary and static seeding enabled more uniform distribution of cells on the staples as opposed to just static seeding. In addition, any excess cells non adherent to the staples would adhere to the well bottom and allowed them to be screened away from the cells adhered to the staples.

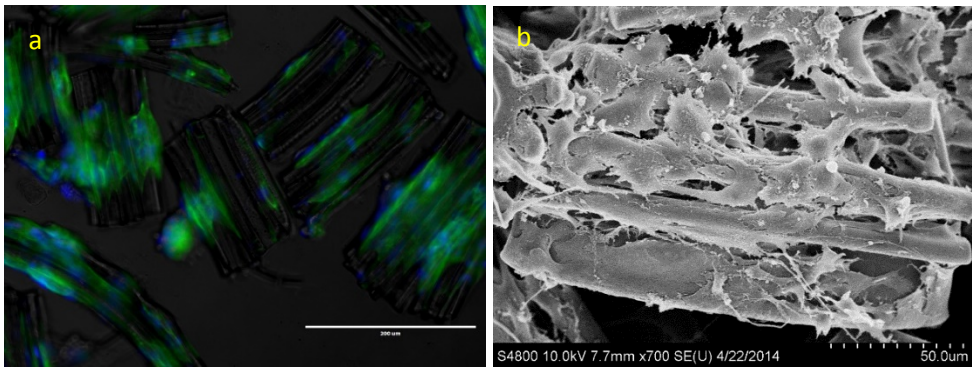


**Fig.4.3.** 3T3 cells on CCP staples after 48 hours in culture (a). Actin filaments (green) and nuclei (blue) indicate spread of cells inside the staple grooves (b). SEM image showing filopodial projections on staple

## Validation of injectability

Staple injectability was tested by injecting CCP staples through 21G needle at concentration of 5mg/ml. Viable adherent cells were stained with Calcein AM before passing through the injection needle. Images were taken before and after the injectability

test. It was found that staples retained viable cells when passed through 21 gauge needle (Fig.4.4).

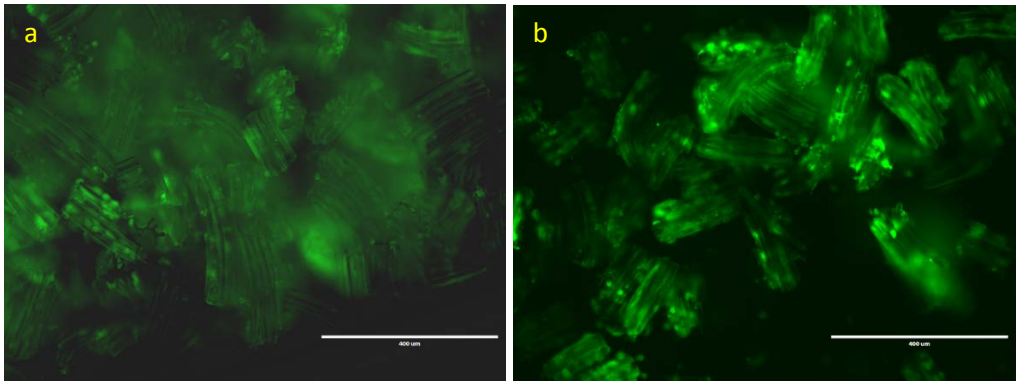


**Fig.4.4.** Injectability of CCP seeded 3T3 fibroblasts stained live with Calcein AM (a).before and (b). after injection through 21G needle (Scale bar = 400 um)

## Cell-staple encapsulation and growth within hydrogel composites

Cell adhesion and proliferation are crucial to designing scaffolds for tissue engineering [36]. In order to employ the microengineered 3D hydrogel-staple composites for tissue engineering applications, encapsulated cells must demonstrate viability and proliferation over time. We encapsulated NIH3T3 fibroblasts as a model cell line in this study. Hydrogel composite semi-IPNs were made by blending PEG-DA macromers, hyaluronic acid and GRGDS-acrylate with CCP staples to investigate the effect of staples as microcarriers for cell growth and proliferation. Gels without staples were used as controls. Each gel contained approximately 225 µg of staples and 69000 cells.

We compared the response of round fiber cross-section staples using the same hydrogel composite system, but cells would aggregate the round staples and prevent homogeneous distribution in the bulk of the hydrogel during crosslinking. The CCP

counterpart, allows the staples to remain non-aggregated and separated during photocrosslinking (Fig.4.5).

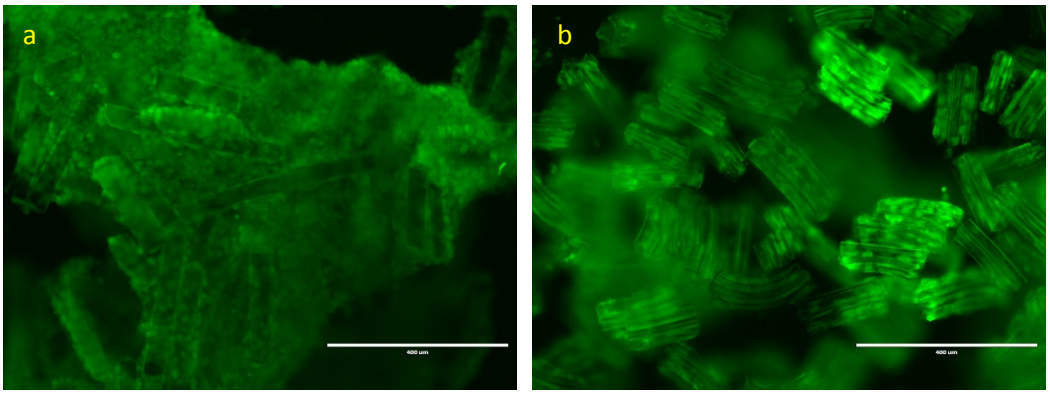


**Fig.4.5.** Cell adhesion to staples 48 hours post seeding (a). Round cross-section staples show aggregate formation (b). CCP cross-section staples show no aggregation and well dispersed. (Scale bar 400um, Magnification 10x, Green = Calcein AM live stain)

Cell growth in the hydrogel composites was qualitatively observed by laser confocal microscopy. Live cell staining showed that the fibroblasts in hydrogel composites were highly viable and proliferating with time during the culture (Fig.4.6). At Day 10, conspicuous signs of increased cell number could be observed with the staples at the core of expanding cell colonies. From day 14 onwards, the cell colonies merged to form high cell density areas as compared to the control gels. The control gels without staples demonstrated round but viable cells over 3 weeks (Fig.4.7). These cells did not exhibit any form of spreading or proliferation but formed aggregates that would exude out of the gel periphery at Day 21. The observations from laser confocal imaging were also be corroborated by macroscopic imaging as shown in Figs. 4.6 & 4.7. 3D rendering of the cell behavior comparison in composite and control gels is also shown at Day 1 and Day 21 time points in Fig. 4.8.

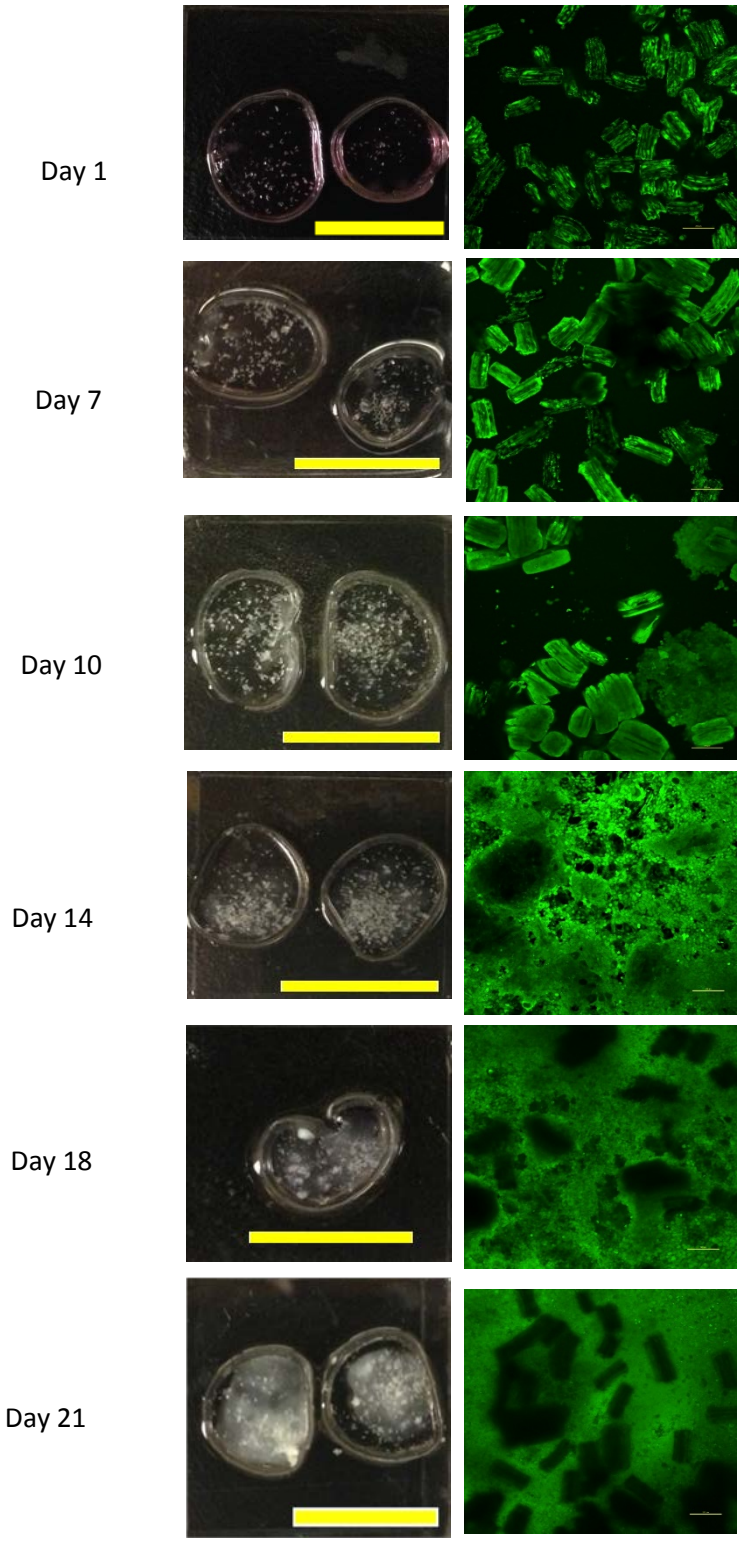


**Fig.4.6.** Fluorescent images of live 3T3 fibroblasts grown in hydrogel composites (PEGdA/HA/PLA staples). Cell seeded staple encapsulation density was 5 mg $ml^{-1}$. 3T3 fibroblasts were labeled with live cell stain Calcein AM. [Scale bar on columns denotes- left 1 cm, right 200µm]

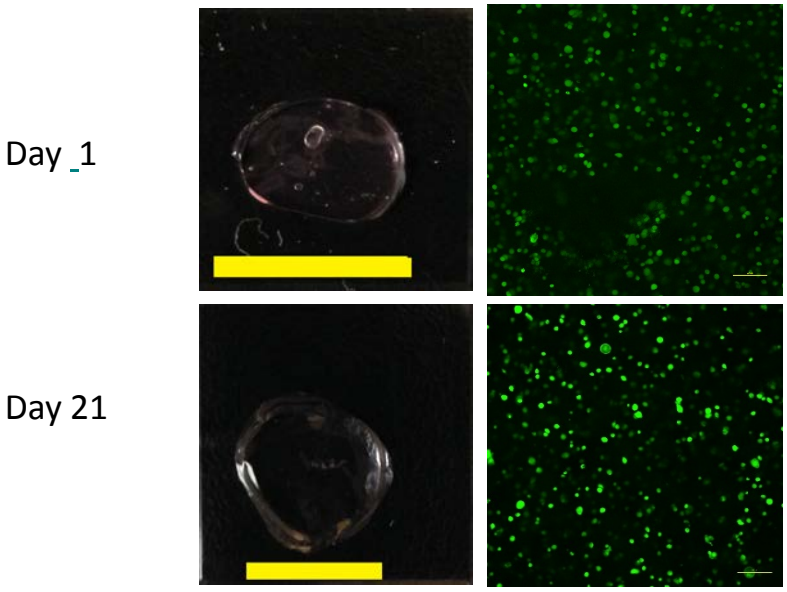


**Fig.4.7.** Fluorescent images of live 3T3 fibroblasts grown in hydrogel controls (PEGdA/HA). Cell encapsulation density was $1.5x10^6$ cells $ml^{-1}$. 3T3 fibroblasts were labeled with live cell stain Calcein AM. (Scale bar on columns denotes- left 1 cm, right 200µm)

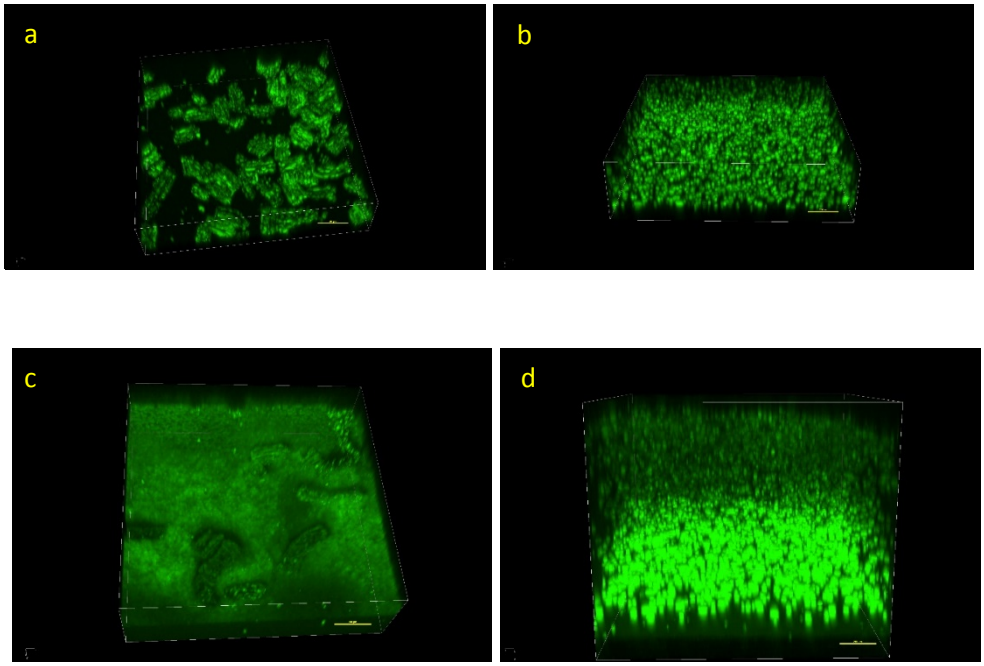


**Fig.4.8.** 3D Z-stack image of fibroblasts grown in (a) Day 1 hydrogel composite (PEGdA/HA/PLA staples) (b). Day 1 hydrogel control (PEGdA/HA) (c). Day 21 hydrogel composite (PEGdA/HA/PLA staples (d). Day 21 hydrogel control (PEGdA/HA). Cell seeded staple encapsulation density was 5 mg $ml^{-1}$. 3T3 fibroblasts were labeled with live cell stain Calcein AM. [Scale bar = 200µm]

In addition to qualitative determination of cell proliferation in the 3D composite gels using confocal imaging, we also quantified the proliferation using Picogreen assay for ds-DNA. The composite hydrogels demonstrated increase in cell number by almost ten-fold by Day 21 when compared to Day 1. No significant difference in cell proliferation was observed among the controls after 21 days (Fig.4.9).

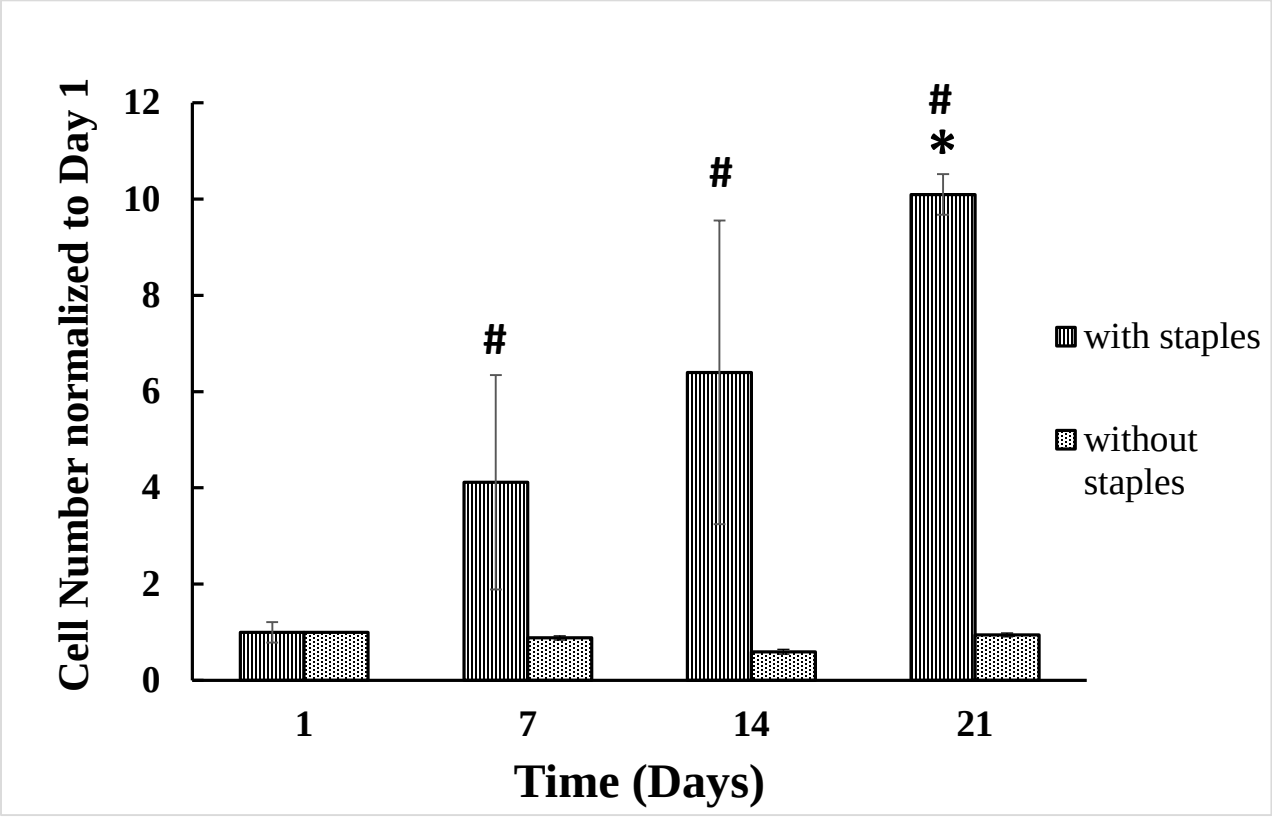


**Fig.4.9.** Proliferation of NIH3T3 fibroblasts in hydrogel composites (PEGdA/HA/Staples) and PEGdA/HA controls. Cells were encapsulated at $1.5x10^6$ cells $ml^{-1}$. Cell number was determined by Picogreen assay for DNA. One way ANOVA revealed differences between Day 1 and Day 21 for the composite gels ($p<0.05$, * vs Day 1 composite, # vs Day 1 control)

## **DISCUSSION:**

In this manuscript, the use of PEGdA/HA-CCP staple composite hydrogel system for cell culture and tissue engineering applications has been demonstrated. PEGdA hydrogels were blended with hyaluronic acid (HA) and cell adhesion motif peptide GRGDS-acrylate. Signals from RGD sequences induce direct and specific $\alpha_5\beta_1$ integrin binding [37] and cells form focal contacts at the integrin-binding sites by synthesizing focal adhesion proteins (namely vinculin, paxillin, talin) that in turn connect to cytoskeletons [38].

The gels were mixed with cell laden microcarrier CCP staples and photocrosslinked. The hydrogel composite showed excellent cell proliferation as compared to control gels. The microcarrier based composite offers a unique method for cell amplification at site of defect *in situ* by serving as substrates for the propagation of anchorage-dependent cells. A composite integrating the microcarriers inside a hydrogel can not only provide a suitable platform for cellular focal adhesion but in addition facilitates the cells to overcome gel enlacement and fully spread out into their natural morphology [34]. This system can be translatable into delivery of expanded culture of undifferentiated or differentiated cells. The encapsulation of the microcarriers within biocompatible and injectable hydrogels enhances the viability of cells at the repair site. For instance, angiogenesis was demonstrated when endothelial cell laden gelatin coated Cytodex-3 microcarriers were entrapped in three dimensional fibrin matrix with fibronectin, basic fibroblast growth factor (bFGF) and vascular endothelial growth factor (VEGF) [39]. It was shown that mere proliferation and migration was not essential for capillary formation, but that inter-cellular adhesion was a crucial factor for efficient neovessel formation. Apart

from promoting intercellular attachment, encapsulation within a matrix can lend a protective and trophic environment for the cells to endure shear forces during injection delivery to the defect site.

One step further would be the development of microcarriers which allow the cells to maintain their natural phenotype. It is widely accepted that the phenotype of cells in two-dimension culture is very different from their behavior in three dimensions [40]. Micro and nano sized scale features can be used to mimic the natural ECM microenvironment of tissues [41]. To that end, we were interested in exploring the role of topographical features on cell adhesion, polarization and proliferation for various tissue engineering applications. In this work, we studied the effect of a uniquely designed capillary channel polymer (CCP) fiber staples and its topographic effect on cell polarization and proliferation inside a synthetic hydrogel. The staples were coated with fibronectin for aiding the adhesion of fibroblasts, in addition the presence of cross-linked peptide cell adhesion motif GRGDS in the bulk of the hydrogel also helps the cells to interact with the otherwise synthetic matrix by integrin binding.

Nanofibrous polyglycerol sebacate (PGS) staples have been explored by Ravichandran et al for injectable cardiomyocytes delivery within an infarct [42]. They observed that the morphology of the short fiber staples was retained after passing through an 18G needle. These fibers were of length 3.8 μm and diameter of 1 μm. However, they did not show how cell laden short fibers would respond to passage through the injection needle. In our work, we have explored the viability of CCP fiber staples in the micron – size range – length ~180μm and diameter ~50 μm with cells adhering and retaining viability and remaining adherent to the staples even upon passing through 21G needle.

The cells in the control gels did not show any proliferation over 3 weeks which supports our hypothesis that physical topographic support plays an important role in cell

proliferation. This NIH3T3 cell response in control gels is contrary to normal human dermal fibroblast (NHDF) response when encapsulated in PEGdA/HA blend gels [16] wherein 1.5 fold proliferation was recorded in 14 days compared to Day 1. This is consistent with Shu et al, who also showed 1.5 times increase in T-31 fibroblast after 15 days culture inside the HA-DTPH-PEGdA hydrogel [43]. In our work, we were able to demonstrate 10 fold increase in cell number in hydrogel composite samples over 3 weeks by Picogreen assay which quantifies the increase in double stranded DNA (dsDNA). The importance of physical support in the form of microcarriers is corroborated by the fact that no increase in cell number was observed in the control gels (Fig.4.9).

The isotropic nature of the hydrogels can be overcome by integrating topographic structures to induce anisotropy and cell polarization. The resulting composite could topographically mimic the ECM to control cell adhesion, morphology and tissue architecture. In the composite gels developed in this work, the presence of physical topographic support by the CCP staples perhaps orients the cell cytoskeleton in a manner which induces higher ECM production and hence proliferation [44-46]. Substratum topography can serve as a means of manipulating cell function because surfaces provide a two-pronged biomimetic extracellular physical milieu and cell stimulating cue.

Of special long term interest to us is the ability to induce adhesion, polarization and thereby differentiation of neural stem cells in an injectable hydrogel system for neural regeneration purposes. This is because for stem cells, the ability to control and regulate cell proliferation in 3D is crucial for cell differentiation fate and proliferation. Using the composite system developed in this work, we can expand NSCs in three dimensions in the bulk by contact with the staples followed by induction of differentiation.

## **CONCLUSION**:

A biodegradable hydrogel-fibrous staple composite demonstrating sustained cell survival and proliferation was developed. 3T3 fibroblasts pre-seeded on CCP staples when encapsulated in PEGdA/HA hydrogel blends, showed high proliferation as compared to control gels without CCP staple microcarriers. The physical properties of the composite system demonstrated cell cluster formation around the staples in 3D by proliferation. This study indicated that the hydrogel-staple composite may have promising potential in various tissue regeneration applications involving stem cell proliferation and differentiation. Future studies could include incorporation of neural stem cells to induce differentiation into neural lineage for targeting CNS trauma and neurodegenerative disease.

## References:


[1] Rutkowski G, Miller CA, Mallapragada S. Processing of polymer scaffolds: solvent casting. Academic Press, San Diego, CA; 2002. p. 681-6.

[2] ON EME. Bone marrow cell colonization of, and extracellular matrix expression on, biodegradable polymers. Cells and Materials 1997;7:223-34.

[3] Harris LD, Kim B-S, Mooney DJ. Open pore biodegradable matrices formed with gas foaming. 1998.

[4] Hall H. Modified fibrin hydrogel matrices: both, 3D-scaffolds and local and controlled release systems to stimulate angiogenesis. Current pharmaceutical design 2007;13:3597-607.

[5] Cai S, Liu Y, Zheng Shu X, Prestwich GD. Injectable glycosaminoglycan hydrogels for controlled release of human basic fibroblast growth factor. Biomaterials 2005;26:6054-67.

[6] Pack DW, Hoffman AS, Pun S, Stayton PS. Design and development of polymers for gene delivery. Nature Reviews Drug Discovery 2005;4:581-93.

[7] Norman JJ, Desai TA. Methods for fabrication of nanoscale topography for tissue engineering scaffolds. Annals of biomedical engineering 2006;34:89-101.

[8] Kim EJ, Boehm CA, Mata A, Fleischman AJ, Muschler GF, Roy S. Post microtextures accelerate cell proliferation and osteogenesis. Acta biomaterialia 2010;6:160-9.

[9] Yang J-H, Lin S-H, Lee Y-D. Preparation and characterization of poly (l-lactide)–graphene composites using the in situ ring-opening polymerization of PLLA with graphene as the initiator. Journal of Materials Chemistry 2012;22:10805-15.

[10] Carlberg B, Axell MZ, Nannmark U, Liu J, Kuhn HG. Electrospun polyurethane scaffolds for proliferation and neuronal differentiation of human embryonic stem cells. Biomedical Materials 2009;4:045004.

[11] Xie J, Willerth SM, Li X, Macewan MR, Rader A, Sakiyama-Elbert SE, et al. The differentiation of embryonic stem cells seeded on electrospun nanofibers into neural lineages. Biomaterials 2009;30:354-62.

[12] Lim SH, Liu XY, Song H, Yarema KJ, Mao H-Q. The effect of nanofiber-guided cell alignment on the preferential differentiation of neural stem cells. Biomaterials 2010;31:9031-9.

[13] Lee KY, Mooney DJ. Hydrogels for tissue engineering. Chemical reviews 2001;101:1869-80.

[14] Davis HE, Leach JK. Hybrid and Composite Biomaterials in Tissue Engineering. Topics in multifunctional biomaterials and devices 2008.

[15] Jia X, Kiick KL. Hybrid multicomponent hydrogels for tissue engineering. Macromolecular bioscience 2009;9:140-56.

[16] Kutty JK, Cho E, Soo Lee J, Vyavahare NR, Webb K. The effect of hyaluronic acid incorporation on fibroblast spreading and proliferation within PEG-diacrylate based semi-interpenetrating networks. Biomaterials 2007;28:4928-38.

[17] Zhu J. Bioactive modification of poly (ethylene glycol) hydrogels for tissue engineering. Biomaterials 2010;31:4639-56.

[18] Almany L, Seliktar D. Biosynthetic hydrogel scaffolds made from fibrinogen and polyethylene glycol for 3D cell cultures. Biomaterials 2005;26:2467-77.

[19] Ifkovits JL, Burdick JA. Review: photopolymerizable and degradable biomaterials for tissue engineering applications. Tissue engineering 2007;13:2369-85.

[20] Van Wezel A. Growth of cell-strains and primary cells on micro-carriers in homogeneous culture. Nature 1967;216:64-5.

[21] Malda J, Frondoza CG. Microcarriers in the engineering of cartilage and bone. Trends in biotechnology 2006;24:299-304.

[22] Varani J, Bendelow MJ, Chun JH, Hillegas WA. Cell growth on microcarriers: comparison of proliferation on and recovery from various substrates. Journal of biological standardization 1986;14:331-6.

[23] Malda J, Van Blitterswijk C, Grojec M, Martens D, Tramper J, Riesle J. Expansion of bovine chondrocytes on microcarriers enhances redifferentiation. Tissue engineering 2003;9:939-48.

[24] Abranches E, Bekman E, Henrique D, Cabral J. Expansion of mouse embryonic stem cells on microcarriers. Biotechnology and bioengineering 2007;96:1211-21.

[25] Fernandes A, Fernandes T, Diogo M, da Silva CL, Henrique D, Cabral J. Mouse embryonic stem cell expansion in a microcarrier-based stirred culture system. Journal of biotechnology 2007;132:227-36.

[26] Yang Y, Rossi F, Putnins EE. Ex vivo expansion of rat bone marrow mesenchymal stromal cells on microcarrier beads in spin culture. Biomaterials 2007;28:3110-20.

[27] Frauenschuh S, Reichmann E, Ibold Y, Goetz PM, Sittinger M, Ringe J. A Microcarrier-Based Cultivation System for Expansion of Primary Mesenchymal Stem Cells. Biotechnology progress 2007;23:187-93.

[28] Cytodex Surface Microcarriers GE Healthcare Biosciences AB. p. Cytodex Surface Microcarriers.

[29] Lafrance ML, Armstrong DW. Novel living skin replacement biotherapy approach for wounded skin tissues. Tissue engineering 1999;5:153-70.

[30] Voigt M, Schauer M, Schaefer D, Andree C, Horch R, Stark G. Cultured epidermal keratinocytes on a microspherical transport system are feasible to reconstitute the epidermis in full-thickness wounds. Tissue engineering 1999;5:563-72.

[31] Bayram Y, Deveci M, Imirzalioglu N, Soysal Y, Sengezer M. The cell based dressing with living allogenic keratinocytes in the treatment of foot ulcers: a case study. British journal of plastic surgery 2005;58:988-96.

[32] Sinclair KD, Webb C, Brown PJ. Capillary channel polymer fibers as structural templates for ligament regeneration. Am Assoc Text Chem Colorists 2008;8:36-40.

[33] Sinclair KD, Webb K, Brown PJ. The effect of various denier capillary channel polymer fibers on the alignment of NHDF cells and type I collagen. Journal of Biomedical Materials Research Part A 2010;95:1194-202.

[34] Wang C, Gong Y, Zhong Y, Yao Y, Su K, Wang D-A. The control of anchorage-dependent cell behavior within a hydrogel/microcarrier system in an osteogenic model. Biomaterials 2009;30:2259-69.

[35] Hern DL, Hubbell JA. Incorporation of adhesion peptides into nonadhesive hydrogels useful for tissue resurfacing. Journal of biomedical materials research 1998;39:266-76.

[36] Khademhosseini A, Vacanti JP, Langer R. Progress in tissue engineering. Scientific American 2009;300:64-71.

[37] Chien H-W, Tsai W-B. Fabrication of tunable micropatterned substrates for cell patterning via microcontact printing of polydopamine with poly (ethylene imine)-grafted copolymers. Acta biomaterialia 2012;8:3678-86.

[38] Ventre M, Causa F, Netti PA. Determinants of cell–material crosstalk at the interface: towards engineering of cell instructive materials. Journal of The Royal Society Interface 2012;9:2017-32.

[39] Nehls V, Drenckhahn D. A novel, microcarrier-based in vitro assay for rapid and reliable quantification of three-dimensional cell migration and angiogenesis. Microvascular research 1995;50:311-22.

[40] Nehls V, Schuchardt E, Drenckhahn D. The effect of fibroblasts, vascular smooth muscle cells, and pericytes on sprout formation of endothelial cells in a fibrin gel angiogenesis system. Microvascular research 1994;48:349-63.

[41] Murugan R, Ramakrishna S. Nano-featured scaffolds for tissue engineering: a review of spinning methodologies. Tissue engineering 2006;12:435-47.

[42] Ravichandran R, Venugopal JR, Sundarrajan S, Mukherjee S, Sridhar R, Ramakrishna S. Minimally invasive injectable short nanofibers of poly (glycerol sebacate) for cardiac tissue engineering. Nanotechnology 2012;23:385102.

[43] Shu XZ, Ghosh K, Liu Y, Palumbo FS, Luo Y, Clark RA, et al. Attachment and spreading of fibroblasts on an RGD peptideâ€“modified injectable hyaluronan hydrogel. Journal of Biomedical Materials Research Part A 2004;68:365-75.

[44] Lee CH, Shin HJ, Cho IH, Kang Y-M, Kim I, Park K-D, et al. Nanofiber alignment and direction of mechanical strain affect the ECM production of human ACL fibroblast. Biomaterials 2005;26:1261-70.

[45] Zhong S, Teo WE, Zhu X, Beuerman RW, Ramakrishna S, Yung LYL. An aligned nanofibrous collagen scaffold by electrospinning and its effects on in vitro fibroblast culture. Journal of biomedical materials research Part A 2006;79:456-63.

[46] Bashur CA, Dahlgren LA, Goldstein AS. Effect of fiber diameter and orientation on fibroblast morphology and proliferation on electrospun poly (d, l-lactic- co-glycolic acid) meshes. Biomaterials 2006;27:5681-8.

# CHAPTER 5

## ENGINEERING STEM CELL FATE USING COMPOSITE SCAFFOLD

### INTRODUCTION:

Biodegradable scaffolds provide a temporal structural support for transplanted stem cells. In addition, the scaffold also delivers bioactive signals for stem cell differentiation, either in the form of released/immobilized trophic factors or through topographic microarchitecture and appropriate biomechanical properties. However, the nervous tissue is extremely complicated. It starts off as the neural plate - a flat sheet of cells on the top surface of the embryo, and undergoes a series of elaborate deformations, resulting in morphogenetic transformation into a hollow tube [1]. One end of this neural tube eventually forms the brain and the other end forms the spinal cord. This complex formation of the nervous system makes it difficult to design an intricate scaffold that would simulate the growth of nervous tissue. While stem cell therapy is a viable option for CNS treatments, many challenges need to be addressed including low cell survival, lack of control on stem cell fate and low cell engraftment and integration with existing neuronal circuitry after transplantation [3]. Though overcoming these obstacles is challenging, the design of structures that mimic the native stem cell niches for transplanted cells can be promising. So, the need to develop a suitable cell laden scaffold which can serve as a cell proliferation platform and also induce differentiation at the transplant site is substantial.

NSCs are self-renewing, multipotent stem cell populations that are present in both the developing and adult mammalian CNS [3]. They are responsible for generating neurons and glia in developing brain and so play a key role in augmenting the otherwise limited ability of the adult CNS to regenerate after injury or disease [4]. NSCs exist as neuroepithelial stem cells in the embryonic neural tube. When the tube undergoes

symmetric division, the NSCs exist as radial glia cells and begin to generate neuronal lineages by asymmetrically dividing within the germinal ventricular zone (GVZ). NSCs then acquire gliogenic competency and produce glial progenitor cells, which proliferate mostly in a second germinal or subventricular zone (SVZ) – located along the lateral wall of the lateral ventricle [5]. By the postnatal stage, most of the radial glia transform into astrocytes and the ventricular zone disappears. Some portion of the SVZ is retained in the adult CNS and serves as one of the primary sites for neurogenesis [6]. These sites are highly significant when considering neural tissue engineering approaches. Two approaches can be considered for NSC mediated regeneration – activation of endogenous stem cells or transplantation of neural stem cells [7, 8]. The regenerative capacity of the endogenous stem cells is very low since they are unable to reconstitute the structural architecture of the CNS.

Transplantation of NSCs is a more promising approach for CNS regeneration although the fate of transplanted cells is determined by the type of injury/disease and the biochemical and biomechanical microenvironment at the site [8]. The hostile environment at the site affects the survival and functionality of the transplanted cells [9]. Rather than direct injection, the creation of the physiological stem cell niche is a more efficient approach [10]. This niche should be a specialized conglomerate providing the correct architecture and containing the required biochemical cytokines/growth factors and signals apart from the right biomechanical properties of native environment [11]. These requirements are important to consider in the development of a biomaterial to mimic the microenvironment [12, 13]. A variety of biomaterials such as hydrogels and nanofibers have been explored towards this end. Hydrogels are of particular interest in this case because of their close resemblance to soft tissues, owing to their cross-linked hydrophilic polymer network. The crosslink density of the polymer network can be tuned to match the

mechanical properties of the CNS tissue. Also, hydrogels are injectable and *in situ* crosslinkable, which makes them a minimally invasive and defect conforming scaffold. Hydrogels can assist in angiogenesis, prevent immune response and inhibit glial scarring as well. However, hydrogels are isotropic and may not strictly control the differentiation fate of NSCs as desired. The fate can be specified by inducing the cells towards a morphological shape that would facilitate their differentiation by cytoskeletal rearrangement of actin filaments and focal adhesion complexes, thus bringing about a signal transduction from the extrinsic mechanical signaling to intrinsic intracellular signaling [14, 15].

The differentiation response of NSCs to surface topography has been widely studied. Aligned nanofibers exhibited higher differentiation into neurons as compared to random counterpart and planar control [16]. Bakhru et al showed that NSCs adhered on and in close proximity to aligned fibers showed more differentiation inclination towards neuronal lineage while cells further away from the fibers differentiated into astrocytes [17]. They also showed that the differentiation into neurons was induced in cells not immediately on fibers by paracrine signaling from cells on the fibers. Hseih et al developed a composite gel-fiber scaffold made of hyaluronan-methylcellulose (HAMC) and polycaprolactone-co-D,L-lactide [P(CL:DLLA)] that induced higher differentiation into neurons and oligodendrocytes than HAMC itself [18].

The process of differentiation into neuronal lineage is not straightforward. The architecture and topography of the scaffold alone does not promote differentiation; so the media is supplemented with chemical inducers that stem the process of cell proliferation and induce biochemical signaling pathways that result in differentiation. Retinoic acid is involved in the induction of neural differentiation, motor axon growth and neural patterning [19]. Axon outgrowth and nerve regeneration are triggered in adults in response to

elevated RA signaling. RA also maintains the differentiated state of adult neurons and altered RA signaling leads to neurodegenerative diseases as Parkinson's and Alzheimer's disease. RA is a metabolic product of vitamin A (retinol). When retinol binds to retinol-binding protein 4 (RBP4), it is taken up by cells through a membrane receptor (STRA6) that interacts with the RBP4. In embryos, retinol dehydrogenase 10 (RDH10) metabolizes retinol to retinaldehyde (Ral), which is then metabolized to RA by retinaldehyde dehydrogenases (RALDHs). RA can be released from the cytoplasm and taken up by the receiving cell (paracrine signaling), or can act back on its own nucleus (autocrine signaling). Cellular retinoic-acid-binding protein 2 (CRABP2) assists RA entry into the nucleus. In the nucleus, RA binds to RA receptors (RARs) and retinoid X receptors (RXRs), which themselves heterodimerize and bind to a sequence of DNA that is known as the retinoic acid-response element (RARE). This binding activates the transcription of target genes. RA is catabolized in the cytoplasm by the CYP26 class of P450 enzymes [19].

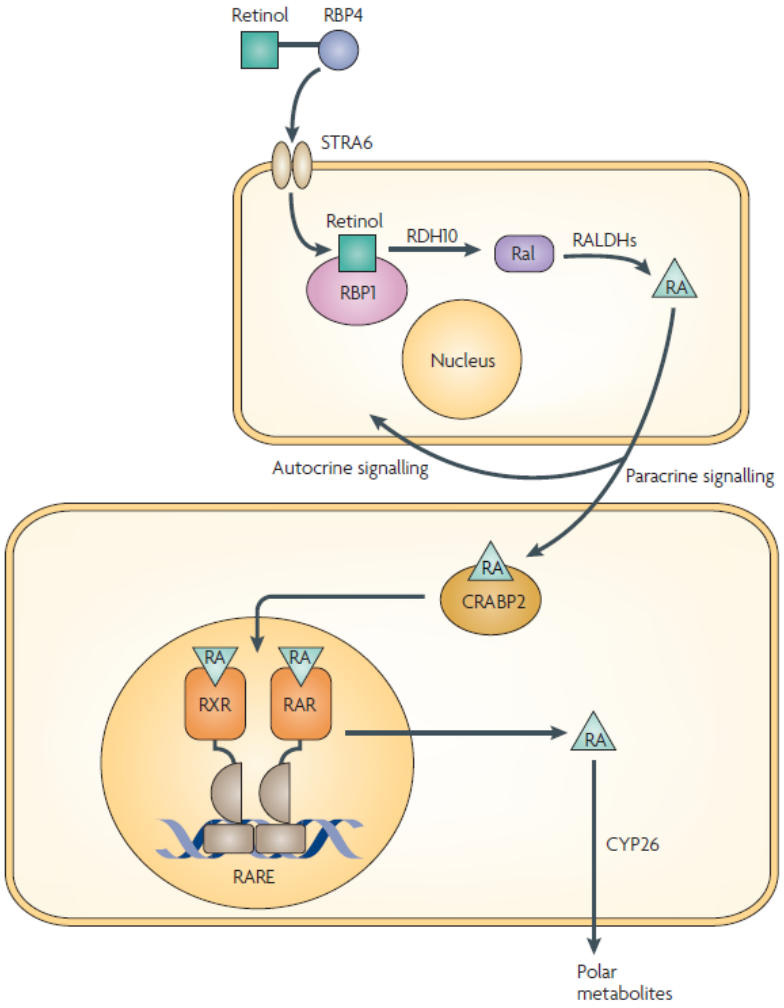


**Fig.5.1.** Pathways that are involved in the generation, action and catabolism of retinoic acid (RA) [19]

In this study, NSCs were adhered to a unique microcarrier and encapsulated within a photocrosslinkable hydrogel. Capillary channel polymer (CCP) fiber staples (~200 µm) were used as microcarriers and crosslinked within PEGdA-HA blend hydrogel. The concept was to induce proliferation of the NSCs, followed by neuronal differentiation on the specialized groove channel topography of the staple with added induction by retinoic acid (RA). The work validates adhesion of NSCs to the microcarriers and investigates the bioactivity of topography by itself or in conjunction with RA. NE-4C mouse neuroepithelial

cell lines were chosen for this study. These NSCs have been established to differentiate into neurons in response to all-trans RA [20].

## MATERIALS AND METHODS

### Preparation of 2D spin cast samples

Microscopic glass slides were cut with a diamond scribe into 2.5 cm x 1.5 cm pieces and cleaned with acetone and water and blow dried with compressed air. The slides were then treated with Piranha solution (3:1 Sulfuric acid : 30% Hydrogen peroxide) and rinsed thoroughly with distilled water. Poly-l-lactide (PLLA, Natureworks, Minnetonka, MN) was dissolved at 10% w/v in dichloromethane and spin coated on the glass slides at 2000 rpm and dried in vacuum for 48 hours to completely remove the dichloromethane. The samples were physisorbed with either fibronectin (20µg/ml, F1141-5MG, Sigma) or laminin (20µg/ml, #23017-015, Life technologies, Carlsbad, CA) overnight at room temperature followed by washing twice with sterile Phosphate Buffer Solution (PBS). For the laminin samples, polylysine (0.01% in water) was pre-coated on the samples for 1 hour, followed by washing twice with sterile distilled water, after which laminin or was adsorbed overnight. For controls, 0.01% polylysine (MW 150000-300000, # P1399-100MG, Sigma) was coated overnight and washed with distilled water twice. The substrates were incubated in cell culture media at 37˚C until seeding within one hour.

**Preparation of fiber samples**

Double sided tape was placed on two opposite edges of round glass cover slips (#26024, Ted Pella, Redding, CA). CCP fibers were aligned and secured between the taped portions of each coverslip. These samples were sterilized by exposure to UV for 1 hour in 12 well plate. The samples were physisorbed with either 15 µg/ml poly-l-lysine (MW 150000-300000, # P1399-100MG, Sigma) or fibronectin (20µg/ml, F1141-5MG, Sigma) overnight at room temperature followed by washing twice with sterile water. The substrates were incubated in cell culture media at 37˚C until seeding within one hour.

**Cell culture and seeding**

Mouse-derived NE-4C neuroectodermal cells (ATCC® CRL-2925) were cultured in poly-l-lysine pre-coated 75cm$^2$ tissue culture flasks with EMEM media (ATCC 30-2003, Manassas, VA) supplemented with 4mM L-glutamine, 10% (v/v) bovine growth serum (Hyclone, Logan UT), and 50 U/mL penicillin and 50 µg/mL streptomycin (Mediatech). Medium was changed every 2 days and cells were maintained in a tissue culture incubator at 37ºC with 5% carbon dioxide ($CO_2$).

For cell adhesion, the staples were incubated with poly-l-lysine (15 µg/ml, MW 150000-300000, # P1399-100MG, Sigma) in a micro-centrifuge tube overnight at room temperature attached to a rotary cell culture system (Synthecon Inc., Houston, Texas) rotating at 15 rpm and then washed with 1X PBS. PLL-coated staples (15mg) were seeded with 1x10$^6$ cells in 1 ml medium in a 1.5 ml micro-centrifuge tube and incubated on a rotary platform (15 rpm) housed in a cell culture incubator for 6 hr. The staples were allowed to settle and the supernatant was discarded. The cell-seeded staples were then transferred to a 24 well plate at 7.5 mg per well and incubated for 42 hours. This method allowed any

remaining non-adherent cells to be removed by attachment to the bottom of the well. The seeding efficiency on the CCP staples was assessed by SEM imaging at 48 hours (Calcein AM, Life Technologies, Carlsbad, CA). For SEM imaging, cell-seeded staples were fixed in paraformaldehyde, dehydrated in a series of ethanol washes, immersed in hexamethyldisilazane (United Chemical Technologies, Bristol, PA) and air dried on glass cover slips at room temperature overnight in fume hood. The samples were then mounted on stainless steel SEM stubs, coated with platinum, and imaged at 10 kV image beam intensity (Hitachi S-4800).

For 2D polystyrene tissue culture plastic (TCP) or 3D CCP fiber samples, NSCs were seeded in 12 well cell culture plate at 1.8 x $10^5$ cells/well.

To induce differentiation of NSCs, culture media containing $10^{-6}$ retinoic acid (RA) was administered 48 hours post cell seeding. A$10^{-2}$ M stock solution of *all-trans* RA (Sigma) in dimethylsulfoxide (DMSO) was stored in -80°C. Culture media was changed every other day and RA supplementation was diluted directly in to the culture medium whenever fresh medium was added.

**Immunostaining of mNSCs**

To evaluate cell morphology and cytoskeletal organization, cells were fixed in 4% paraformaldehyde for 1 hour, permeabilized with 0.1% Triton X-100, and stained with Anti mouse β-III Tubulin produced in Rabbit (1:500, mouse IgG, Sigma, MO) to identify neurons. As secondary antibody goat anti-rabbit IgG Alexa 488 (Life Technologies, Carlsbad, CA) was used at 1:200 dilution in staining media. The nuclei were stained with

4',6-diamidino-2-phenylindole (DAPI, Life Technologies). Fluorescence images were captured using an AMG EVOS microscope (Fisher Scientific, Pittsburgh, PA).

**Synthesis of PEG-dA macromers with ester linkages containing variable alkyl spacers**

Three different types of PEG-DA macromers with varying susceptibility to hydrolytic degradation were synthesized by a two-step process as previously reported [32]. Briefly, PEG (4000 MW, Fluka, Buchs, Switzerland) was reacted with either choroacetyl chloride, 2-chloropropionyl chloride, or 4-chlorobutuyrl chloride (Sigma-Aldrich, St. Louis, MO) in the presence of triethylamine (TEA, Sigma-Aldrich) at a 1:4:1.8 molar ratio in dry dichloromethane (Sigma-Aldrich). After 24 hours reaction at room temperature, the reactants were filtered, washed with sodium bicarbonate and water, dried with anhydrous sodium sulfate, and then precipitated in ethyl ether. After recovery, each resulting intermediate product was reacted with sodium acrylate (5X molar ratio) in dry dimethylformamide (Acros, Morris Plains, NJ) for 30 hours at 50, 85, and 100 ºC to yield PEG-bis (acryloyloxy acetate) [PEG-bis-AA], PEG-bis-(acryloyloxy propanoate) [PEG-bis-AP] and PEG-bis-(acryloyloxy butyrate) [PEG-bis-AB], respectively. The products were purified by filtration, rotary evaporation, and precipitation in ethyl ether and dried under vacuum.

**Preparation of staple-hydrogel composites**

HA (2% w/v, 1.5 MDa, LifeCore Biomedical, Chaska, MN) and PEG-DA (30% w/v) stock solutions were prepared in 1X-PBS (0.1M, pH 7.4). Acryl-PEG-GRGDS was synthesized by conjugating GRGDS peptide (Bachem, Torrance, CA) to acryl-PEG-NHS

(Jenkem, Beijing, China) as previously described [21]. Gel precursor solutions were prepared containing PEG-DA (6% w/v), HA (0.36% w/v 1.5 MDa), acryl-PEG-GRGDS (1 mM), 2-hydroxy-1-[4-(hydroxyethoxy) phenyl]-2-methyl-1-propanone (I-2959, BASF, Florham Park, NJ, 0.1% w/v), and cell seeded staples (5 mg/ml). Sample volumes (45 µl) were pipetted in between glass coverslips separated by 1 mm Teflon spacers and exposed to low intensity UV light (365nm, 10mW/cm$^2$, Black-Ray B100-AO, Upland, CA) for 5 minutes on each side of the disc. Hydrogels with encapsulated staples were cultured in 12 well plate wells with 2mL culture medium per well.

## RESULTS AND DISCUSSION:

### Validation of CCP staple as NSC microcarrier

The seeding efficiency and adherence of NE-4C NSCs to polylysine coated polylactide staples (~180 µm) using the rotary and static seeding method was validated by SEM imaging. As can be seen in Fig.5.2, the cells are adhered to the staple and also extending filopodia.

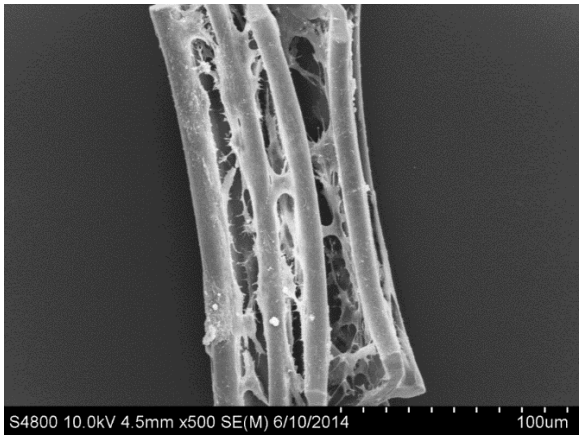


**Fig.5.2.** SEM image showing NSCs on CCP staples after 48 hours in culture SEM image

## Investigation of NSC differentiation

NSCs being anchorage dependent cells, different ligands were tested as effective adhesion molecule to support the adhesion and growth of NSCs. First, the response of NSCs on two dimensional polylactide films was investigated, followed by the response on three dimensional CCP fibers. Polylysine coated tissue culture plates were used as controls while polylactide films were coated with cell adhesive ligands – fibronectin or laminin. Laminin was coated in the traditional Polylysine/laminin manner. RA was administered 24 hours after cell seeding.

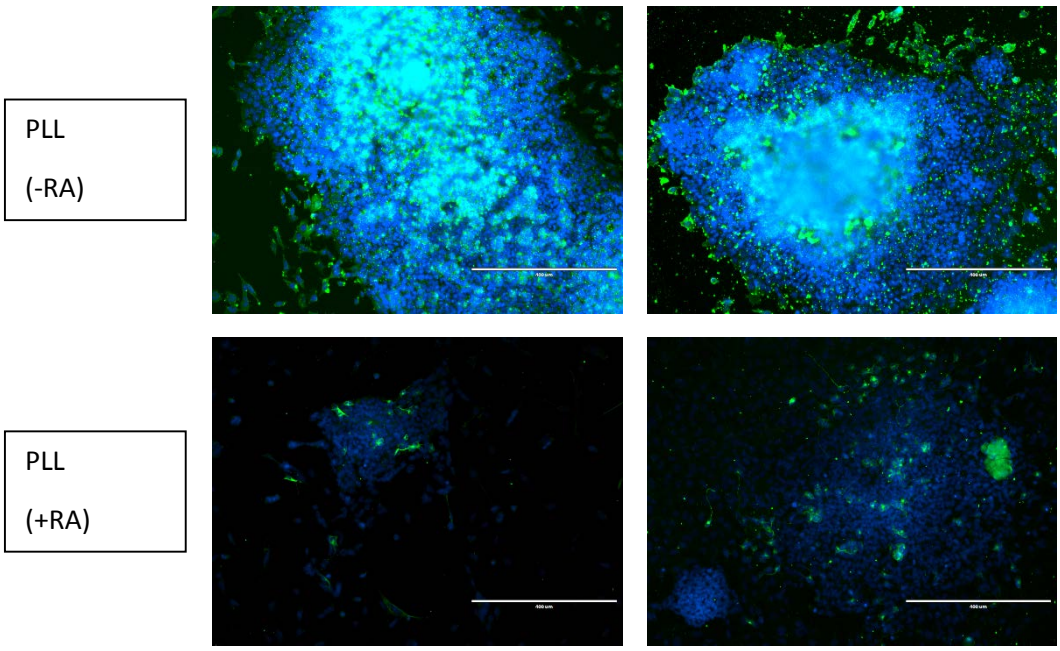


**Fig.5.3.** Fluorescence mages of NSCs polylysine coated TCP (tissue culture plastic) after 8 days of cell culture. For differentiation induction, cells were cultured with 1µM RA (-1/+7) [Green stain = β-III tubulin neuronal marker, Blue stain = DAPI; Scale bar = 400 um]

The controls demonstrated high cell proliferation and aggregate formation when cultured in absence of RA, while proliferation was reduced by RA administration though no specific differentiation trend could be recorded in presence of RA (Fig.5.3). Similar to the polylysine controls, no neuronal differentiation could be observed specifically in

response to RA induction. Higher cell aggregation and proliferation was observed without RA (Fig.5.4).

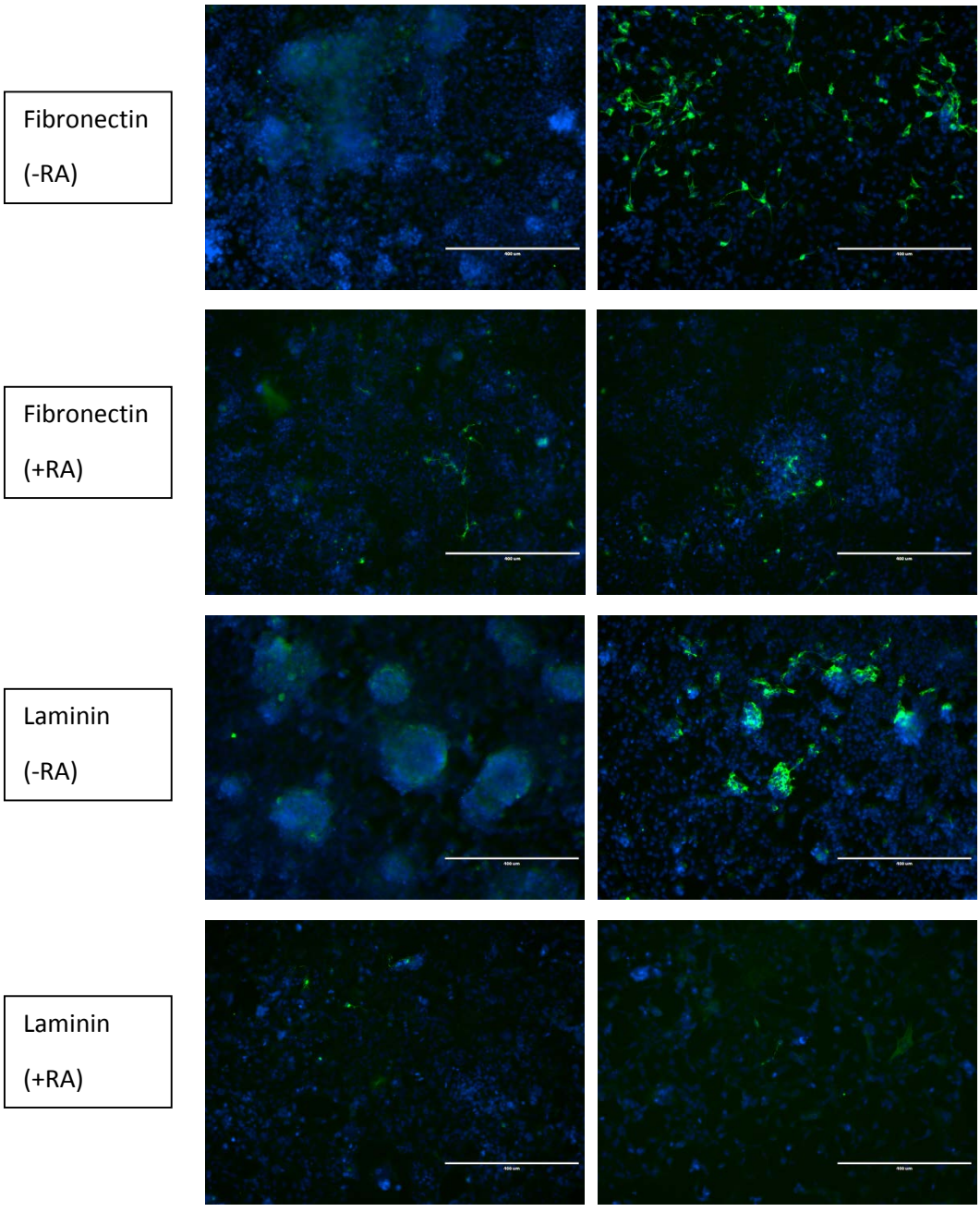


**Fig.5.4.** Fluorescence mages of NSCs on two dimensional planar polylactide (PLA) films after 8 days of cell culture. For differentiation induction, samples were cultured with 1µM RA (-1/+7) [Green stain = β-III tubulin neuronal marker, Blue stain = DAPI; Scale bar = 400 um]

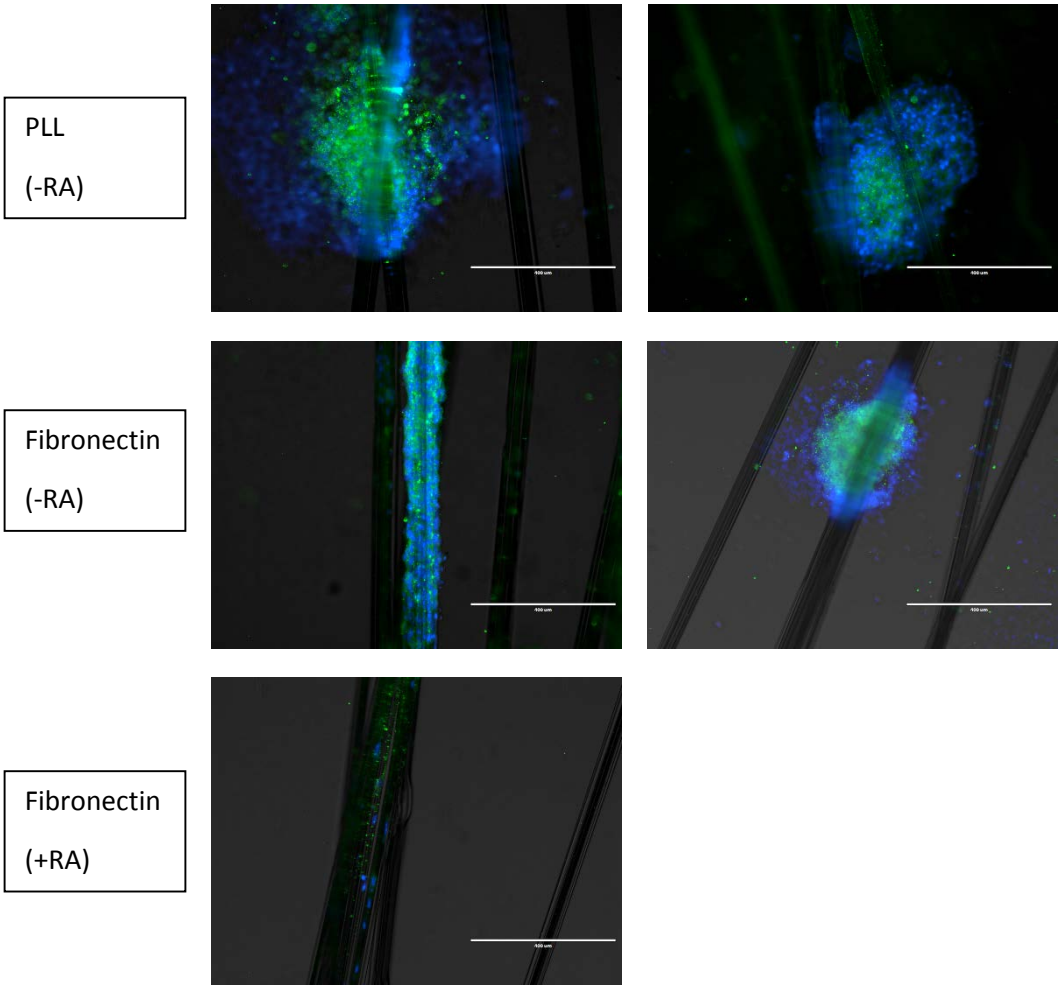


**Fig.5.5.** Fluorescence mages of NSCs on three dimensional CCP fibers after 8 days of cell culture. For differentiation induction, samples were cultured with 1µM RA (-1/+7) [Green stain = β-III tubulin neuronal marker, Blue stain = DAPI; Scale bar = 400 um]

NSCs were seeded on 3D CCP fiber samples to test for the bioactivity of the topography with or without RA induction. The result on 3D CCP fibers was similar to the results on 2D surfaces described earlier. As can be seen in Fig.5.5, some neuronal differentiation could be seen on CCP fibers without RA administration. Cell proliferation was drastically reduced upon RA induction, but no neurons could be observed.

**Discussion**:

NE-4C cells are immortalized neuroectodermal progenitor cell line, which have been established to differentiate into neurons and astrocytes in presence of all-trans retinoic acid (RA) [20]. However, these cells only differentiate when RA administration is in concert with formation of adequate intercellular contacts via aggregation [22]. In order to achieve differentiation, the timing of RA administration appears to be critical, otherwise cell death occurs owing to the 'contact lateral inhibition' phenomenon of these cells. Various factors such as signaling by the membrane anchored receptor/ligand pair, Notch and Delta are known to interact to determine the repression or expression of neurogenic genes, consequently inhibiting or inducing neuronal commitment in NE-4C cells [23]. These facts indicate that gap junctions between these cells communicate signals that control cell proliferation and differentiation [24, 25].

Schlett et al found that the first neurons appear on the $3^{rd}$ day after induction and a dense network of morphologically differentiated neurons develop by the $7^{th}$ day [20]. However, differentiation into neurons only takes place when RA-treated cell aggregates are formed, if RA is absent, the cells in the aggregate die. The formation of aggregates indicated the importance of 3D contacts in neuronal cell fate decision. Cells with astroglial characteristics appear only by the $10^{th}$ -$12^{th}$ day of RA induction. These facts indicate that apart from RA, local biochemical cues are involved during *in vitro* induction of neuronal differentiation. Treatment with RA strengthens the cell-to-cell adhesion at the expense of cell-to-substrate interaction. The appropriate formation of aggregates is also contingent on the initial cell seeding density, a critical density of 25000 cells/$cm^2$ is necessary for neuron formation after the initial 24 hours of induction. The importance of paracrine signaling in neurogenesis was established by blocking gap junction communication with

high concentrations of glycyrrethinic acid (GRA) and carbenoxolone (CRX), which highly reduced rate of neurogenesis in human and mouse cell lines [26].

In this work, RA was administered after 24 hours post cell seeding (-1/+7). When no significant and specific neuronal differentiation could be observed in response to RA, some adjustments were made for a new experimental design. For the last experimental trials (data not shown), the media used was devoid of FBS (fetal bovine serum), the rationale being that serum withdrawal could encourage differentiation and subdue proliferation. The experimental design consisted of 3D CCP fibers and 2D TCP with or without RA induction (-3/+10), which would give adequate time for cells to proliferate and form aggregates over the first three days and then induce the formation of neurons till Day 7 and astrocytes by Day 10. However, high cell death was observed throughout the experiment and by Day 10, most cells were dead (results not shown).

It can be inferred from these experiments with NE-4C NSCs that they do not differentiate in response to the topography of the grooved fibers, but can only respond to meticulously timed induction by RA. The formation of healthy aggregates of RA induced cells can differentiate into neurons by paracrine signaling through gap junction formation. Since NE-4C cells have not been previously used for studying effect of physical topography of scaffold, it will be feasible to select a stem cell line that has been used for such investigations by other research groups. Bakhru et al have used adult rat hippocampal NSCs (Chemicon, Billerica, MA, USA) to demonstrate differentiation in response to proximity to aligned fibers; cells on and in close proximity to fibers differentiating into neurons while those further away from the fibers differentiating into glial phenotypes [17]. NSCs have also been isolated and purified from Fischer 344 rat hippocampi, and shown to differentiate in response to different diameters of electrospun fiber substrates [27]. A suitable alternative choice of NSCs for future work should be able

to respond to the groove topography of CCP fibers by exhibiting enhanced survival, reduced apoptosis and changes in gene expression via cytoskeletal and nuclear elongation. It is known that nuclear distortion results in decreased proliferation and induction of neurogenic pathways via canonical β-catenin/Wnt signaling [28-30].

**Conclusion**:

Stem cells have been shown to change their morphology in response to topography of the substrate and this results in changes on cell proliferation, survival and differentiation gene expression. In this study NE-4C neuroepithelial cells have been used to investigate the response to groove topography of CCP fibers; this study was the first of its kind. No differentiation could be induced in these cells in response to topography even when supplemented by retinoic acid as inducer. Future studies will be focused on using a different cell type such as commercially available adult rat hippocampal NSCs that have already been found to respond by differentiation to fiber topography.

## **References**:


[1] Meinhardt A, Eberle D, Tazaki A, Ranga A, Niesche M, Wilsch-Bräuninger M, et al. 3D Reconstitution of the Patterned Neural Tube from Embryonic Stem Cells. Stem Cell Reports 2014.
[2] Jain KK. Neuroprotection in spinal cord injury. The Handbook of Neuroprotection: Springer; 2011. p. 255-80.
[3] Li X, Katsanevakis E, Liu X, Zhang N, Wen X. Engineering Neural Stem Cell Fates with Hydrogel Design for Central Nervous System Regeneration. Progress in polymer science 2012.
[4] Temple S. The development of neural stem cells. Nature 2001;414:112-7.
[5] Doetsch F, Caille I, Lim DA, García-Verdugo JM, Alvarez-Buylla A. Subventricular zone astrocytes are neural stem cells in the adult mammalian brain. Cell 1999;97:703-16.
[6] Conti L, Cattaneo E. Neural stem cell systems: physiological players or in vitro entities? Nature Reviews Neuroscience 2010;11:176-87.
[7] Okano H, Sawamoto K. Neural stem cells: involvement in adult neurogenesis and CNS repair. Philosophical Transactions of the Royal Society B: Biological Sciences 2008;363:2111-22.
[8] Okano H. Neural stem cells and strategies for the regeneration of the central nervous system. Proceedings of the Japan Academy Series B, Physical and biological sciences 2010;86:438.
[9] Ronaghi M, Erceg S, Moreno-Manzano V, Stojkovic M. Challenges of stem cell therapy for spinal cord injury: human embryonic stem cells, endogenous neural stem cells, or induced pluripotent stem cells? Stem Cells 2010;28:93-9.
[10] Miller FD, Gauthier-Fisher A. Home at last: neural stem cell niches defined. Cell stem cell 2009;4:507-10.
[11] Guilak F, Cohen DM, Estes BT, Gimble JM, Liedtke W, Chen CS. Control of stem cell fate by physical interactions with the extracellular matrix. Cell stem cell 2009;5:17-26.
[12] Straley KS, Foo CWP, Heilshorn SC. Biomaterial design strategies for the treatment of spinal cord injuries. Journal of Neurotrauma 2010;27:1-19.
[13] Nomura H, Tator CH, Shoichet MS. Bioengineered strategies for spinal cord repair. Journal of Neurotrauma 2006;23:496-507.
[14] Reilly GC, Engler AJ. Intrinsic extracellular matrix properties regulate stem cell differentiation. Journal of biomechanics 2010;43:55-62.
[15] Chen CS. Mechanotransduction–a field pulling together? Journal of cell science 2008;121:3285-92.
[16] Lim SH, Liu XY, Song H, Yarema KJ, Mao H-Q. The effect of nanofiber-guided cell alignment on the preferential differentiation of neural stem cells. Biomaterials 2010;31:9031-9.
[17] Bakhru S, Nain AS, Highley C, Wang J, Campbell P, Amon C, et al. Direct and cell signaling-based, geometry-induced neuronal differentiation of neural stem cells. Integr Biol 2011;3:1207-14.
[18] Hsieh A, Zahir T, Lapitsky Y, Amsden B, Wan W, Shoichet MS. Hydrogel/electrospun fiber composites influence neural stem/progenitor cell fate. Soft Matter;6:2227-37.
[19] Maden M. Retinoic acid in the development, regeneration and maintenance of the nervous system. Nature Reviews Neuroscience 2007;8:755-65.
[20] Schlett K, Madarász E. Retinoic acid induced neural differentiation in a neuroectodermal cell line immortalized by p53 deficiency. Journal of neuroscience research 1997;47:405-15.
[21] Hern DL, Hubbell JA. Incorporation of adhesion peptides into nonadhesive hydrogels useful for tissue resurfacing. Journal of biomedical materials research 1998;39:266-76.

[22] Tárnok K, Pataki Á, Kovács J, Schlett K, Madarász E. Stage-dependent effects of cell-to-cell connections on in vitro induced neurogenesis. European journal of cell biology 2002;81:403-12.
[23] Beatus P, Lendahl U. Notch and neurogenesis. Journal of neuroscience research 1998;54:125-36.
[24] Bani-Yaghoub M, Underhill TM, Naus CC. Gap junction blockage interferes with neuronal and astroglial differentiation of mouse P19 embryonal carcinoma cells. Developmental genetics 1999;24:69-81.
[25] Bittman K, Owens DF, Kriegstein AR, LoTurco JJ. Cell coupling and uncoupling in the ventricular zone of developing neocortex. The Journal of neuroscience 1997;17:7037-44.
[26] Bani-Yaghoub M, Bechberger JF, Underhill TM, Naus CC. The effects of gap junction blockage on neuronal differentiation of human NTera2/clone D1 cells. Experimental neurology 1999;156:16-32.
[27] Christopherson GT, Song H, Mao HQ. The influence of fiber diameter of electrospun substrates on neural stem cell differentiation and proliferation. Biomaterials 2009;30:556-64.
[28] Kasai M, Satoh K, Akiyama T. Wnt signaling regulates the sequential onset of neurogenesis and gliogenesis via induction of BMPs. Genes to Cells 2005;10:777-83.
[29] Inestrosa NC, Arenas E. Emerging roles of Wnts in the adult nervous system. Nature Reviews Neuroscience 2009;11:77-86.
[30] Gulacsi AA, Anderson SA. β-catenin–mediated Wnt signaling regulates neurogenesis in the ventral telencephalon. Nature neuroscience 2008;11:1383-91.

# CHAPTER 6

# CONCLUSIONS AND FUTURE WORK

## Conclusions:

The first objective of this research was to demonstrate long distance axonal growth on L1-CAM immobilized capillary channel polymer (CCP) fibers as a potential scaffold. L1-CAM was chosen for its critical role in proper nervous system development and its selectivity of neuron adhesion in the presence of astrocytes. Dose dependent response of L1-CAM was established by demonstration of higher neurite extensions with higher concentrations. In addition the superiority of L1-CAM to widely used laminin for axon extension was shown. The studies showed that primary dissociated neurons and explants would align along the direction of the grooves of the fibers and could serve as a suitable scaffold for SCI injury model.

The second objective of this research was to fabricate fiber 'staples' and test their utility as cell laden microcarriers within hybrid hydrogels. This aim was driven by the rationale that micron scale topographic features can be employed to mimic the natural cellular surroundings of the ECM for nerve regeneration application. A biodegradable hydrogel-fibrous staple composite demonstrating sustained cell survival and proliferation was developed. 3T3 fibroblasts pre-seeded on CCP staples when encapsulated in PEGdA/HA hydrogel blends, showed 10 times more proliferation as compared to day 1 samples and to control gels (without CCP staple microcarriers) as well. The physical properties of the composite system demonstrated cell cluster formation around the staples in 3D by proliferation. This study indicated that the hydrogel-staple composite may have

promising potential in various tissue regeneration applications involving stem cell proliferation and differentiation. Future studies could include incorporation of neural stem cells to induce differentiation into neural lineage for targeting CNS trauma and neurodegenerative disease.

The third objective of this research was to evaluate the gel-staple composite on NSC differentiation. In this study NE-4C neuroepithelial cells have been used to investigate the response to groove topography of CCP fibers; this study was the first of its kind. The adherence of NSCs in grooves of polylysine coated staples was validated. However, no differentiation could be induced in these cells in response to topography even when supplemented by retinoic acid (RA) as inducer. Upon delving into the possible reasons of this behavior, it was found that these cells differentiate only upon RA induced aggregation which causes paracrine signaling by gap junction formation, which was contrary to confluence mediated aggregation induction that was being attempted in this study. Although, it was obvious from this study that these cells did not respond to the bioactivity of topography and relied on RA induction only for neuronal differentiation. Thus, future studies will be focused on using a different cell type such as commercially available adult rat hippocampal NSCs that have already been found to respond by differentiation to fiber topography.

**Future Project Recommendations**:

- Investigate the differentiation of a different NSC line such as adult rat hippocampal NSC in response to retinoic acid on 2D tissue culture plastic.
- Upon optimization conditions of NSC differentiation on 2D surfaces, investigation of differentiation on 3D CCP fibers

- Investigate the proliferation and differentiation of NSCs in 3D gel-staple composite
- Conjugation or immobilization of magnetic nanoparticles to staples and development of a system to align staples for a suitable SCI scaffold.
- Investigation of the composite scaffold towards differentiation of human mesenchymal stem cells into osteogenic cells.
- In vivo animal studies for investigating the feasibility of injectable in situ crosslinkable composite scaffold for SCI/TBI models.